Vehicle-to-Vulnerable roAd user cooperaTive communication and sensing teCHnologies to imprOVE transpoRt safety

D4.1 – Communication technologies specifications

Project contract n.:	FP6-2004-IST-4 – 027014
Workpackage, workpackage title:	WP4, Communication and Sensing Technologies
Task, task title:	T4.1, Communication technologies scouting and selection
Deliverable n.:	D4.1
Document title:	D4.1 – Communication technologies specifications
Deliverable type:	PUBLIC
Document preparation date:	20.12.2006
Authors:	A. Sikora (SFIDK)

Consortium:

Centro Ricerche Fiat, DaimlerChrysler AG, Piaggio & C. S.p.A., Robert Bosch GmbH, MIRA Limited, Technische Universität Chemnitz, ARC Seibersdorf research GmbH, Centre for Research and Technology Hellas, University of Stuttgart, Steinbeis Stiftung für Technologie Transfer, Faber Software S.r.l., LogicaCMG Nederland B.V., Università di Modena e Reggio Emilia

Project co-funded by the European Commission
DG-Information Society and Media
in the 6th Framework Programme

1 Document Control Sheet

Project name: WATCH-OVER

Workpackage, workpackage title: WP4, Communication and Sensing Technologies

Task, task title: T4.1, Communication technologies scouting and selection

Document title: WATCH-OVER D4.1 – Communication technologies specifications

Main author(s): A. Sikora (SFIDK)

Other author(s): G.-J. van Bakel (LogicaCMG), M. Erschig (SFIDK), A. Guarise (CRF), G. Humer (ARCS), D. Lill (SFIDK), U. Neubert (TUC),

Date of submission to consortium: 15.01.2007

Date of submission to European Commission: 05.02.2007

Revision history:

VERSION	DATE	AUTHOR	SUMMARY OF CHANGES
1.0	31.01.2007	A. Sikora	Implementation of Comments from Peer Review
0.6	11.01.2007	A. Sikora	Included review information from G. Humer (ARCS), G.-J. van Bakel and M. Konijn (LogicaCMG)
0.51	04.01.2007	A. Sikora	list of abbreviations supplemented
0.5	20.12.2006	A. Sikora A. Guarise	general review image compression
0.42	13.12.2006	A. Sikora U. Neubert G. Humer	input for chapter 2.2 (TUC) input for chapter 5.1 (ARCS)
0.41	1.12.2006	A. Sikora, A. Guarise	input for chapter 2.1 (CRF); rework of 2.3 (SFIDK)
0.4	27.11.2006	A. Sikora, M. Erschig, G. Humer, U. Neubert	enhanced chapter 3 (SFIDK, TUC, ARCS); measurement report self localisation (TUC); measurement report CSS and UWB-AOA (SFIDK) added chapter 2.2.3 (SFIDK)
0.3	16.10.2006	A. Sikora, G. Humer	Enhanced chapter 3 (SFIDK, LogicaCMG, ARCS)
0.21	6.9.2006	A. Sikora	Responsibilities for chapters (SFIDK) Delete 2.1 (SFIDK)
0.2	14.08.2006	A. Sikora, G.-J. van Bakel	enhancements mainly to ch. 3 (SFIDK) first generation of 3.7 (LogicaCMG)
0.1	22.07.2006	A. Sikora, D. Lill	first generation (SFIDK)

2 List of abbreviations

ACKs	Acknowledgements
ACL	Asynchronous Connectionless Link
AES	Advanced Encryption Standard
AFH	Adaptive Frequency Hopping
AG	Aktiengesellschaft
AOA	Angle-Of-Arrival
AP	Access Points
ASTM	American Society for Testing and Materials
BER	Bit Error Rate
BO	Beacon Order
BP	Beacon Period
BSIG	Bluetooth Special Interest Group
BSS	Basic-Service Set
BTproduct	Time-Bandwidth Product
B.V.	Besloten Vennootschap (e.g. LogicaCMG B.V.).
BWA	Broadband Wireless Access
CAN	Controller Area Network
CAP	Contention Access Period
CBC	Cipher Block Chaining
CCM	Counter Mode Encryption with CBC-MAC
CE	Communautes Europeennes
CEP	Circular Error Probable
CEPT	Conférence Européenne des Postes et Télécommunications.
CFP	Contention Free Period
COST	COoperation Européenne dans le domaine de la recherche Scientifique et Technique
CSMA/CA	Carrier Sense Multiple Access/Collision Avoidance
CSS	Chirp Spread Spectrum
CTR	Counter Mode
DAA	Detect And Avoid
DCF	Distributed Coordination Function
DDL	Dispersive Delay Line
DGPS	Differential GPS
DIN	Deutsches Institut für Normung
DG	Directorate General
DOP	Dilution Of Precision
DPSK	Differential Phase Shift Keying
DRP	Distributed Reservation Protocol
DS	Distribution System
DSSS	Direct Sequence Spread Spectrum
DSRC	Dedicated Short Range Communications
EBM	Energy Budget Management
EC	European Commission
ECC	Electronic Communications Committee
ECU	Electronic Control Unit
ED	Energy Detection
EGNOS	European Geostationary Navigation Overlay Service
EMI	Electromagnetic Interference
EU	European Union
EUI	Extended Unified Identifier
FDD	Frequency Division Duplexing
FHSS	Frequency Hopping Spread Spectrum
FFD	Full Function Devices

FEC	Forward Error Control
GmbH	Gesellschaft mit beschränkter Haftung
GNSS	Global Navigation Satellite System
GPS	Global Positioning System
GSM	Global System for Mobile Communication
GTS	Guaranteed Time Slots
HCF	Hybrid Coordination Function
HCI	Host Controller Interface
HDOP	Horizontal Dilution Of Precision
H-FDD	Half- Frequency Division Duplexing
HMI	Human Machine Interface
HSDPA	High Speed Downlink Packet Access
HSUPA	High Speed Uplink Packet Access
Hz	Cycles per second (with TGMk prefixes).
IEEE	Institute of Electrical and Electronics Engineers
IPS	Intrusion Prevention System
IR	infrared
	Impulse Radio
ISO	International Standard Organisation
IST	Information Society Technologies
IV	Initialisation Vectors
LAN	Local Area Network
LCD	Liquid Crystal Display
LEP	Linear Error Probable
LFM	Linear Frequency Modulated
LLC	Logical Link Control
LM	Link Manager
LNA	Low Noise Amplifier
LOS	Line-Of-Sight
LQI	Link Quality Indicator
MAC	Medium Access Control
MAS	Medium Access Slots
MBOA	Multiband OFDM Alliance
MDMA	Multi Dimensional Multiple Access
MIMO	Multiple-Input Multiple Output
MT	Multi-Tone
NLOS	Non-Line-Of-Sight
OBU	On Board Units
OEM	Original Equipment Manufacturer
OFDM	Orthogonal Frequency Division Multiplex
OWR	One Way Ranging
PA	Power Amplifier
PAN	Personal Area Networks
PC	Personal Computer
PCA	Prioritis Contention Access
PCF	Point Coordination Function
PDOP	Position Dilution of Precision
PHY	Physical
PPS	Precise Positioning Service
PTW	Powered Two Wheeler
RF	Radio Frequency
RFD	Reduced Function Devices
RFID	Radio Frequency Identification
RMS	Root Mean Square
ROI	Region Of Interest

RSS	Received-Signal Strength
RSSI	Received Signal Strength Indication
RTLS	Real Time Localisation Systems
RTOF	Roundtrip-Time-Of-Flight
RX, Rx	Receive
SA	Standards Association
SAW	Surface Acoustic Wave
SBAS	Satellite Based Augmentation System
SCO	Synchronous Connection Oriented
SDS-TWR	Symmetric Double Sided – Two Way Ranging
SEP	Spherical Error Probable
SIR	Signal to Interference Ratio
SO	Superframe Order
SPA	Società per azioni
SPS	Standard Positioning Service
SSCS	Service Specific Convergence Sublayer
SRWN	Short Range Wireless Network
SRL	Società a responsabilità limitata
TCP	Transmission Control Protocol
TDD	Time Division Duplexing
TDM	Time Division Multiplex
TDMA	Time Division Multiple Access
TKIP	Temporal Key Integrity Protocol
TDOA	Time-Difference-Of-Arrival
TOA	Time-Of-Arrival
TWR	Two-Way Ranging
TX, Tx	Transmit
T*x.y*	Task (number *x.y*)
UDP	User Datagram Protocol
UMTS	Universal Mobile Telecommunications System
UWB	Ultra Wide Band
VDOP	Vertical Dilution of Precision
VRU	Vulnerable Road User
WAAS	Wide Area Augmentation System
WAVE	Wireless Access in Vehicular Environment
WiMAX	Wireless Metropolitan Area Access Worldwide Interoperability for Microwave Access
Wi-Fi	Wireless Fidelity
WLAN	Wireless LAN
WMA	WiMedia Alliance
WMAN	Wireless Metropolitan Area Network
WPA	WiFi Protected Access
WPAN	Wireless Personal Area Networks
WP*x*	Work Package (number *x*)

This project has been co-funded by the European Commission DG-Information Society and Media in the 6th Framework Programme. The content of this publication is the sole responsibility of the project partners listed herein and does not necessarily represent the view of the European Commission or its services.

3 Table of contents

This project has been co-funded by the European Commission DG-Information Society and Media in the 6th Framework Programme. The content of this publication is the sole responsibility of the project partners listed herein and does not necessarily represent the view of the European Commission or its services.

This project has been co-funded by the European Commission DG-Information Society and Media in the 6th Framework Programme. The content of this publication is the sole responsibility of the project partners listed herein and does not necessarily represent the view of the European Commission or its services.

4 List of Figures

5 List of Tables

1. Executive Summary

The WATCH-OVER project started in January 2006. It is a specific targeted project co-funded by the European Commission Information Society Technologies (IST) in the strategic objective "eSafety Co-operative Systems for Road Transport".
The goal is the design and development of a cooperative system for the prevention of accidents involving vulnerable road users in urban and extra-urban areas. The innovative concept is represented by an on board platform and by a vulnerable user module. The system is based on short range wireless communication and vision sensors.
WATCH-OVER intends to examine the detection of vulnerable road users in the complexity of traffic scenarios in which pedestrians, cyclists and motorcyclists are walking or moving together with cars and other vehicles.

The document represents an overview of the most relevant information collected for the development of the communication part for the WATCH-OVER system. It is the main output of the Project Task 4.1: “Communication technologies scouting and selection” within the Work Package WP4: “Communication and Sensing Technologies”. It describes the requirements to the system (cf. ch. 2), examines the possible candidates for wireless communication purposes (cf. ch. 3), investigates on the available localisation technologies (cf. ch. 4), and reports on the results and experiences with the examined candidates (cf. ch. 5). It finally gives a recommendation for the use in the WATCH-OVER system (cf. ch. 6).

2. System Specification

2.1. Specification

2.1.1. Basic Specification

Traditional driver assistance systems for recognising external obstacles are usually based on vision sensing technologies, as laser, laser scanners or cameras. The experiences collected in the Protector and SAVE-U projects lead to the observation that an integrated system where the vehicle surrounding scenario is analysed also from a communication link able to exchange localisation data with external entities would be highly valuable to gather a better status evaluation on how the traffic events evolve in front of the vehicle.

In the WATCH-OVER system the use of an IR camera and a wireless communication system is envisaged. The communication system shall support a two-way communication between vehicles and VRU's. In addition, this WATCH-OVER communication system shall also support ranging and localisation. Ranging and localisation belong to today's most complicated tasks in communication technology.

- Ranging is determining the distance between the vehicle and the VRU, typically in a circle around the vehicle
- Localisation is to determine the exact position of the VRU, either in absolute coordinates or relative to the vehicle.

If there is a good localisation, there is no need for ranging anymore.

There are a number of research projects that handle the issue of localisation and ranging. [79] describes some examples. However, suitable mass products for localisation and ranging can hardly be found on the market, at least not for the time being.

The task of communication between Vehicle and VRU can be solved by a lot of standard products. In this system specification we will essentially concentrate on localisation.

Research question

The requirements and constraints of the overall system formulated in the annex I of the WATCH-OVER project lead to the fundamental question, what is the minimum distance between vehicle and VRU in which the vehicle can be stopped, given the instantaneous speed of the vehicle?

This minimum distance determines the minimum performance for the detection system. To solve this question the following physical parameters for the design of the localisation system will be applied.

- Urban traffic, maximum speed: $v = 50\ kmh^{-1} \approx 14\ ms^{-1}$
- Response time of humans: $t_r = 0.5 ... 1s$. Even though reaction time might be smaller (e.g. 0,1 … 0,2 s), this estimation is on the safe side.
- Braking distance: $s_b \approx 25$ m (good road and tyre conditions, response time regarded)
- Maximum reliable detection range for a human shape ≈ 30 m (by the planned infrared (IR) camera)
- Horizontal viewing angle of the IR camera $\Delta \approx 60^0$
- Frame rate of the IR camera 25 Hz, corresponds 40 ms
- Stopping distance: $s_s = s_r + s_b$ (response distance + braking distance)
- Stopping time: $t_s = t_r + t_b$ (response time + braking time)
- Emergency braking deceleration: $a_e = 7.72\ ms^{-2}$

With the following equations

$$v = \frac{s}{t}, \quad \text{(Eq. 1)}$$

for constant velocity, and

$$v = a \cdot t; \qquad s = \frac{a}{2} \cdot t^2; \qquad t = \sqrt{\frac{2s}{a}} \quad \text{(Eq. 2)}$$

for constant acceleration, the braking time results in t_b = 1.8 s and the total stopping time in t_s = 2.8 s. The distances result accordingly. The complete situation is represented in Figure 1.
That means that the IR camera specified in the project with a detection range of about 25 m has only tenth parts of seconds for identification of a VRU to generate a warning signal for the driver to avoid an impact in worst case situation. So we need earlier support by a localisation system, at least in a distance of about 50 m in order to have approximately 1.5 s more available for a reliable detection. Very good road conditions were assumed. Under worse conditions the situation could become even more complicated.

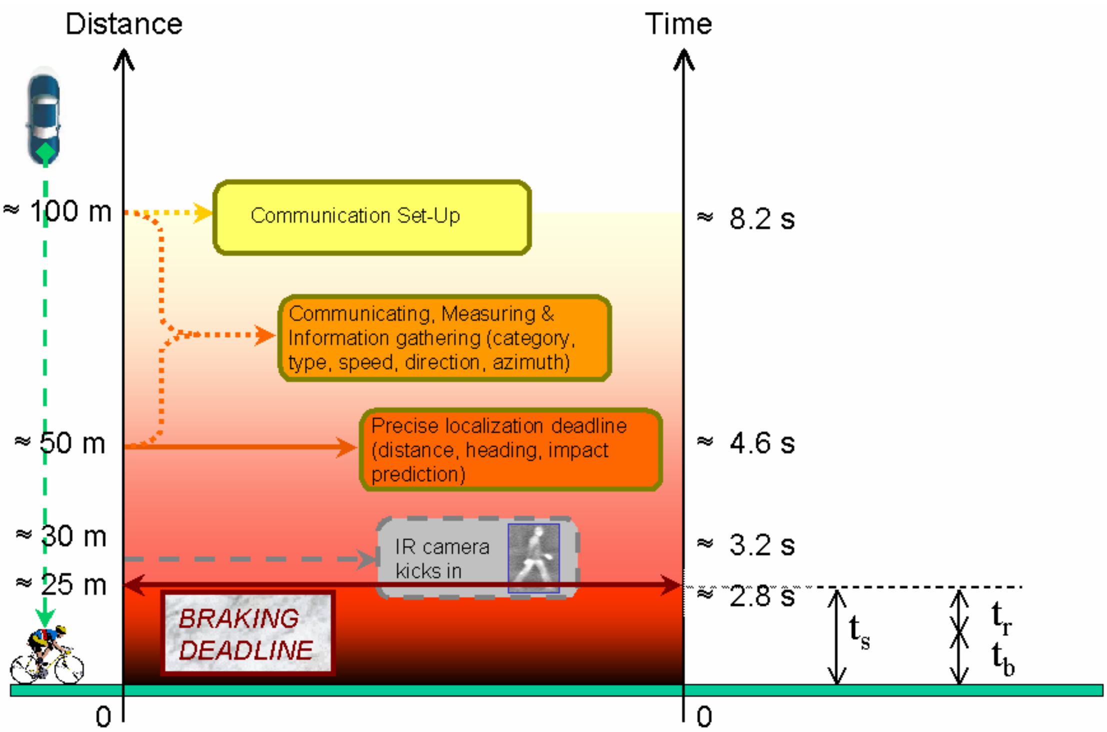

Figure 1: Basic Timeline and Distances for the Localisation System

For using the localisation system in a car there are typical constraints because of the physical dimensions of the vehicle. Normally we can expect a triangulation method for localisation, furthermore a data fusion principle made of IR camera and localisation system is used. That leads to the definition of a region of interest (ROI) in the camera image, which is determined by means of the localisation procedure. The ROI covers a limited area of the camera picture, which contains interesting objects, e. g. VRUs. This reduced region makes a substantially faster and more reliable detection of VRUs and the recognition of dangerous situations possible. Finally the distance information between the vehicle and the VRU delivers generally more confidence in estimation of the actual traffic scenario and allows a relatively precise calculation of the time to a possible collision to generate a warning signal.

The triangulation method for the calculation of the position of the VRU, that means the determination of the position of the wearable unit, needs at least two reference nodes with a known position to each other. The accuracy of the position information increases with the distance between the reference nodes. In our localisation task to detect relevant objects in front of a driving car we use most likely the rear-view mirrors as the mounting locus of the communication devices suitable for localisation (Ant#1 and Ant#2 in the figures). So we get a maximum baseline b ≈ 2 m between the mirrors applicable for a typical car. We assume the IR camera is located at the midpoint between the mirrors.

As the result of the localisation process we get an estimation of the distance d between the object and the IR camera position and an estimation of the heading angle ϑ of the object regarding the IR camera position. Because the images of the objects have a two dimensional shape and finally because of the measurement errors for both parameters the exact geometrical locus of the targeted object spreads into a ROI.

There are two fundamental methods for triangulation:

- Measurement of the distances d1 and d2 between the reference nodes and the interesting object (VRU) and calculation of the distance d and the heading angle ϑ between the IR camera position and the object. This principle is shown in Figure 2.
  For instance, the angle α between the baseline and the object is given by

$$\alpha = \arccos\left(\frac{d_1^2 + b^2 - d_2^2}{2d_1 b}\right), \qquad \text{(Eq. 3)}$$

the distance d by

$$d = \sqrt{\left(\frac{b}{2}\right)^2 + d_1^2 - bd_1\cos\alpha}, \qquad \text{(Eq. 4)}$$

and the heading angle ϑ results in

$$\vartheta = \arccos\left(\frac{d^2 + \left(\frac{b}{2}\right)^2 - d_2^2}{db}\right). \qquad \text{(Eq. 5)}$$

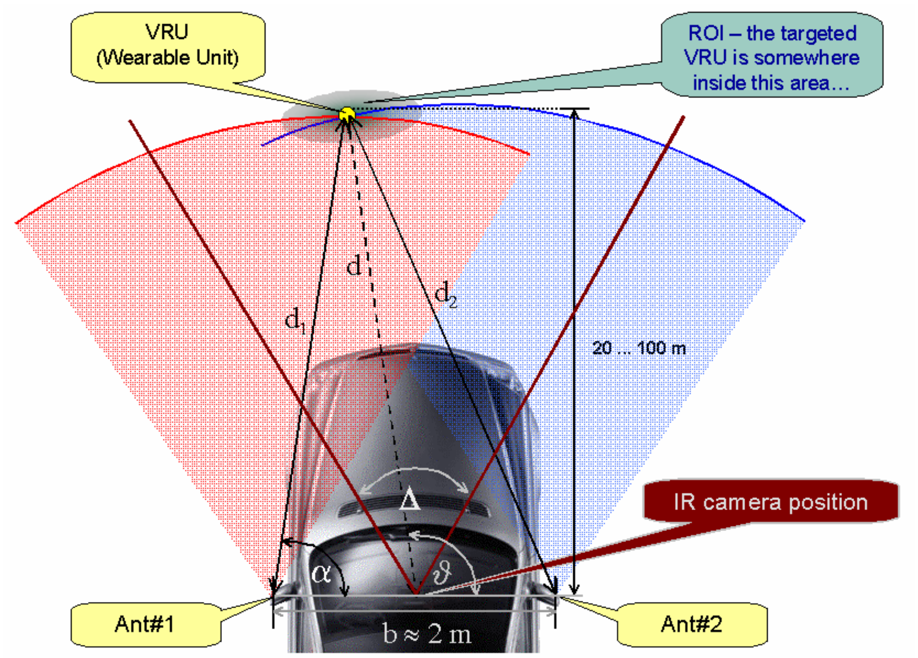

Figure 2: Arrangement of the localisation system, distance measurement approach

- Measurement of the angles α and β between the incoming wave generated by the wearable unit of the answering VRU and the baseline and calculation of the distance d and the heading angle ϑ between the IR camera position and the object. This principle is shown in Figure 3.

  In a triangle γ is given by

  $$\gamma = 180^0 - \alpha - \beta \,, \qquad \text{(Eq. 6)}$$

  the distances d1 and d2 are calculated to

  $$d_1 = \frac{b}{\sin\gamma} \cdot \sin\beta \;\; \text{and} \;\; d_2 = \frac{b}{\sin\gamma} \cdot \sin\alpha \;\; \text{respectively.} \qquad \text{(Eq. 7)}$$

  Thus the distance d and the heading angle ϑ can be computed by the equations (Eq.4) and (Eq. 18), respectively.

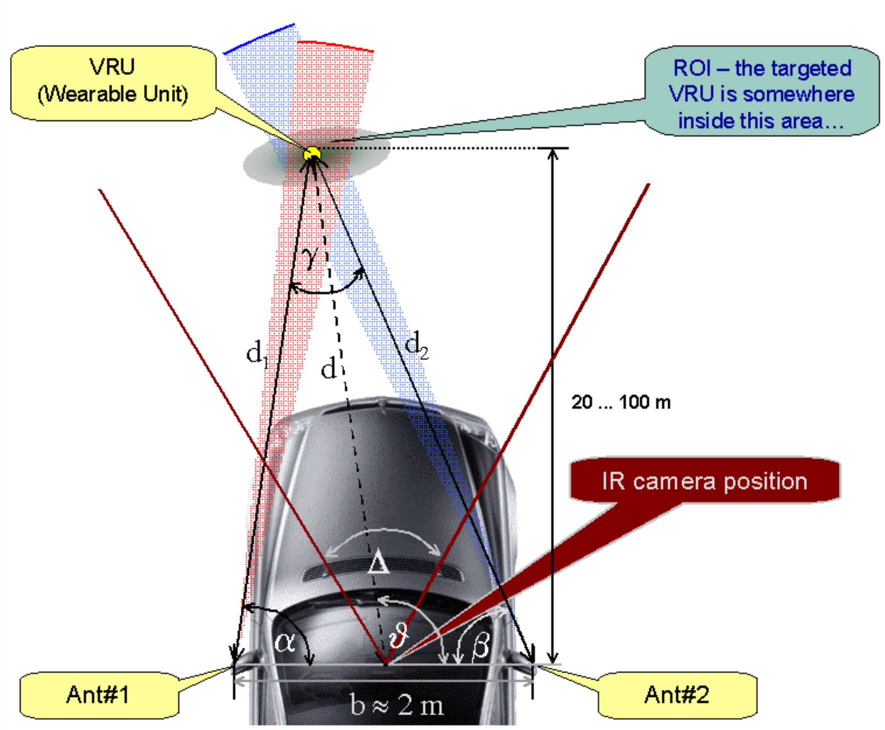

Figure 3: Arrangement of the localisation system, angle measurement approach

Figure 4 shows the consequences for the heading angle accuracy based on a realistic assumption for the reachable distance measurement precision in our measurement scenario with a baseline b of about 2 m. We can expect a relatively good distance accuracy and resolution of about or slightly below 1 m, but this results in a poor heading angle estimation with an uncertainty of about 60° because of the small baseline. Unfortunately, this is the viewing angle Δ of the IR camera itself. Therefore we can not determine a useful ROI, and so we have an unsatisfying situation regarding the cooperation of both sensors. There are two possibilities to solve this problem:

- Improvement of the accuracy of distance measurement. Very difficult to receive because for the above made calculations the parameters of the best products on the market or in development have been taken into account. Additionally, we impact on the physical and regulatory limits respecting the usable bandwidth of the communication system.
- Artificial enlargement of the baseline by using the movement of the car. This seems a good approach, in particular if we take into consideration that we need a sequence of distance measurements for statistical stabilisation of the parameters at any rate.

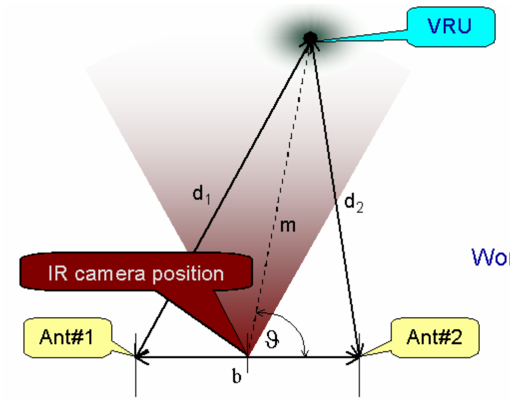

$$\vartheta = \arccos\left(\frac{m^2 + \left(\frac{b}{2}\right)^2 - d_2^2}{m \cdot b}\right)$$

$$\Delta\vartheta_{worst} \approx 60^0$$

Figure 4: Triangulation with two antennas for azimuth estimation
Two antennas are used at a baseline distance b = 2 m. The distance measurement error is assumed to be Δd = 1 m.

2.1.2. Refined Specification

2.1.2.1. opening angle

In principle the basic arrangement of the localisation system can detect VRUs unambiguously in an opening angle of 180°, if they are situated in front of the car. In the other cases the position information is ambiguous because two intersection points exist. This situation is solvable by using at least one additional reference node or directed antennas. We should use the 180° opening angle so that the IR camera based VRU detection system can be prepared in time for those situations where objects occur with a certain probability in the range of sight of the IR camera.

It should be mentioned that the supervision of the vehicle's rear part is not considered within this project.

2.1.2.2. angle resolution

A distinct angle resolution is necessary to separate different VRUs located close together, a ballpark figure of this is below 5°. For instance, to distinguish two VRUs standing together in 1 m distance located in a total distance of 40m from the car needs an angle resolution of 1.50°. Because of the physical constraints of the localisation measurement setup mentioned above, it seems not realistic to achieve this aim. The task to distinguish different VRUs has to be solved by the cooperative IR camera sensor.

A useful contribution of the communication device would be the clear identification of several VRUs in the surrounding of the vehicle by transmitting a unique VRU identifier, if both communication devices come into contact.

2.1.2.3. angle accuracy - pre processing

We need accuracy for the azimuth estimation in direction of travel of the car of 30° or better for reduction of the extent of ROI in the viewing area of the IR camera to accelerate IR image processing. Because of the small baseline for triangulation and the limited bandwidth this can not be achieved by using the communication device in a direct way, so we need additional mathematical tools to improve the precision of the localisation. Kalman filtering is a commonly approved method for this; always a series of measurements is necessary for reliable results of the filtering process. In our measurement situation we optimistically assume a time of approximately 4s from the measurement set-up to the beginning of IR image processing with the defined ROI (see Figure 1 and ch. 2.1.2.6). On this condition and an update rate of the measurement values of at least 100 Hz as well as a permanent communication link during the localisation procedure, we expect an improvement of the azimuth estimation of factor 2 to 3 based on experiences of other applications of Kalman filtering.

Additional problems arise when difficult circumstances for the wireless communication like multipath propagation exist in an urban environment. Especially problematic propagation situations occur when the link between vehicle and VRU is temporarily lost because in the course of movement of the car obstacles are located in the signal path or other signal drop-out effects may happen. In these cases a well adapted Kalman filter is able to predict the movement during a certain time and to keep virtually the communication link in this way. When the signal appears again the filtering process resumes with the actual data. In the end we can expect relatively reliable measurement results, in any case they are much more better than the heavily fluctuating single measured values.

Due to the physical conditions it is probable that a sufficiently exact angle estimation is not possible for the definition of an angle limited ROI. In this case we still can use the relatively exact distance estimation, in order to determine at least the dimension of the ROI in the IR image according to the VRU patterns we are looking for. Despite this restriction, however, an acceleration of the image processing should be achievable.

2.1.2.4. angle accuracy - under multipath conditions

Multipath propagation means that the transmitted signal reaches the receiver on different ways because of reflections on objects. Only one of them is travelling the direct way (line-of-sight, LOS); this signal represents the correct distance. Commonly, the communication devices used for localisation are logging the fastest signal and all others are discarded. So, in most cases we have no serious additional accuracy problems under multipath conditions as long as a direct line-of-sight propagation path exists.

One situation may be critical, when the receiving signal is too weak for a reliable detection because of destructive superposition of the signals arriving the receiving antenna via different propagation paths. This may be temporarily happen in course of the movement of the car. In this case Kalman filtering according to chapter 2.1.2.3 may be very helpful.

2.1.2.5. angle accuracy - under NLOS conditions

If there is no direct line-of-sight between both antennas of the car and of the VRU we can expect very inaccurate measurement results with quick changes during the car movement. It seems a very problematic situation. Therefore, we made a mathematical estimation of the effects resulting of non-line-of sight (NLOS) propagation conditions. The geometrical set-up of the considered propagation situation is shown in Figure 5.

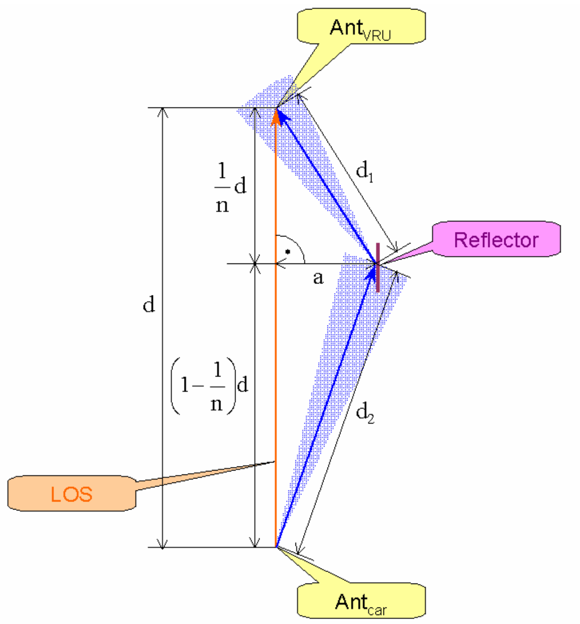

Figure 5: Detour of the signal because of NLOS propagation conditions

If no direct line-of-sight *d* exists the signal has to go a longer detour consisting of the sum of the distances d_1 and d_2 between the antennas and the reflecting object. The length of the detour depends on the shortest distance *a* between the LOS and the reflector and the relative position 1 / *n* of the reflector referring to the antennas. It should be realistic to assume that in almost all cases a reflecting object exists between both antennas as shown in Figure 5 and not only outside in extension of LOS, thus the parameter *a* dominates the accuracy effects due to multipath propagation.

The effects on accuracy depending on the parameters *a* and *n* are exemplary illustrated in Figure 6 and Figure 7. For the calculations we have used a direct distance of 40 m and a region for the offset *a* from 0 to 5 m. A parameter value of *n* = 100 means a very close position of the reflector to the endpoints of LOS, whereas *n* = 2 denominates a position in the middle of LOS. This parameter set-up seems reasonable according to the expected situations in urban areas. For longer distances the relative error decreases because the absolute error is nearly constant. The measurement of shorter distances should be efficiently supported by the IR camera, at least for the angle estimation.

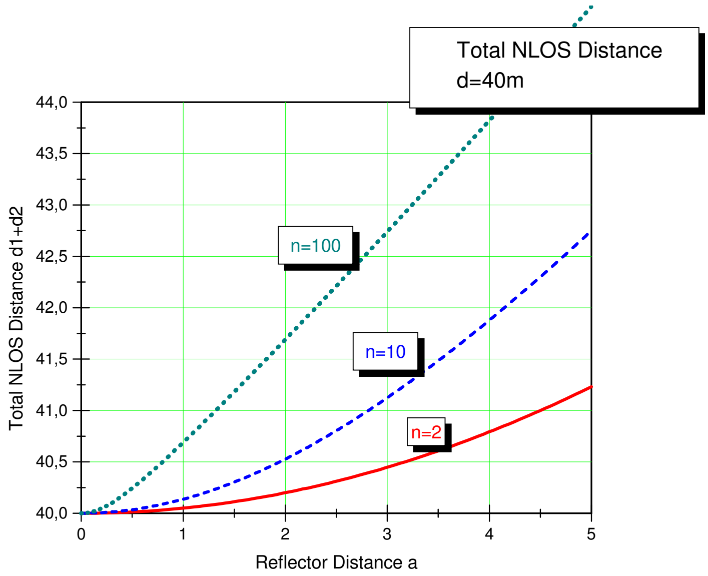

Figure 6: Total NLOS Distance for d = 40 m

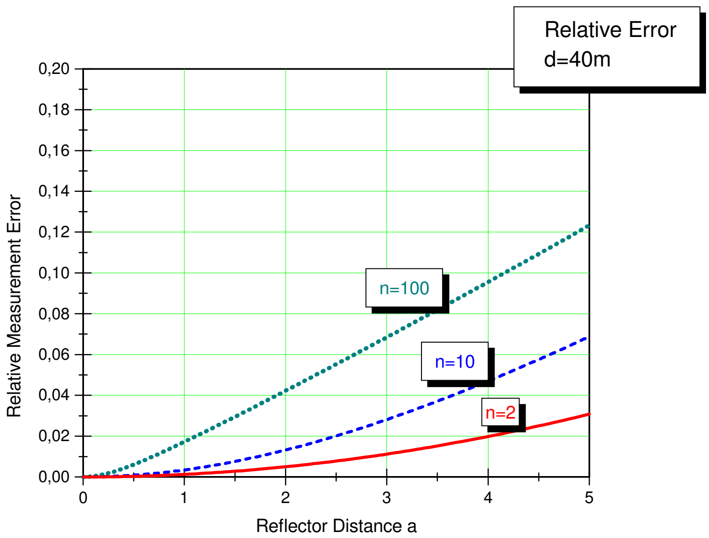

Figure 7: Relative NLOS Measurement Error for d = 40 m

In the plots we see that the error remains below 1 m and 3 % respectively if the offset *a* ranges up to 3 m with the exception that the reflector is located very close to the endpoints of LOS. This

This project has been co-funded by the European Commission DG-Information Society and Media in the 6th Framework Programme. The content of this publication is the sole responsibility of the project partners listed herein and does not necessarily represent the view of the European Commission or its services.

scenario is a realistic assumption of a propagation situation to calculate a feasible prediction of the behaviour of the measurement system.

In summary we can note that the additional error caused by NLOS conditions lies within the area of inaccuracy we have anyway, as mentioned in ch. 2.1.2.8. Therefore we can deduce that no dramatic deterioration of the measurement results happens under NLOS conditions. This corresponds with the results of first measurement campaigns done with the ranging system [81] (cf. ch. 5.3).

2.1.2.6. range

For an in time preparation of the IR based VRU detection system of the car we suppose a range of the localisation system of about 100 m as described in ch. 2.1.1 and shown in Figure 1. That matches with the expected borders of the communication devices coverage. Hence, we have time for communication link set-up, information gathering about category of the VRU, distinguishing between several VRUs, direction and speed of the movement of VRUs etc. of about 3 to 4 s. This time ensures a very reliable first detection of VRUs with a relatively large safeness reserve. In particular that is of importance if we consider the firstly still unstable radio communication link on the border of the covered area. This time is used to initialise the Kalman filter and stabilise the distance calculation process for reliable results by means of a series of measurements. Especially for an usable estimation of the angle between the vehicle movement direction and the VRU (heading angle ϑ in Figure 2) as described in ch. 2.1.2.3 we need a longer set of measured values.

2.1.2.7. distance resolution

Due to elementary physical reasons according to the usable and allowed bandwidth in current Wireless LAN (WLAN) systems of about 100 MHz we have a limit in resolution of about 1 m. Latest prototypes of ranging devices approximately accomplish this limit. Advanced GPS units supported by the EGNOS/WAAS service as described in ch. 4.5 can potentially deliver this performance, too.

UWB devices are able in principle to push the distance resolution in a very much better region because of its huge bandwidth. First products are available on the market, however not yet ready for automotive applications.

2.1.2.8. distance accuracy - pre processing

The reachable distance accuracy corresponds to the resolution described in ch. 2.1.2.7. As mentioned in ch. 2.1.2.3, Kalman filtering of the raw measurement results delivered by the communication units opens the possibility to improve significantly the accuracy and reliability of the final results. In case of distance we can not expect a considerable improvement of accuracy because of the basic bandwidth limits, but a remarkable enhancement of reliability and stability of the measurement results. By means of Kalman filter, the large fluctuations of the several measurements during gathering a series of values may be reduced drastically. At the end we have distance estimation with a much lower deviation from the true value in a statistical sense.

2.1.2.9. information update rate

The aspired WATCH-OVER sensor system update rate is at least 10 Hz. For fast initialisation and converging of the Kalman filter an update rate of about 100 Hz would be useful. This is not a problem for communication devices but for commercially GPS units, which have only a maximum update rate of approximately 10 Hz – mostly due to accuracy reasons.

2.1.2.10. bandwidth of data communication

The physical bandwidth is fundamental for localisation accuracy. But for communication purposes in our application only few bytes per second are necessary, therefore bandwidth of data communication is not a real issue. More important is the set-up time for the communication link between car and VRU which should be not more than 100 … 200 ms.

This project has been co-funded by the European Commission DG-Information Society and Media in the 6th Framework Programme. The content of this publication is the sole responsibility of the project partners listed herein and does not necessarily represent the view of the European Commission or its services.

2.1.2.11. coexistence / interference issues for scalability

Coexistence and interference issues strongly influence the scalability with multiple VRUs. Communication devices compliant to IEEE WLAN standards group 802.xx are designed to work properly in noisy environment and under coexistence conditions other concurrently active devices [82]. A loss in range is expected under such conditions, but the aspired maximum range of about 100 m in free space should be reachable without serious problems. More investigation efforts could be necessary to identify and separate different VRUs, especially if they are located close together.

2.1.2.12. coexistence issues with other EMI

Fundamentally, all candidate communication devices have to comply the basic directives regarding electromagnetic interference (EMI) like the European standards concerning unwanted electrical emissions and immunity on electrical emissions, respectively. All devices, which possess the CE marking (Communautes Europeennes) [80], correspond to this demand. Regardless of this, performance degradation may happen in an environment with many concurrently active communication devices, but this effect is covered by the relevant WLAN standards.

2.1.2.13. maturity: time to market

All investigated communication products suitable for localisation according to the minimum demands are in a prototype state and still under development. Therefore, the device prices are not calculated under real market conditions and also the technical properties are not yet finalised. For commercial use and prices we expect device availability in 2007, earliest.

2.1.2.14. state of standardisation

There are strong efforts to introduce localisation features in common WLAN standards like IEEE 802.xx. For instance, Nanotron's Chirp technology has been a part of the emerging IEEE draft standard 802.15.4a [83]. Other technologies or devices seriously taken into consideration as candidates are also covered by existing standards.

2.1.2.15. radiation exposure to VRU

The evaluated communication devices wear the CE marking and are compliant to relevant standards regarding the allowed maximum radiation values. Thus, they keep the permitted limit values. For comparison, a GSM mobile phone radiates in average about 0.5 W whereas a sophisticated WLAN device emits only 1 mW. That means the limit values are smaller for some orders of magnitude. Hence no negative consequences for the VRUs are to be feared, just as in a permanent use of the devices. If an intelligent power management is used and the device does not radiate more power than it is necessary an additional depletion of radiation exposure to VRU can be achieved [84].

2.1.2.16. power consumption

Saving energy is a great challenge especially for the wearable VRU unit to get longer battery life and thus to reduce the maintenance costs, but should also be considered at the car. Key features are [84]:

- Radiates only the energy needed to communicate with a partner device
- Does not radiate more power than is necessary
- Energy is conserved, which means battery power can be saved
- Implementation of a standby mode with very low power consumption (below 10 µW range)
- Fast wake-up time from standby to active mode (below 10 ms range)

The standby and wake-up feature is important in particular because one can expect that only in a fraction of time contact exists between vehicles and VRUs, therefore a large energy saving potential is present. These features are typical for state-of-the-art active RFID (Radio Frequency Identifier) tags like the Nanotron transceiver NA1TR8 which contains energy budget management (EBM) and sleep/wake-up circuitry to fulfil these demands [85]. For car mounted communication

This project has been co-funded by the European Commission DG-Information Society and Media in the 6th Framework Programme. The content of this publication is the sole responsibility of the project partners listed herein and does not necessarily represent the view of the European Commission or its services.

devices power consumption is not a real issue because the expected total power consumption is in range of only few Watts.

2.1.2.17. cost

Cost is a key feature for both sides, at VRU and at car. Because of the relatively immature state of communication devices suitable for localisation it is very difficult and speculative to make a realistic prediction for the market prices in future under mass production conditions. Especially the wearable unit for VRUs would be very sensitive to high cost and these should not exceed the range of several 10 EUR.

Present prototype prices spread out between several hundred and thousand Euros per unit, they are not representative and hence not appropriate for a serious economical calculation.

2.1.2.18. packaging issues

The car mounted communication and localisation unit have to be integrated in the car electronic system and placed properly regarding the electromagnetic needs, for instance in both rear-view mirrors.

Much more efforts have to be done to motivate VRUs to wear such a device, especially children and young persons. May be it is a good idea to combine the localisation unit with popular entertainment devices like MP3 players or up-to-date mobile phones. In this way also the power supply problem is elegantly solved or at least reduced.

Elderly people will probably be fully aware of the benefit in road safety by wearing this unit. The unit can be designed in a manner like a bunch of keys or a purse so that the device is easy to handle and is likely not forgotten.

2.2. System Architecture

2.2.1. Introduction

The WATCH-OVER system architecture together with the functional specification will be described in Deliverable “D3.1 – System architecture and functional specifications”. In this section a brief highlight is presented of the foreseen physical components that will constitute the WATCH-OVER framework and their relation, in order to allow the reader a better understanding of the method used for the communication technology scouting.

The WATCH-OVER system enables the cooperation of different actors who can communicate to exchange data and share information. The overall architecture is divided into different elements, with a vehicle sensing part aiming at the identification of vulnerable road users that are in front or surrounding a vehicle, and then able to share this information with external entities.

While the vehicle moves along a road there are two sensing system in charge of collecting information of the external scenario, a vision sensor device and a communication module.

The vision sensor device focuses on the frontal part of the car and recognises objects and their motion on the image pattern. The communication module searches for responding signals in the area covered from the antenna(s) and calculates the relative position of each answering radiowave. The on-board intelligence collects the different input and with mean of data fusion evaluates the risk level for possible colliding trajectories. In case the risk level passes a certain threshold there will be both an alert to the driver and a message sent to the VRU module.

A VRU could be represented from a pedestrian, a bicycle or a powered two wheeler.

The reference architecture for the WATCH-OVER system is presented in Figure 8. It shall consider building all the components that are defined by the actors in scenario’s of the participants:

- The car vehicle shall be equipped with the vision based sensor, the communication device, eventually a Global Positioning System (GPS) module for absolute localisation and an on-board unit that performs data fusion and evaluates the objects relative positioning.
- The motorbike (or the moped) shall be installed with a communication system, eventually a Global Navigation Satellite System (GNSS) receiver and an on-board unit able to collect and store information on the surrounding traffic flow.
- The VRU (pedestrian or bicyclist) shall use a wearable communication module for its recognition from the WATCH-OVER vehicles.

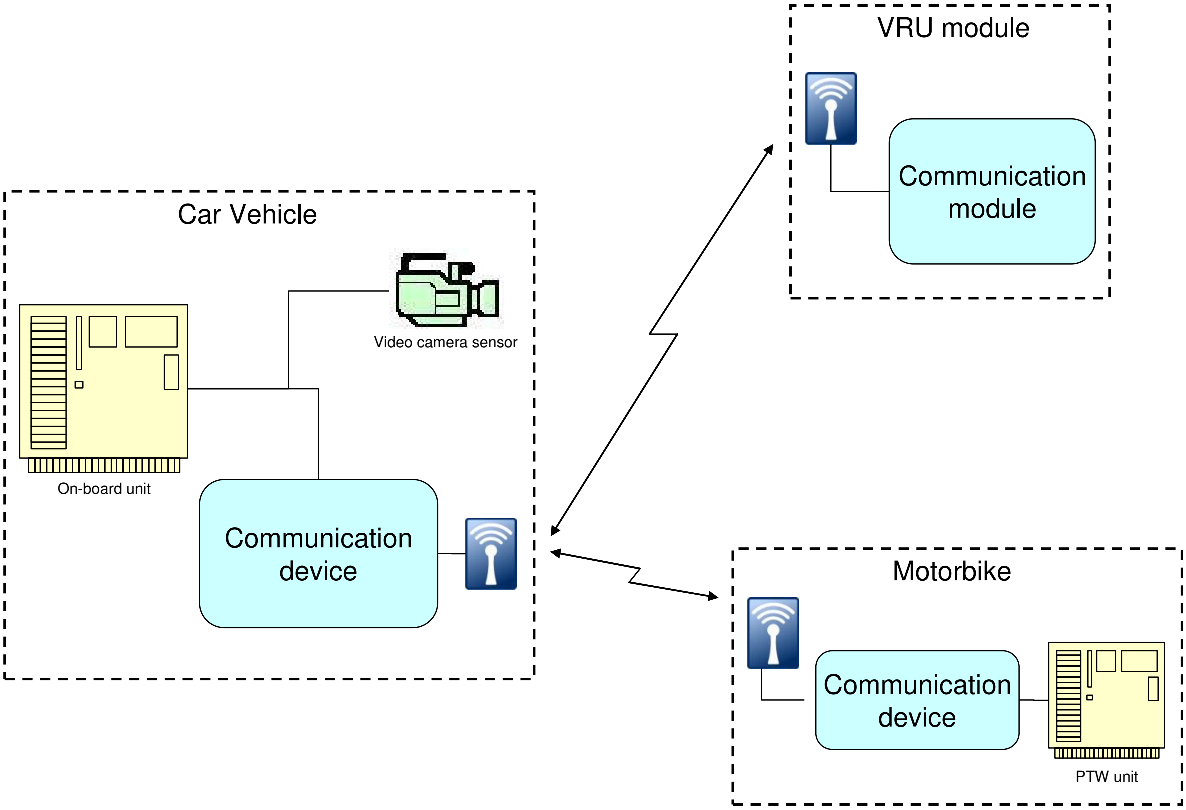

Figure 8: WATCH-OVER reference architecture scheme

The depicted system organisation is a general representation from which each test application will use some of the components or devices. As a general observation the video camera sensor is used on all car makers vehicle, the communication module, whose analysis is considered in the present document, will be present in one of the car manufacturer vehicle and in the PTW vehicle and also there will be a VRU module that implements the communication short range technology.

2.2.2. Localisation

Many of today's systems providing real-time localisation services (RTLS) are based on so called anchor points or base stations with a known position. Typically, those anchor points are located around the object to be localized (interpolation).
In difference to that, the WATCH-OVER topology previews extrapolation, as the VRU is far outside the anchor points at the car.

2.2.3. Communication

2.2.3.1. Topology

The communication system shall allow a two way communication between vehicles and VRUs. One VRU can communicate with several vehicles, and one vehicle can communicate with several VRUs. This means that broadcast, multicast and unicast addresses shall be used.

At any rate, the car shall be the central point of communication, as it comes with virtually unlimited resources of energy. In addition, it can be assumed that the on-board unit will not be as price sensitive as the wearable unit.
However, both on-board and wearable units shall have identical functionality regarding their Radio-Frequency-(RF)-modules. Due to energy and price reasons, it could be envisaged that the on-board unit comes with additional amplifiers on the input path (Low-Noise Amplifier, LNA) and output path (Power Amplifier, PA) to relief the wearable unit from power hungry transceivers.

2.2.3.2. Two way communication flow

The two way communication is required due to the following reasons:

- It should be possible to send out data from the VRU to the vehicles, so that the on-board unit can be informed about the position and the activity of the VRU. In addition, the RF-waves help to determine the local position of the VRU with regard to the vehicle.
- It should also be possible to send data from the vehicle to the VRU. This data might include
    - information about the actual results of the on-board unit, e.g. a warning to the VRU about a potential risk. As it can be presumed that the decision about a possible critical case is by far to complex to be taken in real-time by a low-cost VRU module, the decision about a possible warning should be shifted to the vehicle station. Due to the presumably very simple Human-Machine-Interface (HMI) of the VRU module, a simple alarm tone is anticipated. It should be kept in mind that the number of false alarms should be kept as low as possible.
    - control information to the wearable unit, e.g. detection of presence to increase the frame frequency.

2.2.3.3. Use case: VRU_1_to_Vehicle_1

This paragraph describes the simplest use case with regard to the communication system, as only one VRU and one vehicle is involved.

1. As a starting point, all vehicle units are in receiving mode, whereas a wearable unit periodically sends out data frame (cf. Figure 9). These data frames shall have
    - destination address: broadcast address
    - source address: own MAC address
    - a frame counter

   The data may already include information about the estimated own position. The frequency of the data frame submission from the wearable unit is relatively slow, in order to enhance power-down cycles to save energy. Before falling asleep, there is a certain time period, when the wearable unit switches to Receive-(Rx)-mode to listen to potential answer frames from the vehicle. However, it should be explicitly mentioned that in this state, the on-board unit does not receive the VRU's signals and therefore remains constantly in the Rx-mode.

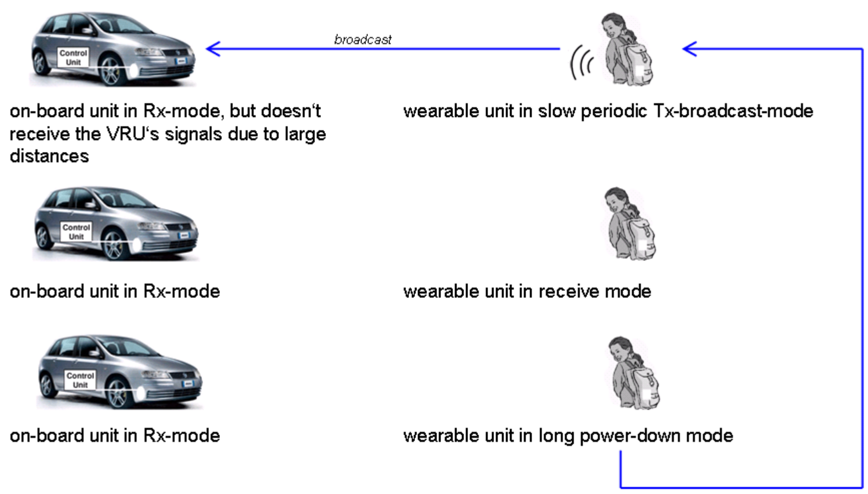

Figure 9: Initial state of communication between wearable and on-board unit

2. This state is left, as soon as the vehicle on-board unit successfully receives data frames from the VRU. In order to increase the stability of the system, one might demand the successful reception of at e.g. least 3 subsequent data frames. Then the vehicle sends out a data frame, which are received from the wearable unit during the Rx-period after the transmission of the broadcast message. Consequently, the wearable unit increases its transmission frequency to enhance the range estimation for the vehicle and decrease the latency for potential danger warnings. This flow is shown in Figure 10.

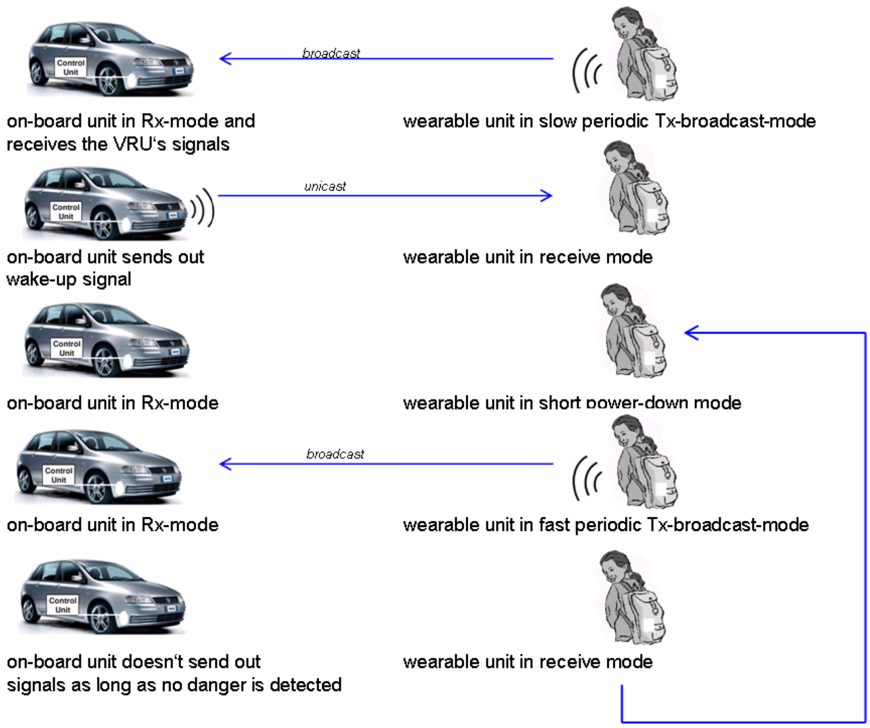

Figure 10: Detected state of communication between wearable and on-board unit

3. As soon as the on-board unit detects a potential risk, a warning is given via the Human Machine Interface (HMI) to the driver. In order to inform the VRU, the on-board unit transmits the corresponding data message with a unicast data frame (cf. Figure 11). This has the effect that the wearable unit remains constantly on and gives an alarm to the VRU.

This project has been co-funded by the European Commission DG-Information Society and Media in the 6th Framework Programme. The content of this publication is the sole responsibility of the project partners listed herein and does not necessarily represent the view of the European Commission or its services.

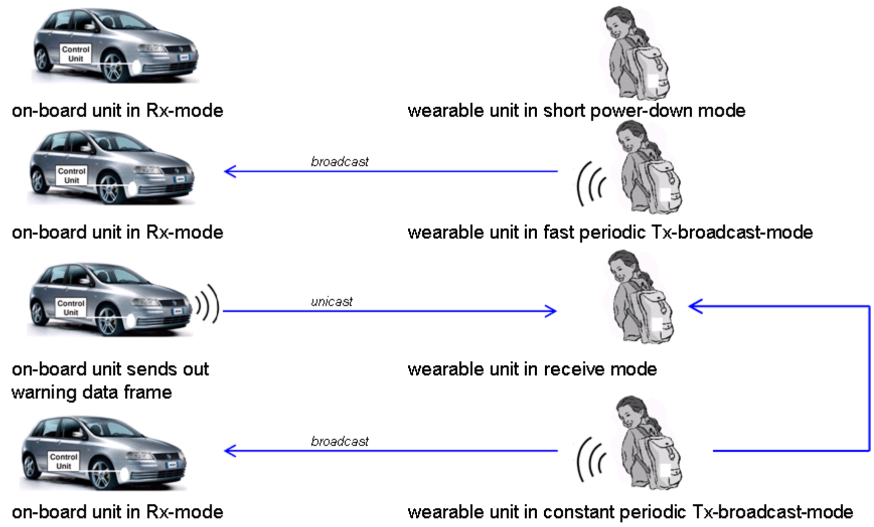

CE

Figure 11: Warning state of communication between wearable and on-board unit

2.2.3.4. Use case: VRU_N_to_Vehicle_1

The use case from ch. 2.2.3.3 can be extended to the communication of *N* VRUs with one vehicle (cf. Figure 12). There are several changes to the *VRU_1_to_Vehicle_1* use case:

- The data frames sent from the VRUs typically share a common channel, and shall therefore coordinate the channel access. Due to the character of the topology, a distributed coordination function (DCF) promises to be the best approach.
- The data frames from the vehicle to the VRU cannot be unicast any more, as presumably the latency would increase too much. Therefore, a broadcast wake-up message seems to be appropriate.

The warning message from the vehicle remains a unicast message, as it can be assumed that it refers to a limited number of persons, only.

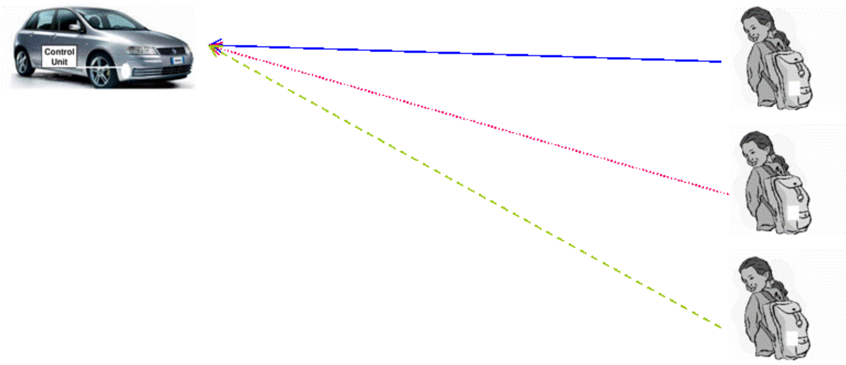

Figure 12: VRU_N_to_Vehicle_1 topology

This project has been co-funded by the European Commission DG-Information Society and Media in the 6th Framework Programme. The content of this publication is the sole responsibility of the project partners listed herein and does not necessarily represent the view of the European Commission or its services.

2.2.3.5. Use case: VRU_1_to_Vehicle_N

The use case from ch. 2.2.3.3 can also be extended to the communication of one VRUs with *N* vehicles (cf. Figure 13). There are also changes to the *VRU_1_to_Vehicle_1* use case:

- It must be made sure that the response frames (wake-up calls) from the vehicles don't interfere. A random back-off seems to be a suitable approach to this problem. A prolonged listen period of the wearable unit doesn't seem to be required, as it is enough to be woken up by one on-board unit.

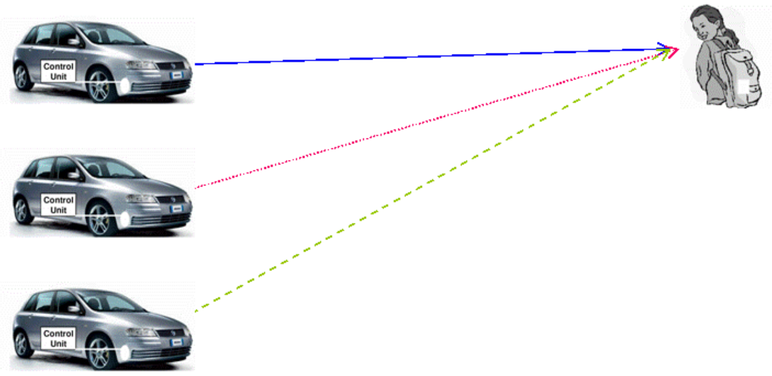

Figure 13: VRU_1_to_Vehicle_N topology

2.2.3.6. Use case: VRU_N_to_Vehicle_N

Based on the topologies described above, also *N* VRUs can communicate with *N* vehicles. The scalability of the system depends on the communication technology and its characteristics and is subject of detailed investigation throughout the project.

2.3. Security and Privacy

2.3.1. Introduction

Wireless communication is especially prone to security issues. This especially holds true for wireless ad-hoc systems, as they are envisaged within this WATCH-OVER project, as autonomous network management is of key importance to fufil the required timing behaviour.
It is common knowledge that security and privacy are amongst the most critical challenges for RF-based data communication in public traffic applications [91].
The most important parameters describing security for communication systems can be detailed along the aspects described in the next paragraphs.

2.3.2. Confidentiality

Although everybody can listen to the network traffic on the shared RF-medium, nobody can understand its content, unless he shares a common secret. Apart from the mere content of the content of the data frame, it is of key importance that the privacy of the nodes (and the persons wearing those nodes) remains anonymous.
In addition, it must be made sure that no tracking of persons or vehicles is possible.

2.3.3. Integrity

Furthermore, it is important that data frames cannot be manipulated, or – if manipulation cannot be ruled out – manipulation can be detected at the receiver.

2.3.4. Authentication and Authorisation

For many systems, it is important that only a predefined set of stations can take part in the communication. For the WATCH-OVER scenario, as many stations as possible shall participate in the mutual detection and localisation. However, it must be ensured that no malicious stations are allowed to the network.

2.3.5. Availability

Although availability is mainly linked to safety, it has its meaning for security as well. This is caused by the fact that the activities and the counter-measures are similar to other security aspects. Availability can be lost due to denial-of-service-attacks, and it can be enhanced through authentication, packet-filtering (firewalling) and intrusion prevention systems (IPS).

3. Investigation on Communication Techniques

3.1. Introduction

The following paragraphs describe the most important technologies and candidates, which promise to be a suitable solution for the WATCH-OVER use-cases. The basic selection is derived from the specification in ch. 2.1. They include

- all of the RF-technologies used in other eSafety projects [77],
- most of the RF-technologies used in other international projects for traffic safety [78]
- some additional technologies, not being considered in those projects, because they gained relevance only during the last months and few years.

The selection includes

- extensively standardised solutions with full hardware and software support, e.g.
    - IEEE802.15.4 (cf. ch. 3.2),
    - Bluetooth (cf. ch. 3.4),
    - and WLAN according to IEEE802.11 (cf. ch. 3.5)
- recently standardised solutions with early hardware and software support, e.g.
    - IEEE802.16 (Wireless Metropolitan Area Access, WiMAX, cf. ch. 3.6)
- upcoming standards with first hardware and software support, e.g.
    - IEEE802.15.4a – Chirp Spread Spectrum (CSS, cf. ch. 3.3)
- generic technologies, which might be applied in various standards and solutions, e.g.
    - Radio Frequency Identification (RFID, cf. ch. 3.7), and
    - Ultra Wide Band (UWB, cf. ch. 3.8).

Besides, other technologies for the detection of object exist. Namely radar should be mentioned, with specification for short- and for long-range. However, these technologies are not included into this survey due to two reasons:

- The cost issue for radar based systems is anticipated much higher than for communication based systems,
- It is known that hidden objects (as they are anticipated in D3.1 of the WATCH-OVER project), cannot be detected by radars.

All chapters follow the same structure. After a general description of the technology and the description of the standardisation bodies and the status of the standardisation, the technology itself is described. The most important part of the technologies is in the physical and the data link layer, which is described in more detail. In the end, the suitability for eSafety-related applications is evaluated. If the result of this evaluation is that the technology might be suitable, then it is examined with real-life tests. Those are described in ch. 5.

3.2. IEEE802.15.4

3.2.1. General Description

3.2.1.1. Overview

IEEE802.15.4 standard has been accepted and published in October 2003. First Silicon products are available since then, with a broad choice from basically all large semiconductor manufacturers. It is operating in an unlicensed, international frequency band, i.e. in the 868/915 MHz or in the 2.4 GHz, with data rates of up to 250 kb/s. The main characteristics of this standard are:

- low power consumption due to extensive power-down modes,
- fast wake-up and association,
- bidirectional communication,
- availability of network management and supervision functions, e.g. Energy Detection (ED) and Link Quality Indicator (LQI),
- solid modulation through spread spectrum technologies,
- low cost due to low complexity of RF-chip and peripherals, and
- low complexity of transceiver control, which can be implemented with a low power low-cost 8 bit microcontroller.

It was chartered to investigate a low data rate solution with multi-month to multi-year battery life and very low complexity. Potential applications are sensors, interactive toys, smart badges, remote controls, and home automation.
The IEEE 802.15.4 describes the PHY and MAC layers, i.e. layers 1 and 2 in a protocol stack. Figure 14 shows the elements of the protocols.

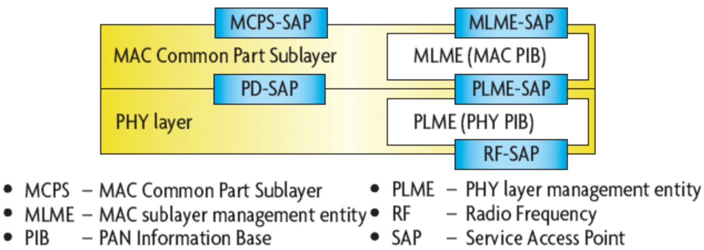

Figure 14: Elements of the IEEE802.15.4 Protocol Stack

3.2.1.2. Standardisation Bodies and Consortia

The IEEE802.15.4 belongs to the standard group of IEEE802.15 WPAN standards [2]. Thus, it is a member of the IEEE802-family, where other wireless systems are specified as well, e.g. IEEE802.11 WLAN [1] and IEEE802.16 WMAN [3].
These efforts are made within the IEEE 802 LAN/MAN Standards Committee within the Standards Association (SA) of the Institute of Electrical and Electronics Engineers, Inc. (IEEE) [4]. They develop Local Area Network standards and Metropolitan Area Network standards, in general. The most widely used standards are for the Ethernet family, Token Ring, Wireless LAN, Bridging and Virtual Bridged LANs. An individual Working Group provides the focus for each area.

The IEEE802.15.4 task group is enhanced through two work groups:

- The IEEE 802.15 Low Rate Alternative PHY Task Group (TG4a) for Wireless Personal Area Networks (WPANs) has defined a project for an amendment to 802.15.4 for an alternative PHY [62].
  The principle interest is in providing communications and high precision ranging / location capability (1 meter accuracy and better), high aggregate throughput, and ultra low power; as well as adding scalability to data rates, longer range, and lower power consumption and cost. These additional capabilities over the existing 802.15.4 standard are expected to enable significant new applications and market opportunities.
  802.15.4a became an official Task Group in March 2004; with its committee work tracing back to November 2002. The committee is actively drafting an alternate PHY specification for the applications identified in accordance with the project timeline.
  The baseline is two optional PHYs consisting of a UWB Impulse Radio (operating in unlicensed UWB spectrum) and a Chirp Spread Spectrum (operating in unlicensed 2.4GHz spectrum). The CSS option is described in more detail in ch. 3.3. Information on the Ultra Wide Band (UWB) technology can be found in ch. 3.8.
- The IEEE 802.15 task group 4b was chartered to create a project for specific enhancements and clarifications to the IEEE 802.15.4-2003 standard, such as resolving ambiguities, reducing unnecessary complexity, increasing flexibility in security key usage, considerations for newly available frequency allocations, and others [63].

3.2.2. Physical Layer

The physical layer of IEEE802.15.4 comes with several options in the 2.4 GHz and in the 868/915 MHz-band. Both options use a simple Direct Sequence Spread Spectrum (DSSS) approach in order to reduce susceptance to failure.

The world-wide available 2.4 GHz-band offers 16 channels with a maximum gross data rate of 250 kbps. The modulation scheme is shown in Figure 15.

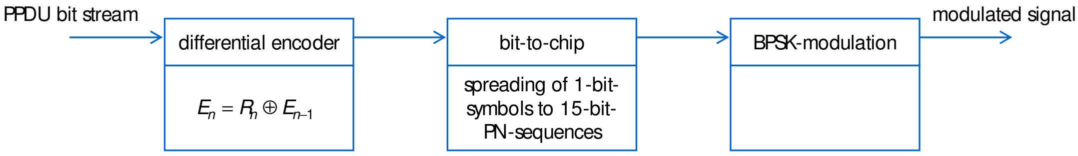

Figure 15: Modulation Techniques for IEEE802.15.4 in the 2.4 GHz frequency band

Additionally, there are two sub-Gigahertz-bands at 868.3 MHz with one channel and up to 20 kbps for Europe and at 915 MHz with ten channels and up to 40 kbps for USA/pacific. The modulation scheme is shown in Figure 16.

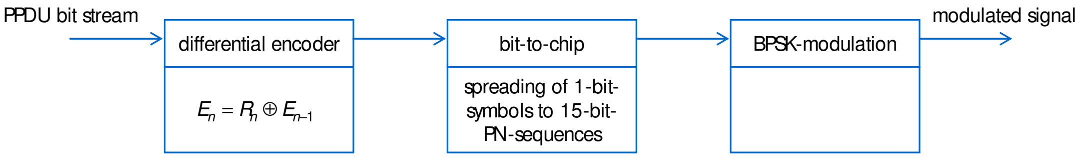

Figure 16: Modulation Techniques for IEEE802.15.4 in the 900 MHz frequency band

3.2.3. Data Link Layer

3.2.3.1. General Architecture

The data link layer of IEEE802.15.4 is subdivided into two portions, which is the common approach with IEEE802-data link layer standards.

- The lower portion is covered by the Medium Access Control (MAC) layer, which specifies the medium access, the frame format and the addressing scheme. When using ZigBee on top of IEEE802.15.4, it directly interfaces to the MAC-layer.
- IEEE802.2 describes the Logical Link Control-(LLC)-sublayer as an interface to higher layers is common to all IEEE802-sub-families (from Ethernet to WMAN). For interfacing IEEE802.15.4 MAC to LLC, a Service Specific Convergence Sublayer (SSCS) is provided. However, for all current approaches in attaching IP to IEEE802.15.4, SSCS is omitted [7] [6] [8] [9] [10].

3.2.3.2. Topologies

The MAC layer specifies two classes of devices, Reduced Function Devices (RFD) und Full Function Devices (FFD). An FFD may communicate with RFDs or other FFDs, whereas a RFD can be a slave to an FFD only. This shall help to implement RFDs on low cost 8-bit-microcontrollers.
With both device classes star- and peer-to-peer-topologies (cf. Figure 17) can be realised, which are referred to as Personal Area Networks (PAN). In such a PAN, one FFD acts as „PAN-coordinator“. It takes care for association and dis-association and may synchronise all stations with the help of beacon frames.

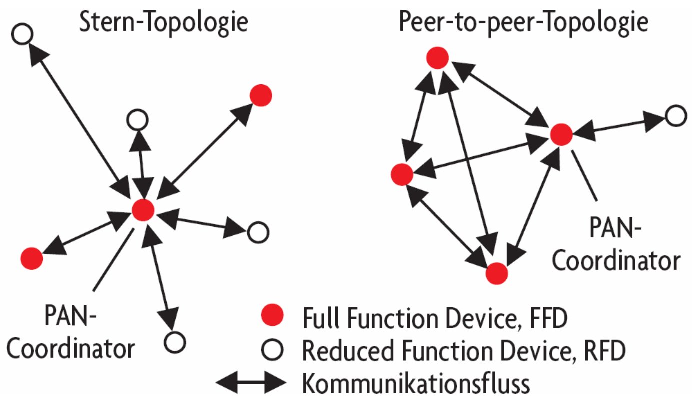

Figure 17: Star- and Peer-to-Peer-Topology for IEEE802.15.4 PANs [11]

3.2.3.3. Medium Access Control

The channel access of IEEE 802.15.4 follows a random Carrier Sense Multiple Access / Collision Avoidance (CSMA/CA)-scheme, which is basically known from the IEEE802.11. From experience with other wireless protocols, it implements several additional features:

- L2-acknowledgements are optional. Using acknowledgements (ACKs) allows the reliable transmission of frame between two nodes. Omitting ACKs helps to improve the net bandwidth.
- IEEE802.15.4 allows the definition of super-frames. All stations in a PAN are synchronised with the help of beacons from the coordinator. The super-frames may be sub-divided into three different types of time-slots (cf. Figure 18):
  - A contention free period (CFP) allows the transmission of periodical data streams, e.g. from regular sensor read-outs. Time-slots may be reserved for dedicated stations
  - The contention access period (CAP) period is open to the normal random access of all stations.
  - All stations may be switched to an inactive state for power saving.

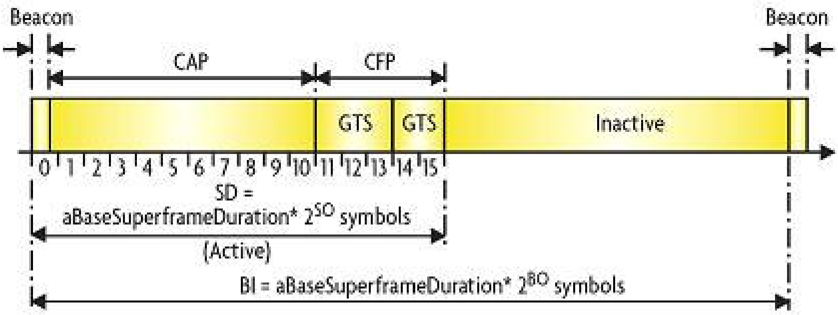

Figure 18: IEEE802.15.4 compatible beacon-enabled superframes

They combine classical CSMA/CA- and periodical traffic in Guaranteed Time Slots (GTS) as well as long inactive phases for power-saving [11]; BO stands for Beacon Order, SO for Superframe Order.

3.2.3.4. Frame Format

The format of IEEE802.15.4 frames is shown in Figure 19. Its maximum payload on PHY level amounts to 127 Bytes.

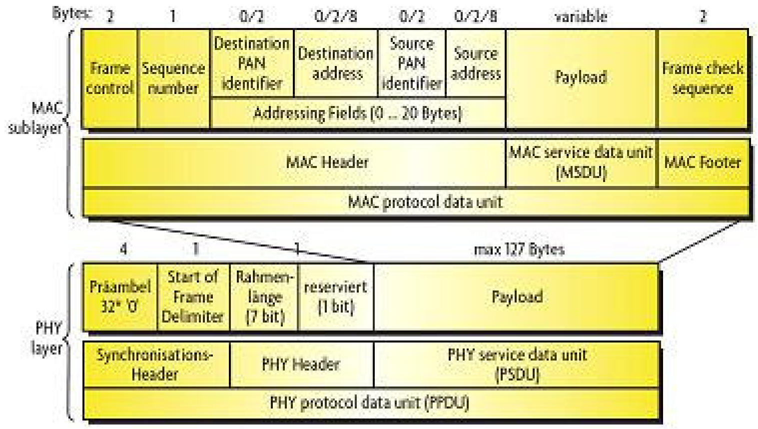

Figure 19: Format of IEEE802.15.4 frames on the PHY and the MAC layer [11]

3.2.3.5. Addresses

The physical MAC-addresses follow the rules for 64bit long IEEE Extended Unified Identifier (EUI-64) [57].

Due to the limited length of the MAC frame, logical MAC addresses can be used, as well. They have a length of 16 Bit and might be assigned during association. It is due to the length of these "short addresses" that one reads about 65,500 nodes within one network. This however, does not seem to be realistic for most of the installations. Apart from pure memory size aspects, in most cases address-wasting structural assignment schemes will be envisaged.

3.2.3.6. Security

The IEEE802.15.4-MAC envisages optional security services. The different options are shown in Table 1.

SUITE	**BITS OF INTEGRITY PROTECTION**	**ACCESS PROTECTION**	**ENCRYPTION**	**INTEGRITY**	**SEQUENTIAL FRESHNESS**
AES-CTR	0	Y	Y	N	Optional
AES-CCM-128	128	Y	Y	Y	Optional
AES-CCM-64	64	Y	Y	Y	Optional
AES-CCM-32	32	Y	Y	Y	Optional

SUITE	BITS OF INTEGRITY PROTECTION	ACCESS PROTECTION	ENCRYPTION	INTEGRITY	SEQUENTIAL FRESHNESS
AES-CBC-MAC-128	128	Y	N	Y	N
AES-CBC-MAC-64	64	Y	N	Y	N
AES-CBC-MAC-32	32	Y	N	Y	N

Table 1: Security options in IEEE802.15.4

CTR – Counter Mode; CCM - Counter Mode Encryption with CBC-MAC; CBC - Cipher Block Chaining; MAC – Message Authentication Code [11]

All are based on the Advanced Encryption Standard (AES) [12], which is commonly rated as one of the best symmetric encryption algorithms.
No rules for key generation or distribution are defined within the current IEEE802.15.4-standard.

3.2.4. eSafety relevant issues

Localisation services are not described within the generic IEEE802.15.4 standard. Proprietary extensions are developed [64] and available as products [65].

3.3. IEEE802.15.4a – Chirp Spread Spectrum

3.3.1. General Description

3.3.1.1. Overview

A chirp is a signal in which the frequency increases ('up-chirp') or decreases ('down-chirp') with time. It is commonly used in sonar and radar, but has other applications, such as in spread spectrum communications. Chirp signals can also be found in nature. They are used by dolphins and bats. A first patent was assigned for radar applications about 1940 to Prof. Huettmann. It was further developed by Sidney Darlington in 1947 ("Pulse Compression Radar“). Later it was patented by Canon for data transmission in fibre optic systems in the mid-90s.

3.3.1.2. Standardisation Bodies and Consortia

The Chirp Spread Spectrum (CSS) was adopted as one technology between two other UWB-based technologies for the IEEE802.15.4a working group in March 2005. The CSS version for IEEE802.15.4a operates in the ISM band at 2.45 GHz and achieves a maximum data rate of 2 Mbps. Each symbol is transmitted with a chirp pulse that has a bandwidth of 80 MHz (an effective bandwidth of 64 MHz is the result of a selected roll-off factor of 0.25) and a fixed duration of 1 µs. Thus, the theoretical system gain of CSS is 17 dB.

3.3.2. Physical Layer

3.3.2.1. CSS and MDMA

In a linear chirp, the instantaneous frequency f(t) varies linearly with time:

$$f(t) = f_0 + kt \,. \qquad \text{(Eq. 8)}$$

where f0 is the starting frequency (at time t = 0), and k is the rate of frequency increase or chirp rate. Chirp pulses are Linear Frequency Modulated (LFM) signals with constant amplitude. They fill out the total available bandwidth B over a predefined duration T. A time-bandwidth product (BT product) can be realised that is much larger than 1. The larger is the time-bandwidth product, the

This project has been co-funded by the European Commission DG-Information Society and Media in the 6th Framework Programme. The content of this publication is the sole responsibility of the project partners listed herein and does not necessarily represent the view of the European Commission or its services.

more resistant the chirp pulses are against disturbances during transmission. A corresponding time-domain function for a sinusoidal chirp is:

$$x(t) = \frac{x_0}{\sqrt{BT}} \sin\left(2\pi\int_0^t f(\tau)d\tau\right) = \sin\left(2\pi\left(f_0 + \frac{k}{2}t\right)t\right) \quad \text{(Eq. 9)}$$

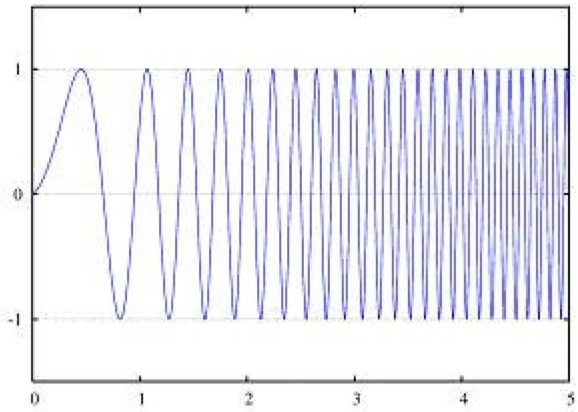

Figure 20: A linear chirp waveform

A sinusoidal wave that increases in frequency linearly over time (up-chirp)

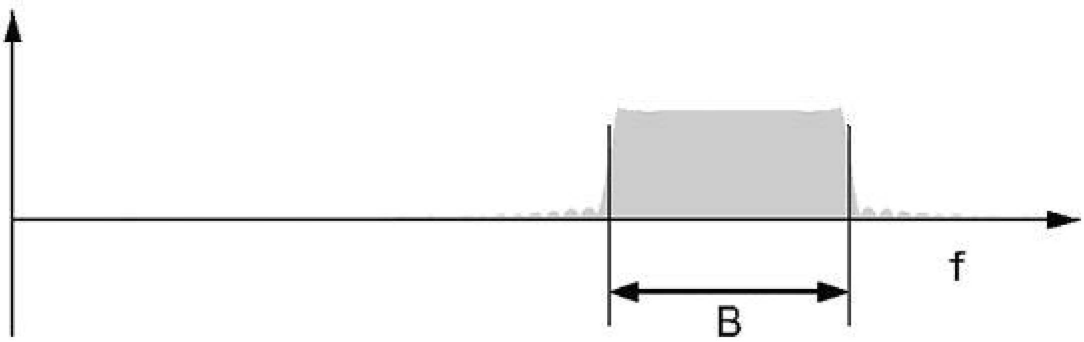

Figure 21: The spectrum of the LFM pulse in the frequency domain

In a geometric or exponential chirp, the frequency of the signal varies with a geometric relationship over time. In other words, if two points in the waveform are chosen, t_1 and t_2, and the time interval between them $t_2 - t_1$ is kept constant, the frequency ratio $f(t_2)/f(t_1)$ will also be constant. The frequency varies exponentially as a function of time:

$$f(t) = f_0 + k^t \quad \text{(Eq. 10)}$$

In this case, f0 is the frequency at t=0, and k is the rate of exponential increase in frequency. A corresponding sinusoidal chirp waveform would be defined by:

$$x(t) = \sin\left(2\pi\int_0^t f(\tau)d\tau\right) = \sin\left(\frac{2\pi f_0}{\ln(k)}\left(k^t - 1\right)\right) \quad \text{(Eq. 11)}$$

This project has been co-funded by the European Commission DG-Information Society and Media in the 6th Framework Programme. The content of this publication is the sole responsibility of the project partners listed herein and does not necessarily represent the view of the European Commission or its services.

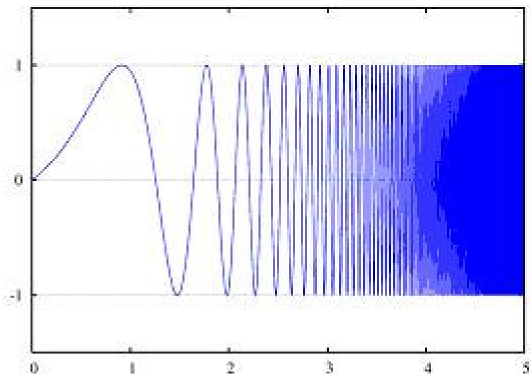

Figure 22: An exponential chirp waveform

a sinusoidal wave that increases in frequency exponentially over time

One speciality of the linear chirp can be used for the so called Multi Dimensional Multiple Access (MDMA). The power spectrum of the LFM pulses in the frequency domain is identical to sinc pulses. Ideal sinc pulses have the shortest possible duration at a given bandwidth B ("Shannon-Limit", very small BT product of 1). Through this, the sequence of the bits in the baseband is optimal. Furthermore, sinc pulses are generated relatively easily in the transmitter and can be detected with simple amplitude discrimination in the receiver.
The properties of sinc pulses in the time domain are shown in Figure 23. The power spectrum is identical to LFM pulses shown in Figure 21.

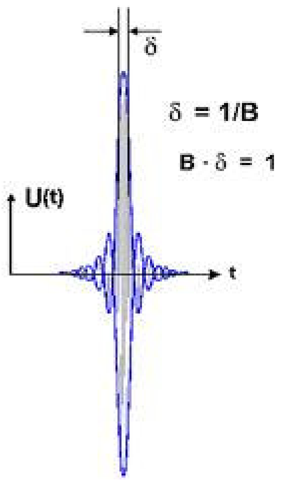

Figure 23: A sinc pulse in the time domain [13]

The sinc pulse in the baseband is described with

$$x(t) = x_o \frac{\sin(\pi B t)}{\pi B t} \qquad \text{(Eq. 12)}$$

The same spectrum is not the only similarity of chirp and sinc pulses. These pulses can be simply and reversibly transformed from one into the other with a Dispersive Delay Line (DDL), for example, a surface acoustic wave (SAW) filter. The combination of these two signals forms the basic principle of MDMA.
The fundamental signal forms of MDMA are shown in Figure 24.

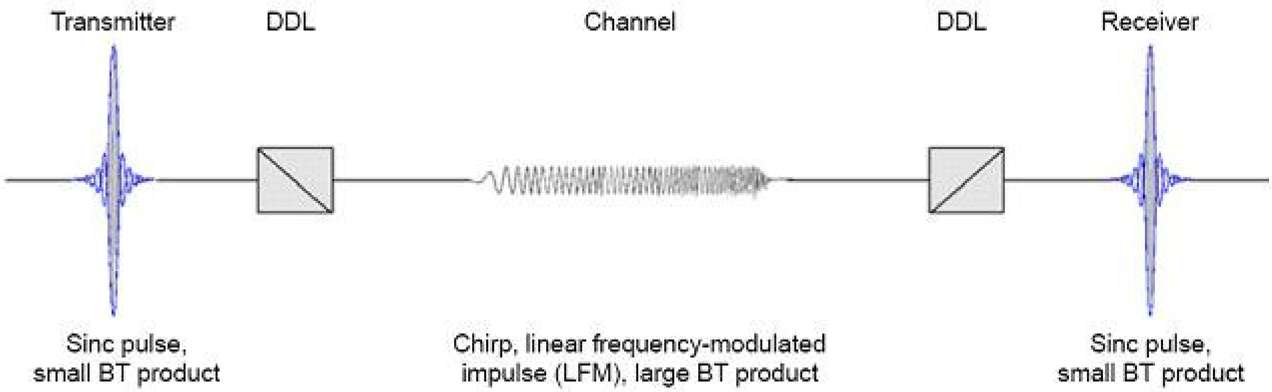

Figure 24: Signal forms of MDMA [13]

As a consequence, MDMA has optimal signal forms for both RF link and baseband, as MDMA it comes with an almost perfect spectrum of the chirp pulse (sharp edges on each side and flat in between). Thus, the available rectangle of bandwidth *B* and power *P* is almost completely filled (small shaping factor of almost 1). This results in a near optimal use of the channel capacity by chirp pulses.

Two parameters describe the characteristics of the MDMA signals:

- The spread factor is defined as bandwidth *B* divided by data rate *R*

$$\mathrm{v} = \frac{B}{R} \qquad \text{(Eq. 13)}$$

- The second parameter is the duration *T* in which the signal passes the full bandwidth (duration *T* of the chirp pulse). This technology is known as Time Spreading. This is the duration *T* of the chirp pulse divided by shortest symbol duration δ:

$$\psi = \frac{T}{\delta} = BT \qquad \text{(Eq. 14)}$$

Chirp Spread Spectrum or CSS is the first and simplest application of MDMA technology. It is customised for the requirements of battery–powered sensor networks with high data rates. In such applications, reliability of the transmission as well as low power consumption are of special importance.

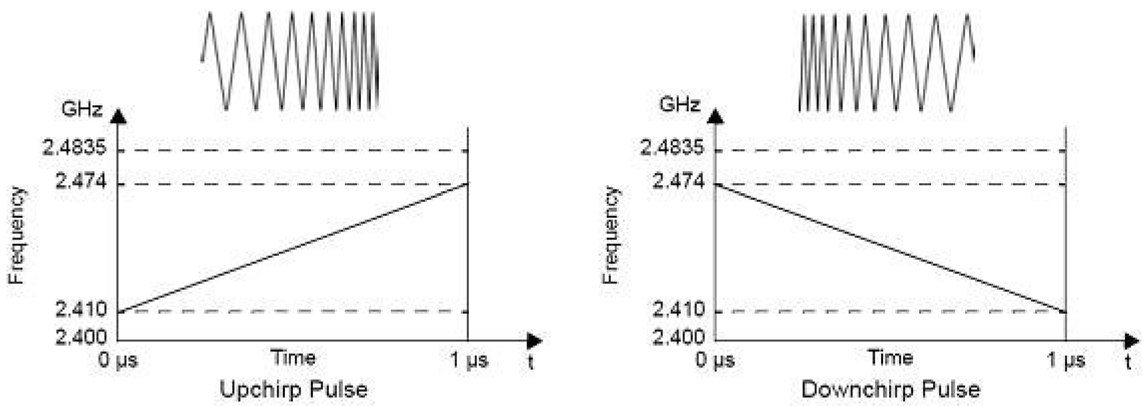

Figure 25: Upchirp and Downchirp pulses in time domain [85]

CSS does not take full advantage of the flexibility of MDMA, i.e. it does not superpose chirp pulses, to keep the system design as simple, cost-effective and power-saving as possible. The frequency and time spread of CSS are, as a special case of MDMA, equal to:

$$v = \psi \qquad \text{(Eq. 15)}$$

3.3.2.2. Chirp modulation

Chirp modulation is an enhancement to CSS, combining chirp-signals with Differential Phase Shift Keying (DPSK).
This approach was jointly developed by Nanotron Technologies GmbH and Orthotron from South Korea. It is denominated as „Differentially Bi-Orthogonal Chirp Spread Spectrum“ (DBO-CSS) [14].
In this case, four sub-chirps form one chirp symbol and four sequences of sub-chirps form a set of four chirp symbols. These four codes help to avoid interference between neighboured piconets, as each piconet uses only one of the four available codes. In addition, frequency division multiple access (FDMA) with three channels can be used. CSS supports 22 MHz mode with identical band plan and spectral mask for coexistence with WLAN systems in 2.4 GHz: Clear Channel Assessment prevents CSS from transmitting if channel in use by WLAN

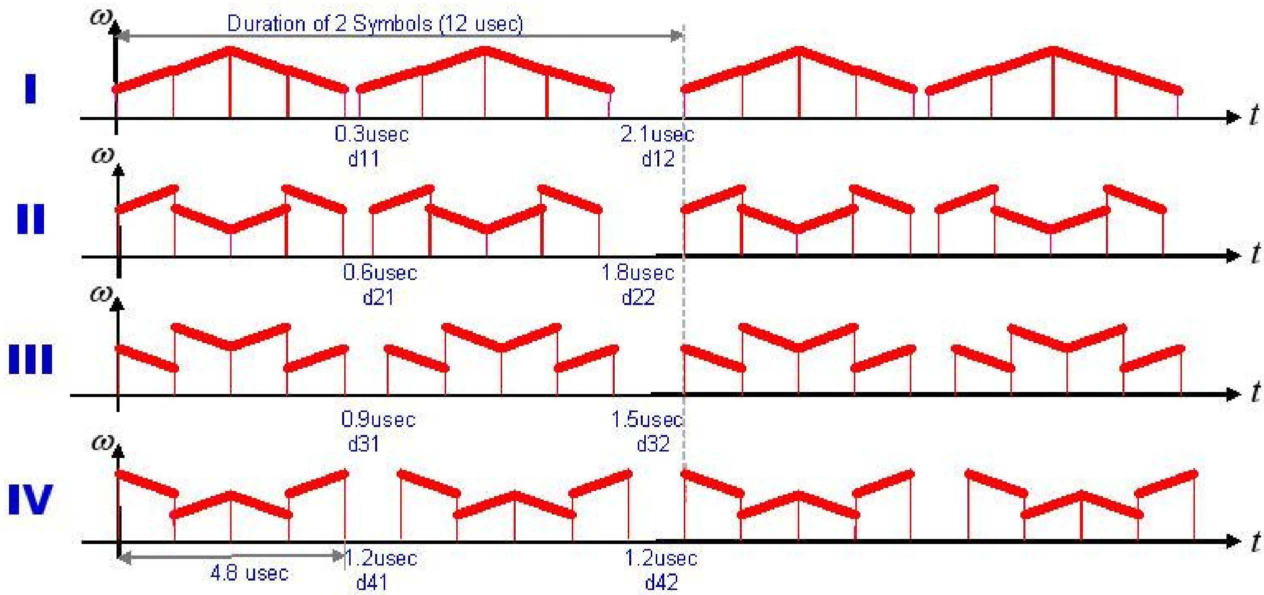

Figure 26: Chirp codes [14]

The chirp symbols are separated by time gaps of alternating duration. The average chirp symbol rate is 1/6 µs.

For the signal acquisition of the synchronisation header, DBPSK is applied, where 1 bit goes into one sub-chirp, and 4 bits form a chirp symbol.
For the data communication, DQPSK with bi-orthogonal coding is used. As 2 bits go into a sub-chirp, 8 bits form chirp symbol. Two bi-orthogonal codes yield two data rates

- Code rate 3/4 -> 3/4 * 8 bit / 6µs = 1 Mbit/s
- Code rate 6/32 -> 6/32 * 8 bit / 6µs = 250 kBit/s

3.3.3. Data Link Layer

For the IEEE802.15.4a version, the MAC layer remains identical to IEEE802.15.4(b).

3.3.4. eSafety relevant issues

In its Informative Annex D, IEEE 802.15.4a defines ranging modes. However, it does not prescribe the technology to be used, but gives semiconductor and system manufacturers the freedom to choose a ranging mode to suit their application.
In addition, IEEE 802.15.4a enables a portfolio of tag solutions from beacon-only tags to data-rich sensor tags.

3.4. Bluetooth V2.0

3.4.1. General Description

3.4.1.1. Overview

The activities around Bluetooth started in 1994, as the Mobile Communication Division of the Swedish manufacturer of mobile telecommunication equipment Ericsson prepared a feasibility study about a wireless replacement for the different cable connections around their mobile phones. As a result of this and many other activities, in 1998, the Bluetooth Special Interest Group (BSIG) was founded by IBM, Toshiba, Intel, Ericsson and Nokia. The first version 1.0 could be adopted already in 1999. A first revision 1.0b followed in December 1999. The first stable version, which was used for real product development, was adopted in February 2001, as V1.1.
In November 2003 the V1.2 added features like Adaptive Frequency Hopping (AFH), Extended SCO for a better voice quality, and Fast Connection Setup (FCS). The attempt to increase the bandwidth up to 4, 8 and 12 MBit/s in a V2.0 led to the adoption of Enhanced Data Rate in June 2004 with a gross bandwidth of 2.2 MBit/s.

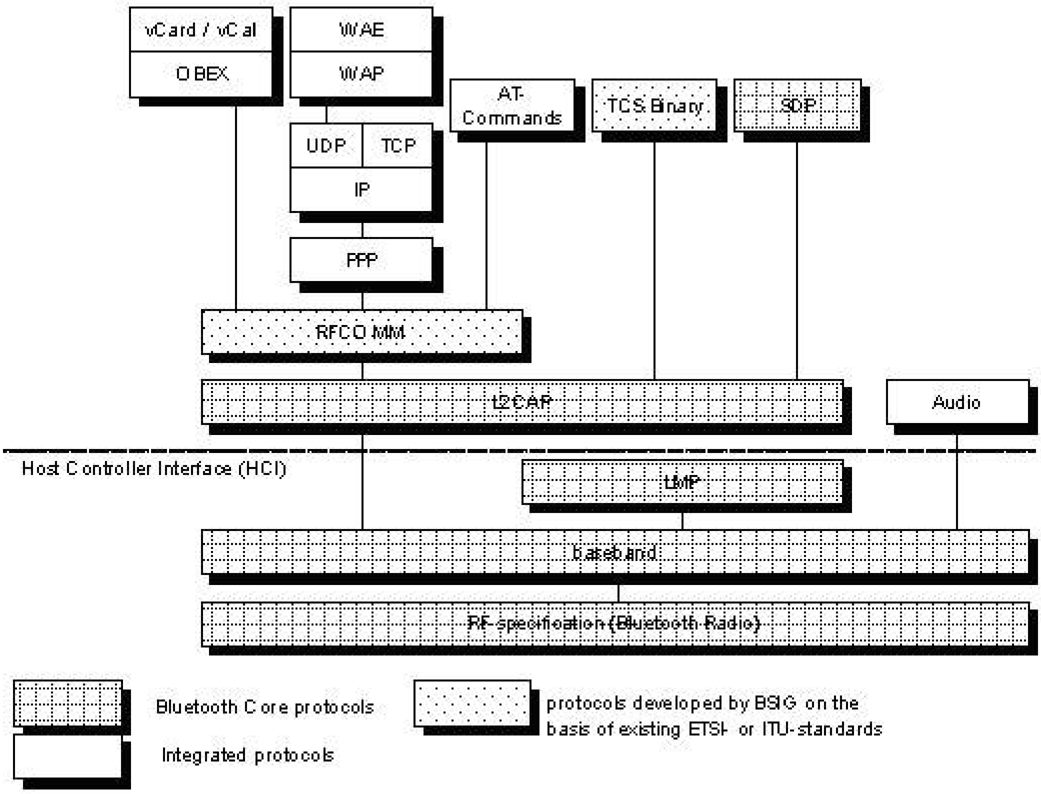

Figure 27: The Bluetooth Stack [23]

Some aspects should be highlighted in the context of the Bluetooth stack:

- Bluetooth covers all layers from physical to application layer.
- Application layer descriptions come with profiles.

The architecture of the stack is not conformant with the traditional OSI- and IEEE-layering, as can be seen in Figure 28. Various attempts have been made to translate the description to those legacy architectures. This was done e.g. in IEEE802.15.1 for physical and data link layer.

This project has been co-funded by the European Commission DG-Information Society and Media in the 6th Framework Programme. The content of this publication is the sole responsibility of the project partners listed herein and does not necessarily represent the view of the European Commission or its services.

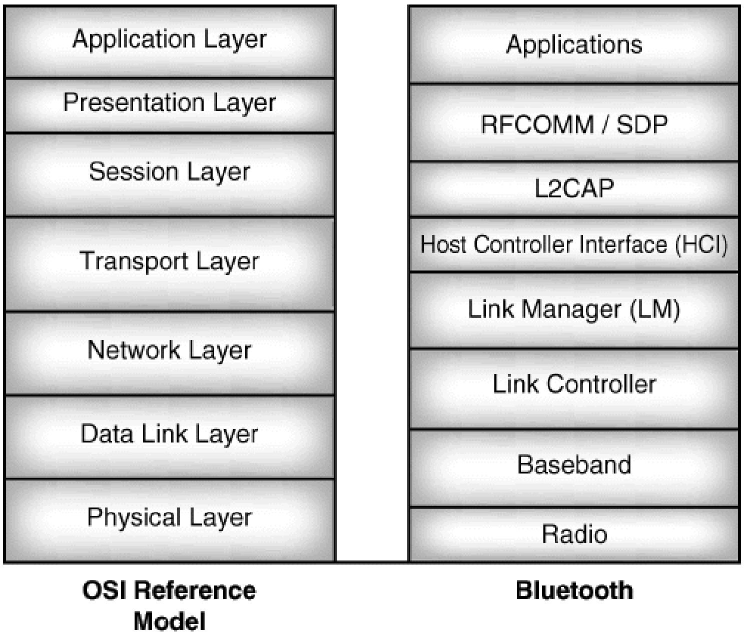

Figure 28: The Bluetooth Stack in comparison to OSI Reference Model [24]

The most common interface to attach a Bluetooth based system to an own application is the Host Controller Interface (HCI), which sits on top of the Link Manager (LM). The LM allows the full management of transparent links for the application.

3.4.1.2. Standardisation Bodies and Consortia

The Bluetooth Special Interest Group (BSIG) is a privately held, not-for-profit trade association. The Bluetooth SIG itself does not make, manufacture, or sell Bluetooth enabled products [25].
The SIG is composed of over 4,000 members who are leaders in the telecommunications, computing, automotive, music, apparel, industrial automation, and network industries, and a small group of dedicated staff in Hong Kong, Sweden, and the USA.
There are three membership tiers at the SIG: Promoter, Associate, and Adopter membership. The Bluetooth SIG's Promoter members include Agere Systems, Ericsson Technology Licensing AB, IBM Corporation, Intel Corporation, Microsoft Corporation, Motorola Inc., Nokia, and Toshiba Corporation.
Small associates (< $100 Mio USD annual turnover) pay an annual membership fee of $7,500 USD, large associates of $35,000 USD.

3.4.2. Physical Layer

Bluetooth is defined for the 2.4 GHz-band. It follows a Frequency Hopping Spread Spectrum (FHSS) scheme, with up to 79 non-overlapping frequency bands with a bandwidth of 1 MHz each (cf. Table 2). The number of channels is limited in Japan and some parts of France and Spain, which leads to a limited number of hopping sequences.

REGION	FREQUENCY BAND	HOPPING FREQUENCIES	# OF HOPPING SEQUENCES
USA	2.4000 - 2.4835 GHz	2.402 - 2.48 GHz	79
Europe	2.4000 - 2.4835 GHz	2.402 - 2.48 GHz	79
Japan	2.4710 - 2.4970 GHz	2.473 - 2.495 GHz	23
France	2.4465 - 2.4835 GHz	2.447 - 2.473 GHz	27
Spain	2.4450 - 2.4750 GHz	2.448 - 2.482 GHz	35

Table 2: Channel assignment of Bluetooth [23]

The actual sequence is calculated along a pseudo-random base sequence of numbers in the range between 0 and 78, where the minimum hopping distance is 6 channels.
If the base sequence is given as, for example:

$$b(i) = 0, 54, 70, 45 \qquad \text{(Eq. 16)}$$

the actual frequency of the k-th element is then calculated as

$$f_k(i) = 2402 + (b(i) + k) \bmod 79 \text{ [GHz]} \qquad \text{(Eq. 17)}$$

where mod is the modulo-function.

As Bluetooth follows a master-slave-architecture, the communication takes place amongst master and slave, where the master polls the slaves. The derived frequency behaviour is shown in Figure 29. Multislots frames remain on the same frequency.

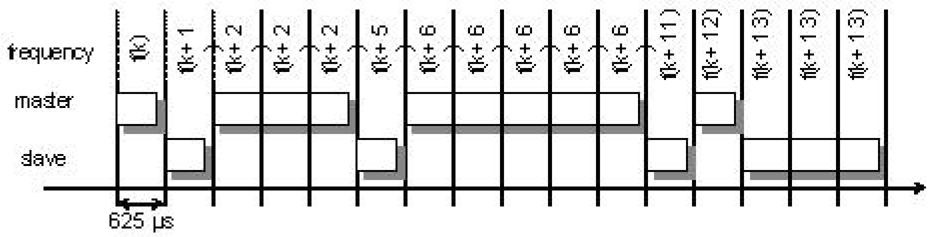

Figure 29: Assignment of Bluetooth channels for single- and multislot-frames [23]

In addition, Bluetooth defines different classes of output power, which then translate in different ranges.

	MAXIMUM OUTPUT POWER		POWER CONTROL	
Class 1	100 mW	20 dBm	4 … 20 dBm	mandatory
			-30 … 4 dBm	optional
Class 2	2,5 mW	4 dBm	-30 … 4 dBm	
Class 3	1 mW	0 dBm	-30 … 0 dBm	

Table 3: Classes of output power for Bluetooth devices [24]

3.4.3. Data-link layer

3.4.3.1. General architecture

The data-link layer architecture of Bluetooth follows a master-slave-architecture, which allows connection-oriented and connectionless communication (cf. Figure 30).
The synchronous connection oriented (SCO) link realises symmetrical point-to-point communication via circuit switching. The asynchronous connectionless link (ACL) sets up a connection between a master and one or more slaves. ACL-links allow packet-switching.

This project has been co-funded by the European Commission DG-Information Society and Media in the 6th Framework Programme. The content of this publication is the sole responsibility of the project partners listed herein and does not necessarily represent the view of the European Commission or its services.

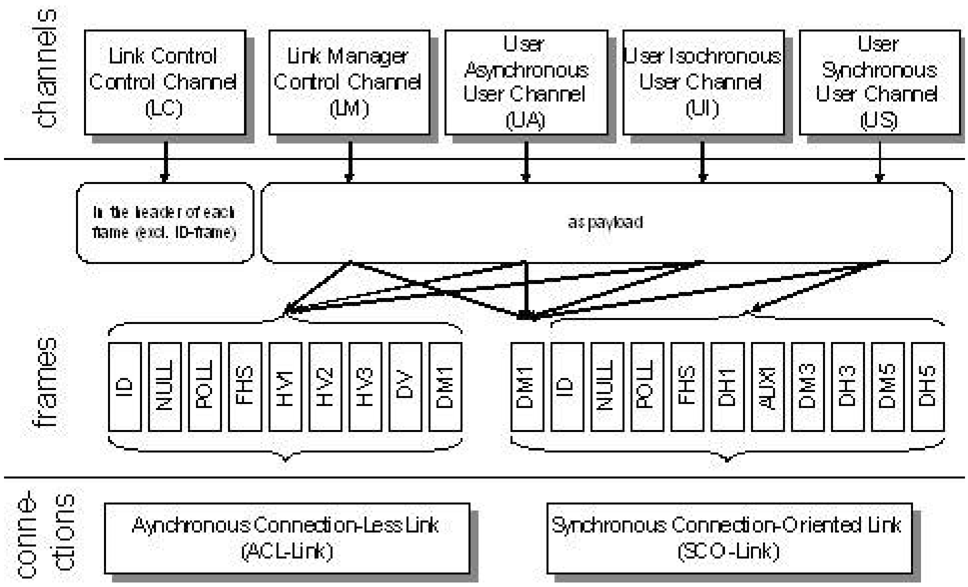

Figure 30: Assignment of Bluetooth channels to frame formats and connections [23]

Within these channels, different frame types can be assigned (cf. Table 4).

	Type	Payload Header [Bytes]	User Payload [Bytes]	FEC	CRC	Symmetric Max Rate [kbps]	Asymmetric Max Rate [kbps]	
							Forward	Reverse
Link Control Packets	ID	-	-	-	-	-	-	-
	NULL	-	-	-	-	-	-	-
	POLL	-	-	-	-	-	-	-
	FHS	-	-	-	-	-	-	-
ACL Packets	DM1	1	0 .. 17	2/3	yes	108,8	108,8	108,8
	DH1	1	0 .. 27	no	yes	172,8	172,8	172,8
	DM3	2	0 .. 121	2/3	yes	258,1	387,2	54,4
	DH3	2	0 .. 183	no	yes	390,4	585,6	86,4
	DM5	2	0 .. 224	2/3	yes	286,7	477,8	36,3
	DH5	2	0 .. 183	no	yes	433,9	723,2	57,6
	AUX	1	0 .. 29	no	no	185,6	185,6	185,6
SCO Packets	HV1	-	10	1/3	no	64,0	-	-
	HV2	-	20	2/3	no	64,0	-	-
	HV3	-	30	no	no	64,0	-	-
	DV*	1 D	10 V + 0 .. 9 D	no V 2/3 D	no (V) yes (D)	64,0 (V) + 57,6 (D)	-	-

* D denominates „data“, V „voice“

Table 4: Frame-Types for different connection types and speed and reliability trade-off [23]

3.4.3.2. Topologies

A Bluetooth network follows a master-slave-architecture. Based on this platform, the following topologies are described (Figure 31):

- A piconet has one master and one (mono-slave) or more (multi-slave) slaves. Due to the addressing scheme of piconet active member addresses, which are 3 Bits long (cf. Figure 32), it is possible to have up to seven active slaves in a piconet.
- When two or more independent, non-synchronised Bluetooth piconets overlap, a scatternet is formed in a seamless, ad-hoc fashion allowing inter-piconet communication. In this scatternet, more than one Bluetooth master is active. A master of one piconet can be a slave in another piconet.

This project has been co-funded by the European Commission DG-Information Society and Media in the 6th Framework Programme. The content of this publication is the sole responsibility of the project partners listed herein and does not necessarily represent the view of the European Commission or its services.

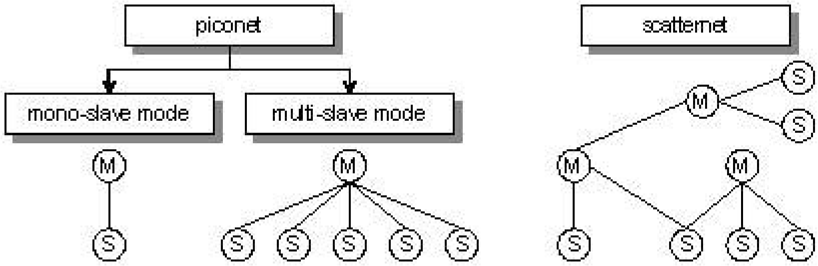

Figure 31: Bluetooth topologies [23]

While the Bluetooth specification stipulates the use of time-division multiplexing (TDM) for enabling concurrent participation by a device in multiple piconets, it leaves the choice of actual mechanisms and algorithms for achieving this functionality open to developers. Due to this high degree of freedom, scatternet was no option for versions 1.0 and 1.1. In v1.2, the situation improved, however, still significant imponderabilities remain [26]. Many Bluetooth scatternet formation protocols are proposed in the literature but most of them don't satisfy the desirable characteristics

3.4.3.3. Medium Access Control

Within a piconet, the medium access is controlled by the master. This enables support of full quality of service under two preconditions:

- the master provides the channel, e.g. capacities for the required SCO are available, and
- no significant error rate on the physical channel occurs.

3.4.3.4. Frame Format

The format of a Bluetooth frame is shown in Figure 32.

Access Code			Header Link Control (LC) information							Payload
72 b			54 b							0… 2745 b
Pre-amble	Sync Word	Trailer	AM_ADDR	Type	Flow	ARQN	SEQN	HEC		
4 b	64 b	4 b	3 b	4 b	1 b	1 b	1 b	8 b		
the following access codes are available ▪ CAC Channel Access Code ▪ DAC Device Access Code ▪ IAC Inquiry Access Code ▪ GIAC General Inquiry Access Code ▪ DIAC Dedicated Inquiry Access Code			Active Member Address	frame type	flow control	acknowledgeent indication	sequential numbering	header error check		

Figure 32: Bluetooth Frame Format [23]

3.4.3.5. Address Range

Bluetooth devices come with a physical address that follows the IEEE-scheme of 48 Bit addresses, as shown in Figure 33.

LSB											MSB
company_assigned						company_id					
LAP						UAP		NAP			
0000	0001	0000	0000	0000	0000	0001	0010	0111	1011	0011	0101

Figure 33: Bluetooth Address Format [25]

For active members in a piconet, a three bits long active member address (AM_ADDR) is assigned.

3.4.3.6. Security

The Bluetooth stack provides link layer security between any two radios. It consists of various elements, which were solely developed for Bluetooth based systems:

- The authentication is based on a symmetrical two-side Challenge/Response system, which follows the E1 algorithm.
- The encryption uses a symmetric stream cipher following the E0 algorithm.
- The key management and usage contains various elements. It cryptographic elements are applied for key generation with the E2 and the E3 algorithms.

User information can be protected by encryption of the packet payload; the access code and the packet header shall never be encrypted. The encryption of the payload shall be carried out with a stream cipher called E0 that shall be re-synchronised for every payload.
The stream cipher system E0 shall consist of three parts:

- the first part performs initialisation (generation of the payload key). The payload key generator shall combine the input bits in an appropriate order and shall shift them into the four LFSRs used in the key stream generator.
- the second part generates the key stream bits this shall use a method derived from the summation stream cipher generator attributable to Massey and Rueppel. The second part is the main part of the cipher system, as it will also be used for initialisation.
- the third part performs encryption and decryption.

The Massey and Rueppel method has been thoroughly investigated, and there exist good estimates of its strength with respect to presently known methods for cryptanalysis. Although the summation generator has weaknesses that can be used in correlation attacks, the high re-synchronisation frequency will disrupt such attacks [27].
Direct attacks to compromise the E0 cipher are known [28], however, remain at a significant complexity.

3.5. IEEE802.11 (WLAN)

3.5.1. General Description

3.5.1.1. Overview

In 1997, after a seven year development and approval process, the IEEE's Standards Association (SA) agreed on the first non-manufacturer-specific standard for transfer protocols in wireless local area networks. This is why the original standard is sometimes referred to as IEEE802.11-1997.

3.5.1.2. Standardisation Bodies and Consortia

The working group 11 within the IEEE802-activities is the core of the technological development. In the mean-time, an extensive list of task groups has been established within this working group (cf. Table 5).
In addition, other committees have been set up within this framework. Above all, the Wireless Ethernet Compatibility Alliance (WECA) should be mentioned, as it does not only certify the interoperability of IEEE802.11-compatible devices, but also introduces own profiles and standard. Incidentally, devices that comply with IEEE802.11 are marketed under the brand name Wi-Fi™ (Wireless Fidelity) [23].
Further committees deal with application specific aspects of Wireless LAN. The Wireless Industrial Networking Alliance (WINA) is a coalition of industrial end-user companies, technology suppliers, industry organisations, software developers, system integrators, and others interested in the advancement of wireless solutions for industry [44].
Dedicated Short-Range Communications (DSRC) was established to provide secure, reliable communication links between vehicles and infrastructure safety subsystems that can increase highway safety [30]. It will be described in chapter 3.5.4.2.

TASK GROUP	DESCRIPTION	STATUS
802.11a	definition of a PHY with OFDM modulation, carrier frequency of 5 GHz and gross data rates up to 54 Mbps	accepted as IEEE Std. 802.11a-1999
802.11b	definition of a PHY with DSSS modulation, carrier frequency of 2.4 GHz and gross data rates up to 11 Mbps	accepted as IEEE Std. 802.11b-1999
802.11b-cor1	corrections of the MIB (Management Information Base) from 802.11	in action
802.11c	supplementary MAC procedures to allow 802.1-compatible bridges	accepted as part of ISO/IEC 10038 (IEEE 802.1D)
802.11d	supplementary PHY definitions (e.g. channel selection, frequency hopping schemes, MIB) to new countries (Regulatory Domains)	accepted
802.11e	MAC-Enhancements for Quality of Service: EDCF and HCF; originally included security issues, which are since May 2001 in 802.11i	accepted
802.11f	InterAccess Point Protocol for Roaming and Load Balancing	accepted
802.11g	extension of 802.11b for higher data rates up to 54 Mbps	accepted
802.11h	Spectrum Managed 802.11a: european extension of 802.11 MAC-Protokolls and 802.11a PHY-Protokolls for 5GHz: TPC and DFS	accepted
802.11i	MAC-Enhancements for Enhanced Security: protocols for improved security and authentication	accepted
802.11j	Japanese extension of 802.11 MAC-Protokolls and 802.11a PHY-Protokolls for 5GHz, add'l band at 4,9 GHz	accepted
802.11k	Radio Resource Measurement Enhancements	in action
802.11m	complete review of other documents and determine a final list of work items	in action
802.11n	Standard for Enhancements for Higher Throughput for up to 300 Mbps	in action
802.11p	Wireless Access for the Vehicular Environment	in action
802.11r	Fast Roaming	in action
802.11s	ESS Mesh Networking	in action
802.11t	Wireless Performance Prediction	in action
802.11u	Wireless Interworking With External Networks	in action
802.11v	Wireless Network Management	in action

TASK GROUP	DESCRIPTION	STATUS
802.11w	Protected Management Frames	in action
802.11y	Contention Based Protocol Study Group	in action
WNG	Wireless LAN Next Generation Standing Committee	in action

Table 5: Task Groups within the IEEE802.11 standard

3.5.2. Physical Layer

Nowadays, the physical layer of IEEE802.11 comes with a large number of frequencies and modulation schemes. They are listed in Table 6.

	FREQUENCY SPREADING	MODULATION	FREQUENCY BAND	DATA RATES
802.11	Frequency Hopping Spread Spectrum (FHSS)	FSK / GFSK	2.4 GHz	1 / 2 Mbps
	Direct Sequence Spread Spectrum (DSSS)	BPSK / QPSK	2.4 GHz	1 / 2 Mbps
	Infrared with no practical implementations			1 / 2 Mbps
802.11a	Orthogonal Frequency Division Multiplex (OFDM)	BPSK / QPSK / 16QAM / 64 QAM	5 GHz	3 – 54 Mbps
802.11b	Direct Sequence Spread Spectrum (DSSS)	CCK	2.4 GHz	5.5 / 11 Mbps
802.11g	Orthogonal Frequency Division Multiplex (OFDM)	BPSK / QPSK / 16QAM / 64 QAM	2.4 GHz	3 – 54 Mbps
802.11h	Physical layer identical to IEEE802.11a			
802.11n	Multiple-Input Multiple Output (MIMO)		2.4 GHz	up to 300 Mbps

Table 6: Short description of the different physical layers within IEEE802.11

3.5.3. Data Link Layer

3.5.3.1. General Architecture

The data link layer definition of IEEE802.11 follows the legacy architecture of IEEE802, which splits the data link layer into two parts:

- the logical link control (LLC) sublayer, which handles the service definitions and traffic types together with a unified service access point structure for all higher layers.
- the medium access control (MAC) sublayer.

Apart from the horizontal layering, a vertical differentiation is made to enable the explicit and autonomous administration of the wireless network.

3.5.3.2. Topologies

An IEEE802.11-compliant network allows either ad-hoc-mode (which should be understood as infrastructureless mode), where all end devices can communicate directly, or infrastructure mode. In the infrastructure mode, access points (AP) are required for each communication. Each cell of an access point with the registered end devices is called basic-service set (BSS). If the access points (AP) are interconnected via a wired or wireless distribution system (DS), the whole architecture is denominated extended service set.

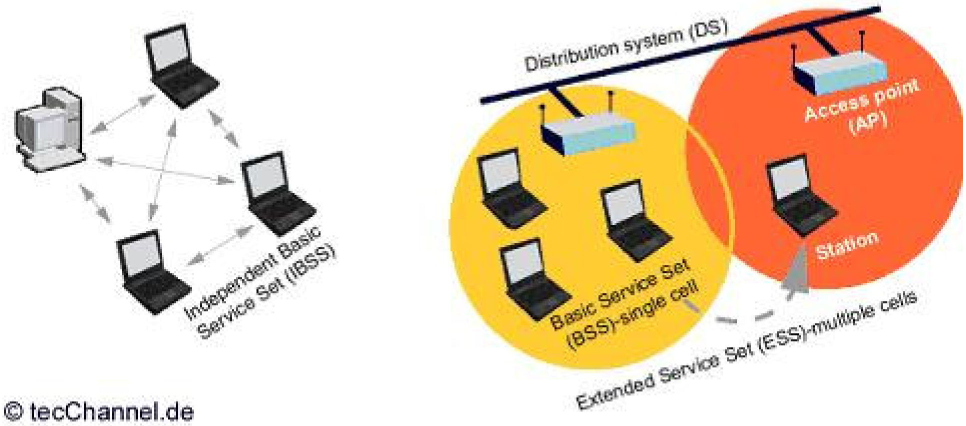

Figure 34: Architectures of the IEEE802.11 operation types [23]

In addition, flat topologies are envisaged within the working group IEEE802.11s. This working group currently describes a standardised way to use the access points as a mesh of traffic distribution as for the interconnectivity of the end devices (cf. Figure 35) [55]. The most prominent real-life example is the roofnet of MIT (see Figure 36) [56].

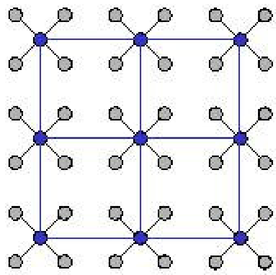

Figure 35: Topology example of a hierarchical 2D grid with local star topology [55]

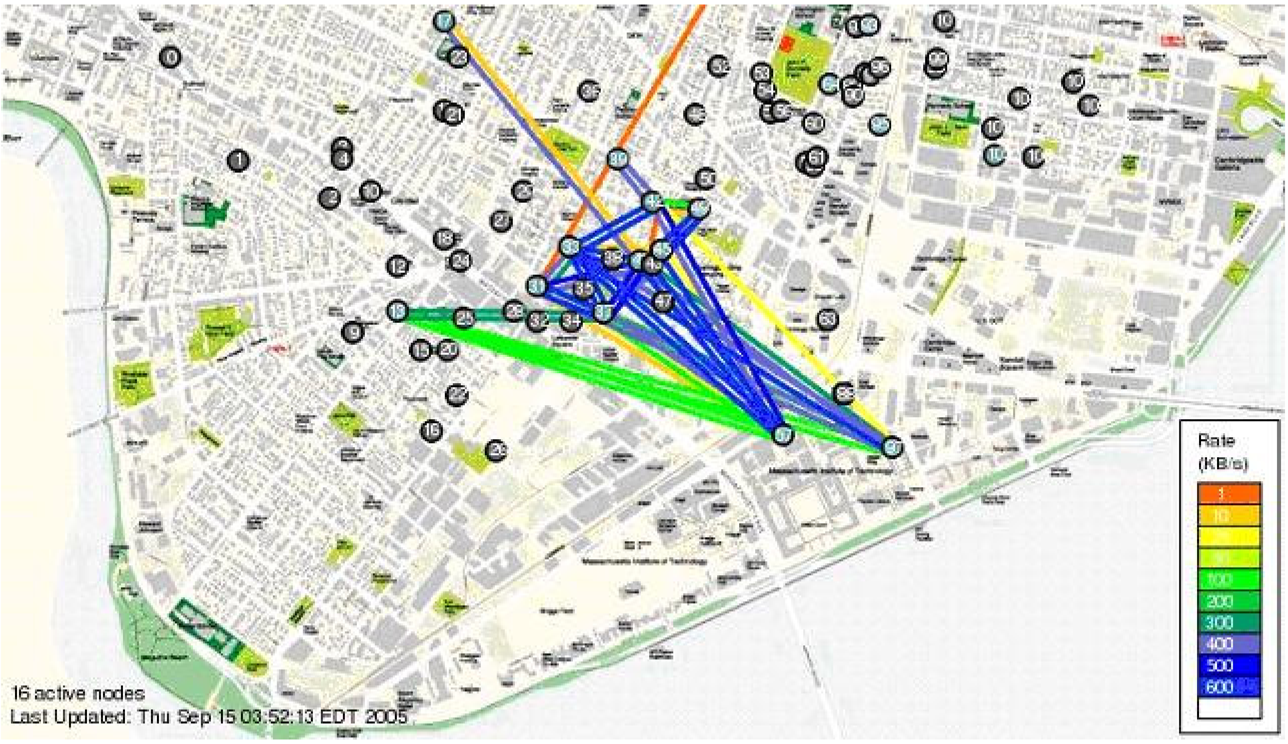

Figure 36: Topology example of a hierarchical 2D grid with local star topology [56]

3.5.3.3. Medium Access Control

The medium access control (MAC) described in IEEE802.11 is very closely related to the definition in the Ethernet standard. However, the wireless standard must also take into account the special features of its transmission routes. In particular, collision monitoring, as carried our on wired transmission media, is impossible for wireless transmissions due to the near/far problem [23].

Two access mechanisms, Distributed Coordination Function (DCF) and Point Coordination Function (PCF), are described within the standard for channel access. However, the PCF was never implemented and is currently replaced by the Hybrid Coordination Function (HCF).

The DCF is based on the CSMA/CA algorithm (Carrier Sense Multiple Access / Collision Avoidance). The collision avoidance attempts to prevent collisions, however, does not give any guarantee for collision-free communication.

It consists of the following elements:

- a random back-off algorithm after a collision has occurred,
- a random back-off algorithm after the channel has been detected busy,
- the optional RTS-CTS (request to send, clear to send) algorithm, which describes a two-way handshake for channel reservation.

3.5.3.4. Frame Format

The frame format follows the structure shown in Figure 37.

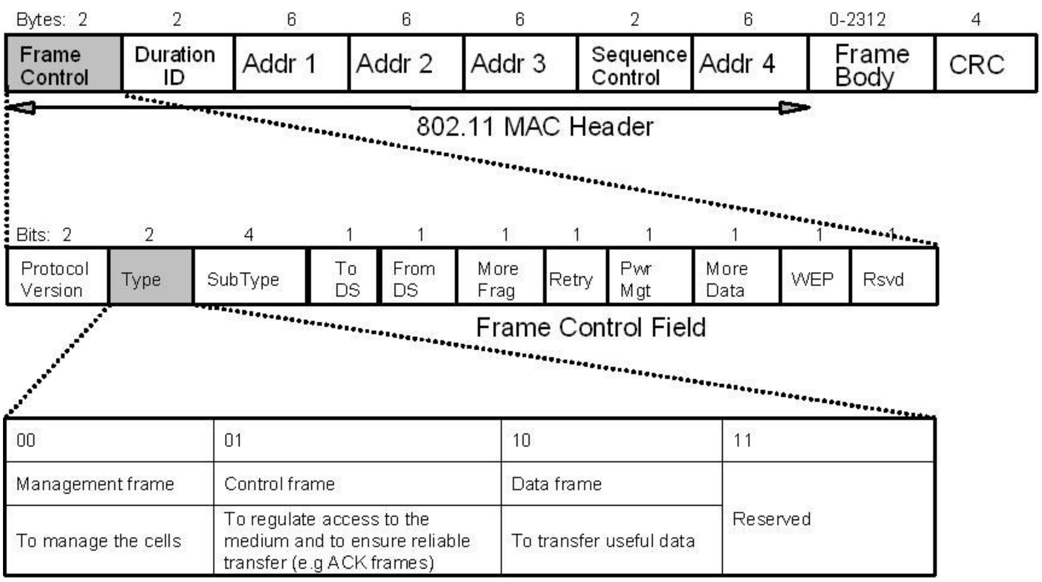

Figure 37: IEEE802.11 frame formats
(1) general MAC frame (2) formal of the control field in a data frame (3) possible frame types and their encoding [23]

3.5.3.5. Addresses

The IEEE802.11 uses standard 48-Bit long IEEE addresses [57].

3.5.3.6. Security

Security is a major stepping-stone for the success of wireless LAN networks. After the detection of major security flaws [58], a variety of security solutions were introduced. Those are described in the IEEE802.11i-standard and the WiFi Protected Access (WPA) specification of the WiFi Alliance. They include:

- improved encryption scheme, i.e. the AES128-block cipher is made an option in IEEE802.11i.

- improved key usage also in case of RC4-strame (*Temporal Key Integrity Protocol*, TKIP)
- longer Initialisation Vectors (IV) to reduce the risk of replay attacks,
- avoidance of weak key through the preselection of Initialisation Vectors (IV),
- the integration into overall network security mechanisms through IEEE802.1x and centralised authentication.

3.5.4. eSafety-relevant issues

3.5.4.1. IEEE802.11p

The task group IEEE802.11p describes physical (PHY) and medium access control (MAC) layers Wireless Access in Vehicular Environment (WAVE) within the 5 GHz range.
The ballot of March 2006 did not achieve the required majority [89], which leads to a current revision of the previous activities.

3.5.4.2. DSRC

Dedicated Short-Range Communications (DSRC) is an emerging technology with intriguing performance and benefits that provides a critical communication link for future Intelligent Transportation Systems. DSRC technology will provide secure, reliable communication links between vehicles and infrastructure safety subsystems that can increase highway safety [30].

The Dedicated Short Range Communication (DSRC) standards group devised a channel switching scheme that includes a control channel in order to support a site licensing system for roadside transponders, a general priority system for applications, and still use the full spectrum of the DSRC band. The spectrum is divided into several channels: control channels and service channels. The basic concept is that the control channel will support very short announcements or messages only, and any extensive data exchange will be conducted on service channels [29].

“DSRC” has different meanings, different technical characteristics and different operating frequencies around the world in the transportation sector. It is closely linked with IEEE802.11p, which describes the lower layers of DSRC.

In most parts of the world, DSRC is generally used only for electronic tolling collection (ETC) and access control applications. In the United States, DSRC/WAVE operates at 5.9 GHz [30]. For the US market, the DSRC activities consist of various elements, which together cover all layers of the communication reference model, as it is shown in Figure 38 [29].

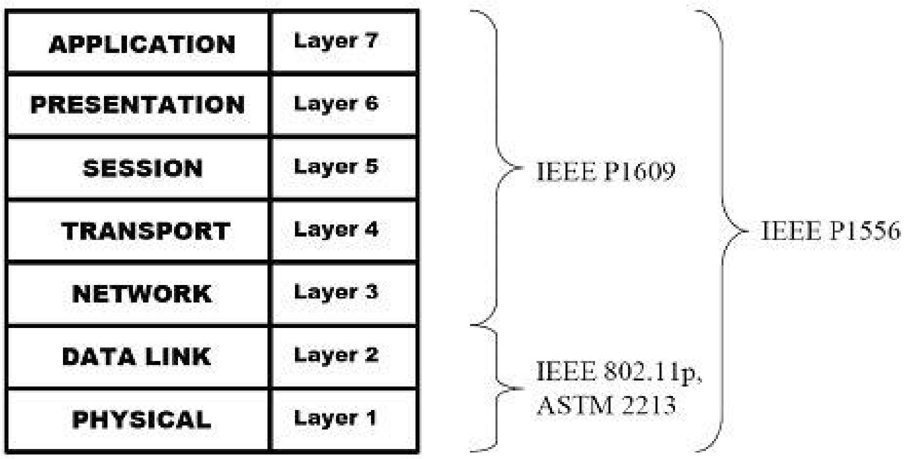

Figure 38: The elements of DSRC within the OSI reference model [29]

This project has been co-funded by the European Commission DG-Information Society and Media in the 6th Framework Programme. The content of this publication is the sole responsibility of the project partners listed herein and does not necessarily represent the view of the European Commission or its services.

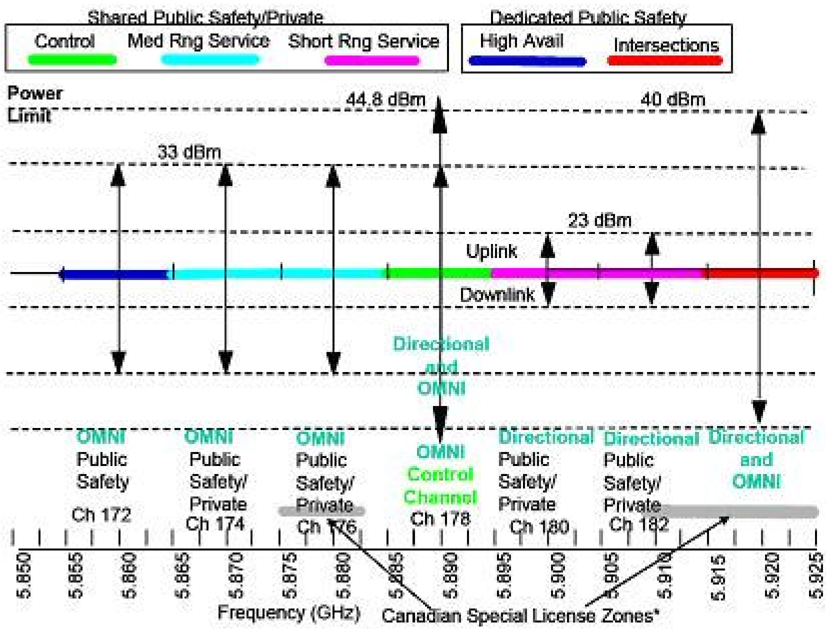

Figure 39: Frequency channel and antenna plan for IEEE802.11p in the FCC regions [30]

- 5.9GHz DSRC is a wireless communication protocol similar to IEEE 802.11a; however, it operates within the 5.9GHz band and is dedicated solely to automotive applications. IEEE 802.11p addresses the physical layer and medium access control layer (MAC) called 802.11p module.
  The FCC ruling for IEEE802.11p Wireless Access in Vehicular Environment (WAVE) is based on the ASTM (American Society for Testing and Materials) standard E2213-03 where the 5.9 GHz (5.850-5.925) band is divided into seven 10 MHz channels (one control and six service) at power levels up to 44.8 dBm (30 Watts) EIRP for road side units (RSUs) and 33 dBm (2 Watts) EIRP for on board units (OBU).
  The channel assignment for IEEE802.11p within the FCC-regions is shown in Figure 39.

- The IEEE P1609 Upper Layer WAVE Standards describe the higher layer and currently consist of the elements, shown in Table 7. The status of the different activities is also shown.

P1609.1/D17	WAVE Resource Manager	Unapproved IEEE Draft Standard
1609.2-2006	Security Services for Applications and Management Messages ("Application Layer")	IEEE Trial-Use Standard
P1609.3/D18	Networking Services ("IP Interface")	Unapproved IEEE Standard
P1609.4/D07	Multi-Channel Operation ("MAC Extensions")	Unapproved IEEE Standard

Table 7: Elements of the IEEE P1609 standard

- The IEEE P1556 had the purpose to define the essential protective mechanisms for DSRC applications and communications technology. The main benefit is to offer confidentiality, integrity, and availability protection for the DSRC communications link and offer security services. However, the 1556 standards project is no longer endorsed by the IEEE [31].

3.6. IEEE802.16 (WiMAX)

3.6.1. General Description

3.6.1.1. Overview

It is already for some decades, that microwave- and laser-links allow high-speed point-to-point-(P2P)- and point-to-multipoint-(P2MP)-connectivity. However, there were only proprietary systems in the past. The objective of IEEE802.16 is the standardisation of these BWA-systems for cost reduction, market and product enhancement.
The technology promises data rate of up to 75 MBit/ s across distances of up to 50 km. Thus, WiMAX is positioned as competing technology to

- high speed mobile networks, i.e. Universal Mobile Telecommunications System (UMTS) with High-Speed Downlink Packet Access (HSDPA) or High-Speed Uplink Packet Access (HSUPA)
- high speed wired access networks, i.e. ADSL-technologies, with a special focus on rural areas with a low-density wired infrastructure,
- meshed WLAN-networks, as they are envisaged from the WLAN IEEE802.11s task group,
- future activities from the IEEE802.20 working group, which goes for Mobile Broadband Wireless Access. However, this group is still in its early phase.

WiMAX is positioned on the Wireless Metropolitan Area Network (WMAN) level. For wired networks, this level was mainly replaced by high-speed Ethernet networks.

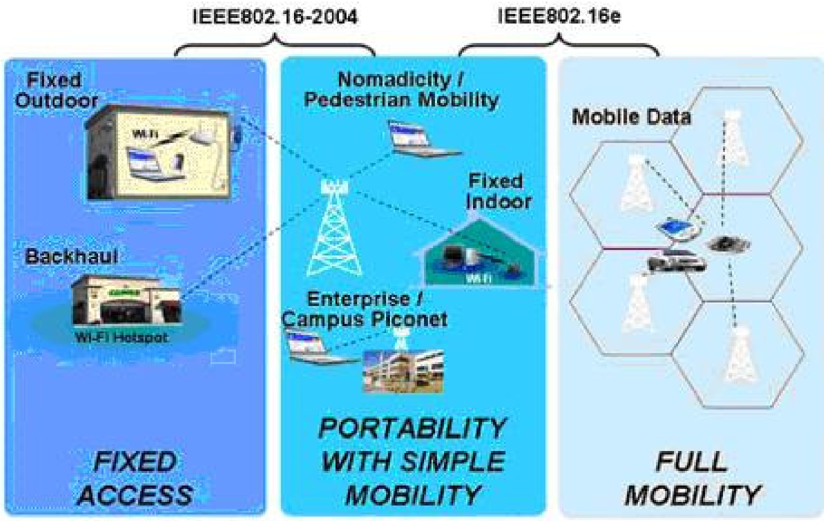

Figure 40: Architectures and Applications of IEEE802.16 (WiMAX) [30]

3.6.1.2. Standardisation Bodies and Consortia

The work group 16 of the IEEE802 activities [43] deals with the Broadband Wireless Access (BWA) for stationary and mobile nodes.
In the field of marketing and compatibility tests, the standard is supported by the WiMAX-Forum [42]. WiMAX stands for "Worldwide Interoperability for Microwave Access". This non-profit organisation (NPO) has already more than 400 company members (as of Jan 2007).
Although the activities started in the late nineties only, IEEE802.16 comes with a plethora of elements and options. This is mainly caused by the fact that this standard derives from proprietary solutions.

- The first standard was proposed in December 2001. It is the first standardised approach for Wireless Metropolitan Area Network (WMAN). The final standard was accepted in April 2002. It covers frequencies between 10 and 66 GHz, and is thus limited to applications with Line of Sight (LOS) only.
- The WiMAX-Forum was founded b/o 2003 under the auspices of Intel, who plan to us the standard for portable end devices. The enhancements IEEE802.16a and IEEE802.16REVd were accepted in the same year. Both were united to IEEE802.16-2004 in July 2004. Frequencies between 2 and 11 GHz shall enable connectivity at lower cost and with Near-Line of Sight-characteristics.
- The next element, which is due in 2006, shall support fully mobile (nomadic) nodes without LOS. It shall support data rates up to 15 MBit/s and ranges up to 5 km. In addition, roaming shall be enabled.

demonination	IEEE802.16	IEEE802.16a IEEE802.16REVd IEEE802.16-2004 (WiMAX)	IEEE802.16e (WiMAX)
date of acceptance	Dec 2001	Jan 2003 - Jul 2004	?
first products	available	m/o 2005	starting in 2006
frequency bands	10-66 GHz	2-11 GHz	0,7-6 GHz
channel characteristics	LOS	Near LOS, Non LOS	Non LOS
max. data rate	32 - 134 Mbit/s in channels of 28MHz	up to 75 Mbit/s in channels of 20MHz	up to 15 Mbit/s in channels of 5MHz
bandwidth	20, 25, 28MHz	scalable between 1,5 and 20MHz	
Modulation	QPSK, 16QAM, 64QAM	OFDM256, OFDMA 64 QAM, 16QAM, QPSK, BPSK	OFDM256, OFDMA 64 QAM, 16QAM, QPSK, BPSK
subscriber station	fixed	fixed outdoor antenna, limited use for mobile and indoor applications	(nomadic) mobile
max range	variable, ? 100km	up to 50km	up to 5km
		typically 15km with outdoor antenna, 5km with indoor antenna	typically 1,5km

Table 8: IEEE802.16 and its derivatives [59]

ETSI is also an important stepping stone towards WiMAX. It is planned to harmonise the HiperMAN-approach from the BRAN-project (Broadband Radio Access Network) with the IEEE802.16-architecture to achieve interoperability.
For the IEEE802.16-2004, various licence exempt and licensed frequency bands are envisaged. The most important candidates are shown in Table 9.

REGION	LICENSED FREQUENCIES	LICENCE EXEMPT FREQUENCIES
Northern America, Mexico	2.5 GHz	5GHz
Central and South America	2.5 GHz, 3.5 GHz	5GHz
Western and Eastern Europe	3.5 GHz	5GHz
Middle East and Africa	3.5 GHz	5GHz
Asian Pacific	3.5 GHz	5GHz

Table 9: International availability of frequency bands for the IEEE802.16-2004 [59]

In Europe, European Telecommunications Standards Institute (ETSI) has planned the 3.5 GHz band for licensed WiMAX solutions. Originally, this band was dedicated to wireless public local loop (WPLL) applications. The policy of the European governments with regard to the licensing of these frequencies currently is very inhomogeneous. In many countries the process is still ongoing.

The licence-free bands correspond to the 5 GHz frequencies of IEEE802.11a and h. This might lead to increased coexistence issues in this band, as well.

This project has been co-funded by the European Commission DG-Information Society and Media in the 6th Framework Programme. The content of this publication is the sole responsibility of the project partners listed herein and does not necessarily represent the view of the European Commission or its services.

3.6.2. Physical Layer

The IEEE802.16-2004 standards use an ***O**rthogonal **F**requency **D**ivision **M**ultiplex* (OFDM) approach to achieve a high spectral efficiency of up to 3 bits/s/Hz. The overall approach shows a number of improvements over IEEE802.11:

- Within the IEEE802.16-2004 256 subcarriers are used, whereas IEEE802.11 uses only 64 subcarriers. The larger the number of subcarriers, the longer the duration of each symbol. This severely helps to alleviate deep fading due to multi-path effects.
- The *Guard Time* or *Cyclic Prefix* (CP) defines the allowed transition time between symbols. For IEEE802.16 the CP can be selected amongst 1/32, 1/16, 1/8 and 1/4 for optimum adaptation to the channel characteristics.
- Based on these and other mechanisms, the IEEE802.16 can handle a delay spread of up to 10 µs. The corresponding value of IEEE802.11 is only 90 ns.

Furthermore, the 802.16e PHY-Layer allows OFD Multiple Access (OFDMA), which describes a further channel segmentation for Up- and Downlink-channels, as well as the usage of different coding algorithms for the different subchannels. In addition, Scalable OFDMA (SOFDMA) allows the adaptation of the modulation scheme to the channel quality, i.e. QPSK, 16QAM or 64QAM, and a dynamic assignment of subcarriers to subscribers (cf. Figure 41).

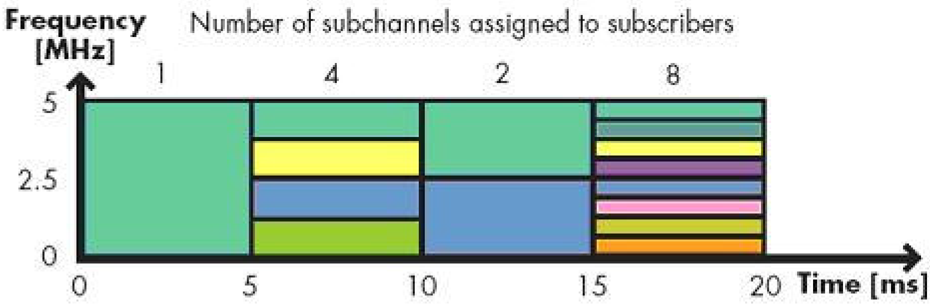

Figure 41: Scalable OFDMA: dynamic assignment of subcarriers to subscribers [61]

In addition, various improvements can be achieved through the use of antenna technology, which is seamlessly integrated into the PHY management.

Channel assignment can be performed with the following architectures:

- Up- und downlink-channels are operated simultaneously on different frequencies in the case of Frequency Division Duplexing (FDD).
- In the case of Time Division Duplexing (TDD) both up- and downlink channels sequentially use the same frequency.
- In addition, Half-FDD (H-FDD) is defined with a fixed downlink frequency.

3.6.3. Data Link Layer

3.6.3.1. General Architecture

The data link layer has to cope with the overall requirements of handling very different data streams with special attention to Quality of Service (QoS) based operation. QoS shall be enabled through

- alleviation of the coexistence issue with the help of Dynamic Frequency Selection (DFS) and Automatic Power Control (APC),
- the improvement of the Bit Error Rate (BER) through Forward Error-Control (FEC), e.g. Reed-Solomon- and Trellis coding,
- reliable transmission through Automatic Retransmission Request (ARQ), and
- seamless integration of Layer 2 QoS-services, such as the Grant Request Protocol and the support of differentiated services (DiffServe).

This project has been co-funded by the European Commission DG-Information Society and Media in the 6th Framework Programme. The content of this publication is the sole responsibility of the project partners listed herein and does not necessarily represent the view of the European Commission or its services.

3.6.3.2. Topologies

In last mile, IEEE802.16 offers infrastructure based star topologies. Figure 42 shows the overall architecture.
Starting with IEEE 802.16a, mesh-networks are made possible to allow direct communication between subscriber stations. Figure 43 shows the corresponding infrastructure.

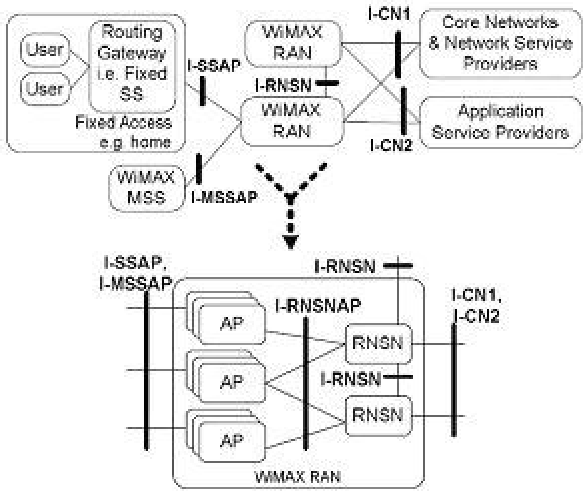

Figure 42: IEEE802.16 reference architecture [60]

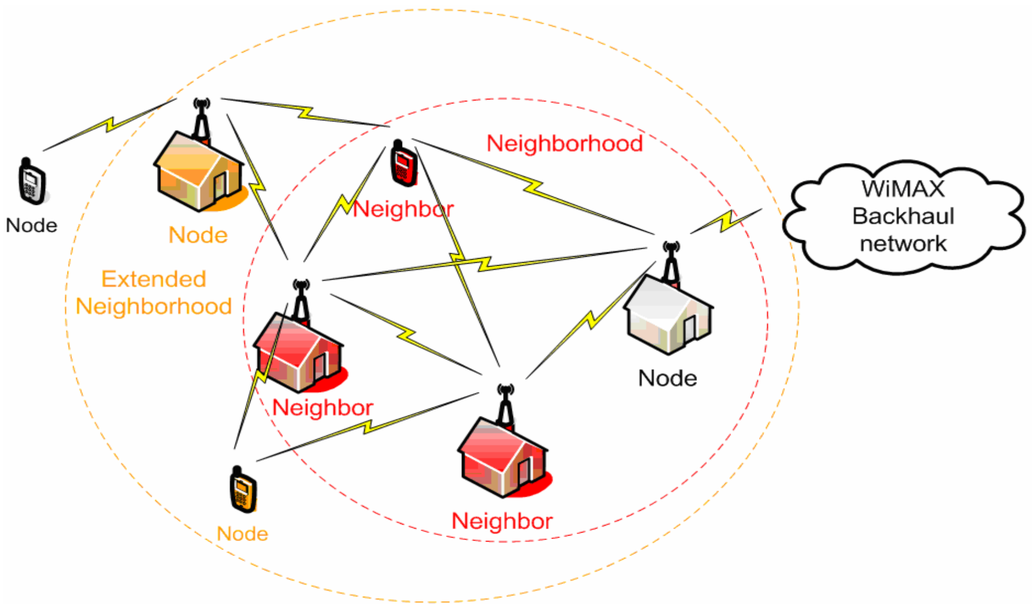

Figure 43: IEEE802.16a mesh topology [70]

3.6.3.3. Medium Access Control

The medium access control of IEEE802.16 is based on Time Division Multiplex (TDM) for downlink connections and Time Division Multiple Access (TDMA) for uplink connections. As the time slots for uplink are managed by the central base stations, no collisions can occur.
The base station multiplexes the traffic in fixed time slots to the different subscriber stations. For the different data streams, individual modulation and coding schemes can be defined. The header describes these options.

This project has been co-funded by the European Commission DG-Information Society and Media in the 6th Framework Programme. The content of this publication is the sole responsibility of the project partners listed herein and does not necessarily represent the view of the European Commission or its services.

3.6.3.4. Frame Format

The format of the MAC frame is shown in Figure 44.

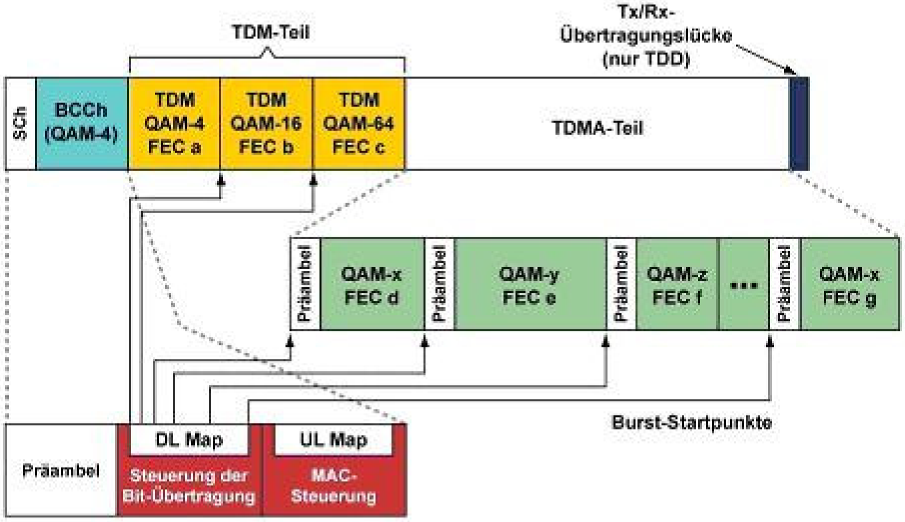

Figure 44: IEEE802.16 MAC frame format [59]

3.6.3.5. Addresses

The IEEE802.16 uses standard 48-Bit long IEEE addresses [57].

3.6.3.6. Security

The IEEE802.16 uses manifold standard approaches for security, i.e.

- 3DES-CBC or AES-CCM encryption for confidentiality,
- SIM- and/or EAP-based mutual authentication.

3.6.4. eSafety relevant issues

For the time being, no major implications of WiMAX to eSafety applications can be expected. This is due to the current characteristics of WiMAX:

- Its current primary focus is on fixed and nomadic installations. Support of mobile installations will enter the market at a later stage. And even after introduction of mobile devices, the traffic flow tends to be static, instead of spontaneous.
- The equipment is very complex and thus expensive.
- The systems are not optimised to low power consumption, so that user equipment would require really large batteries.

3.7. RFID

3.7.1. General Description

3.7.1.1. Overview

RFID (Radio Frequency IDentification) is the general name for any technique that utilises modulation of a radio-frequency signal, travelling in free space, with a digital ID. The signal is sent by an RFID-transmitter (“tag”) that is attached to an item, case, container or person [53]. The RFID-receiver (“reader”) can infer the close presence of the tag by detecting the ID. Examples of tags are shown in Figure 45. Some tags also allow for programmable data, in addition to the fixed ID.

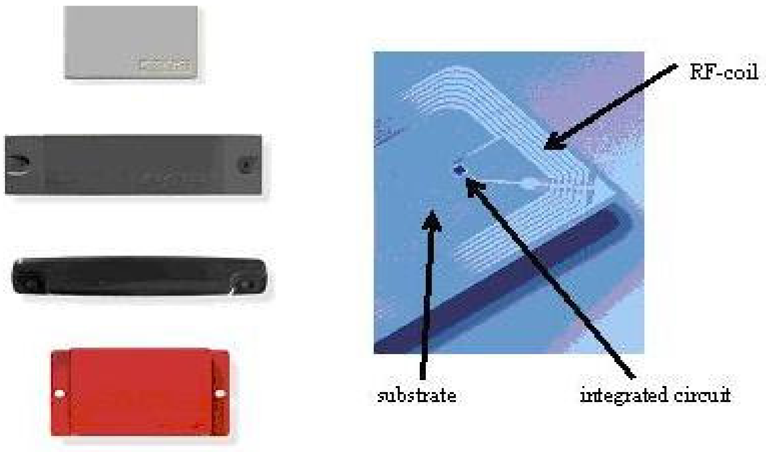

Figure 45: Examples of RFID-tags

3.7.1.2. Regulation and Standardisation

The transmission frequency bands are LF (130 kHz), HF (13.56 MHz), UHF (434, 868/902 MHz) to microwave (2.4 GHz), with variations depending on the country or global region. The most important possibilities are shown in Table 10.

STANDARD	SUBJECT OF THE STANDARD	FREQUENCIES
Auto-ID Class 0	Parameters for air interface communication	860 - 930 MHz
Auto-ID Class 1	Parameters for air interface communication	860 - 930 MHz
EPCglobal Gen 2	Parameters for air interface communication, intended 860 - 930 MHz as replacement for Class 0 and Class 1, submitted to the ISO at the beginning of 2005	860 - 930 MHz
ISO 14443	Regulation for contactless / proximity IO cards, reading 13.56 MHz distance 7 -15 cm.	13.56 MHz
ISO 15693	Regulation of contactless / vicinity cards, reading 13.56 MHz distance up to 1m	13.56 MHz
ISO 18000	Family of RFIO air interface standards, examples:	
ISO 18000-1	Generic parameters far air interface of globally accepted frequencies.	
ISO 18000-2		125, 134.2 KHz
ISO 18000-3	Reading distance max. 1.5 m, successor of 13.56 MHz ISO 15693	13.56 MHz
ISO 18000-4		2.45 GHz
ISO 18000-5	Has been withdrawn.	5,8 GHz
ISO 18000-6	EPCglobal Generation 2 Tags (under development)	860 - 960 MHz

Table 10: ISO and EPCglobal standards [52]

A set of standards exists (BSR INCITS 371.1 for 2.4 GHz air interface, 371.2 for 433 MHz air interface) that depend on active tags for Real Time Localisation Systems (RTLS) using RSSI (Received Signal Strength Indication) within an infrastructure of readers. Still, manufacturers tend to develop proprietary protocols that do not provide interworking. The range of active tags is 100+ meters, depending on the transmission power. For RTLS-applications, proprietary systems based on UWB RFID-tags are emerging, that do not suffer from the multipath effect that hinders RSSI based RTLS.

3.7.2. Physical Layer

In case the tag and reader are less than one wavelength apart (i.e. speed of light / frequency), the interaction is of an inductive rather than an electro-magnetic nature. In other words, the tag's and reader's RF-circuits make up the primary and secondary coil of an ac-transformer. The signal transfer function drops off more steeply ($1/r^3$) than for isotropic electromagnetic waves ($1/r^2$),

This project has been co-funded by the European Commission DG-Information Society and Media in the 6th Framework Programme. The content of this publication is the sole responsibility of the project partners listed herein and does not necessarily represent the view of the European Commission or its services.

resulting in a pronounced proximity effect. This effect is utilised in typical RFID-applications, in which tags are tracked as they pass along an infrastructure of readers. By constraining the motion of items to pass so-called choke-points (see Figure 46), the location of the items can be inferred from the sequence of reader-tag interactions. In case the motion cannot be constrained, the readers must be spaced sufficiently close, such that their proximity zones just overlap (cf. Figure 47).

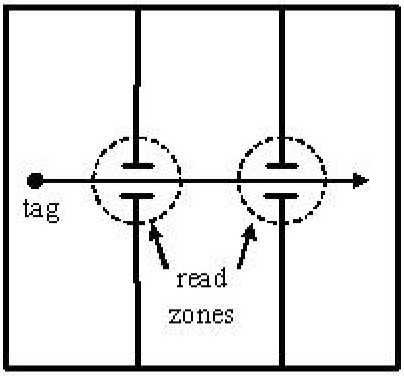

Figure 46: Non-overlapping read zones with choke-points

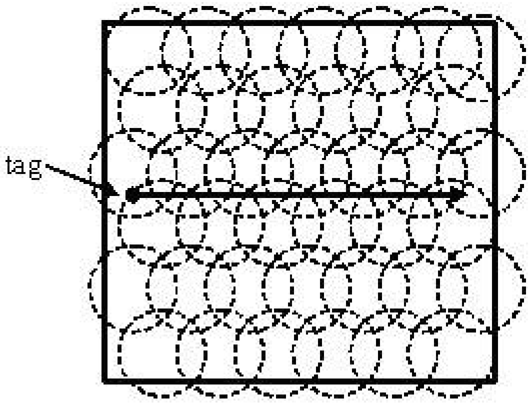

Figure 47: Overlapping read zones

For business applications, such infrastructure of readers is connected to specialised software ("edgeware") that processes reader-tag events and provides higher-level information to enterprise middleware applications.
To be able to send a modulated signal of limited duration, a tag needs to accumulate a certain amount of energy. This energy is either stored in a battery (active tag), or retrieved from the reader via a -contactless- inductive circuit (passive tag). Active tags are set up to transmit in a periodic fashion ("beacon"), and often convey dynamic data, in addition to a fixed ID and programmable static data. In this sense, they are assuming the role of wireless sensors. Passive tags only transmit when being prompted by the reader. Because the range of passive tags is invariably small (up to several meters, which requires large reader coils), only active tags are considered for WATCH-OVER application.

Active tags are set up to send a packet (modulated signal of milliseconds duration) periodically, usually once every couple of seconds (beacon mode). A set of standards exists (BSR INCITS 371.1 for 2.4 GHz air interface, 371.2 for 433 MHz air interface) that depend on active tags for Real Time Locating Systems using RSSI (Received Signal Strength Indication) within an infrastructure of readers. Still, proprietary protocols exist that do not provide interworking. The range of active tags is 100+ meters, depending on the transmission power. For RTLS-applications, proprietary systems based on UWB are emerging, that do not suffer from the multipath effect that hinders RSSI-based RTLS.

This project has been co-funded by the European Commission DG-Information Society and Media in the 6th Framework Programme. The content of this publication is the sole responsibility of the project partners listed herein and does not necessarily represent the view of the European Commission or its services.

3.7.3. Data Link Layer

The operation of RFID systems often involves a situation where numerous transponders are present within the interrogation zone of one reader.

The simplest of the multi-access procedures is the Aloha algorithm [54]. This procedure is applied only for read-only transponders with only a small amount of data to be transferred [53]. Aloha is based on a request of all serial numbers within the readers range. When the reader sends a request-command to all transponders, each transponder waits a random backoff time, before answering with its unique serial number (UID) and the data. The data frame must be short so that the collision probability remains low.

The binary search algorithm alleviates this problem. It is based on the fact that collisions may occur, however, they can be located within the data frame. Thus, the binary search identifies the collided bits and steps through the possibilities bit by bit, as it is shown in Figure 48. A binary search algorithm consists of a predefined sequence of interactions (request, select(UID), read_data, and unselect) between the reader and several transponders with the objective to select any desired transponder.

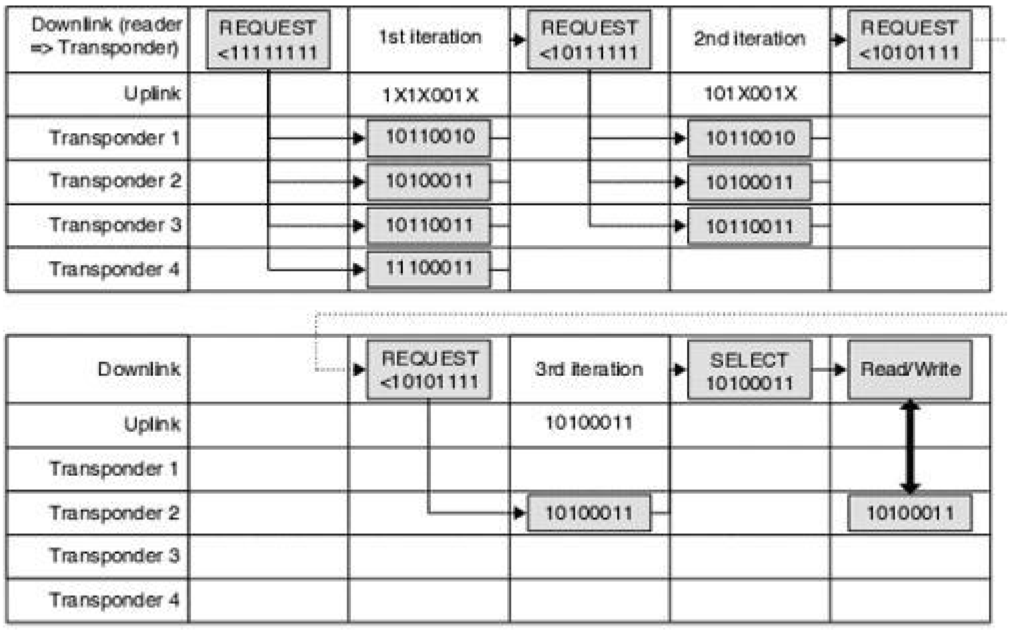

Figure 48: Binary search algorithm [53]

3.7.4. eSafety relevant issues

No major activities are known for RFID-based eSafety architectures. Within the WATCH-OVER project, a demonstrator was built for illustration purposes that employ a set of readers to be attached to the side of a vehicle, and a tag to be attached to a VRU. It is described in ch. 5.4.5.

3.8. UWB

3.8.1. Introduction

3.8.1.1. General Description

The origins of UWB technology stem from work begun in 1962 that was generally referred to as impulse radio, baseband or carrier-free communications. The term “ultrawideband” was first coined by the U.S. Department of Defence in 1989, and early applications leveraged the technology’s properties as ground-penetrating radar [33]. Ultra-wideband (UWB) systems were used for radar, sensing, military communications and niche applications in the past 20 years. In February 2002, the FCC issued a ruling that UWB could be used for data communications, which was a substantial change [32].

Ultra-wideband (UWB) is a generic denomination and does not relate to a specific technology. The prevailing definition comes with two preconditions to be ultra-wideband [34]:

- It has a bandwidth larger 500 MHz, or
- It has a fractional bandwidth B_f larger than 0.2, where

$$B_f = 2\frac{f_H - f_L}{f_H + f_L} \qquad \text{(Eq. 18)}$$

and f_H is the higher and f_L is the lower -10 dB points in the spectrum. In other words, the occupied spectrum is greater than 20 percent of the center frequency.

UWB has a number of advantages that make it attractive for consumer communications applications. Those are shown in Table 11, before the challenges and problems are itemised in Table 12.

ADVANTAGE	BENEFIT
coexistence with current narrowband and wideband radio services	avoids expensive licensing fees.
large channel capacity	high bandwidth can support real-time high-definition video streaming.
ability to work with low SNRs	offers high performance in noisy environments.
low transmit power	provides high degree of security with low probability of detection and intercept.
resistance to jamming	reliable in hostile environments.
high performance in multipath channels	resistant to multipath fading
simple transceiver architecture	potentially enables ultra-low power, smaller form factor, and better mean time between failures, all at a reduced cost.
very good time domain resolution	allows for location and tracking applications.

Table 11: Advantages and benefits of ultra-wideband systems [34] [35] [36]

CHALLENGE	PROBLEM
pulse-shape distortion	low performance using classical matched filter receivers.
channel estimation	difficulty predicting the template signals.
high-frequency synchronisation	very fast ADCs required.
multiple-access interference	detecting the desired user's information is more challenging than in narrowband communication.
low transmission power	information can travel only short distances.

Table 12: Challenges and Problems of ultra-wideband systems [36]

3.8.1.2. Regulations

The radiation limits stated by FCC in 2002 are shown in Figure 49 and Figure 50. As a concession to the very early regulation, very low power levels were made available. If the entire 7.5 GHz band is optimally utilised, the maximum power available to the transmitter is approximately 0.5 mW [34].

This project has been co-funded by the European Commission DG-Information Society and Media in the 6th Framework Programme. The content of this publication is the sole responsibility of the project partners listed herein and does not necessarily represent the view of the European Commission or its services.

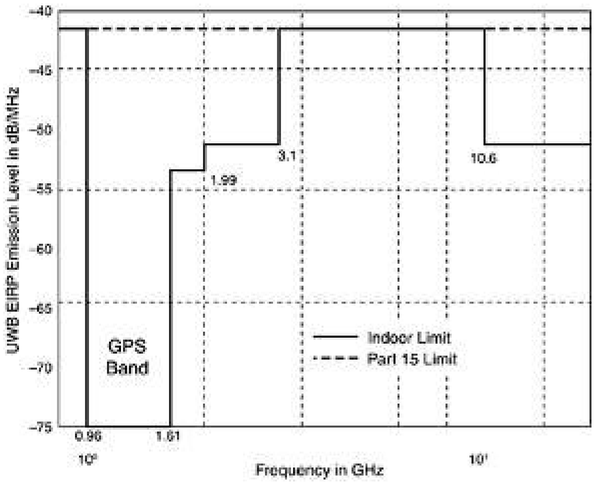

Figure 49: UWB emission limits for indoor communications systems [36]

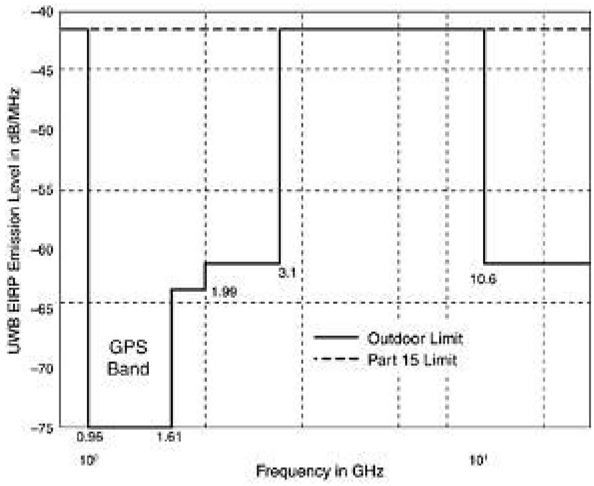

Figure 50: UWB emission limits for outdoor communications systems [36]

For the ETSI, no decisions have been taken yet. However, it is clear that the European approach will be somewhat more cautious than that of the USA, although heavily influenced by the FCC decision [34].

The ECC TG3 currently develops provisions for a CEPT regulation. It has presented the "Report 64" in December 2004. A "Draft Decision" was due in December 2005, which was modified in March 2006. This specification was proposed to the Radio Spectrum Committee (RSC) of the EC for public comments [41]. The actual specification is shown in Table 13.

FREQUENCY RANGE [GHZ]	MAXIMUM MEAN E.I.R.P. DENSITY [DBM/MHZ]	MAXIMUM PEAK E.I.R.P. DENSITY [DBM/50MHZ]
Under 1.6	-90	-50
1.6 to 3.8	-85	-45
3.8 to 4.8	-70	-30
4.8 to 6	-70	-30
6 to 8.5	-41,3	0
8.5 to 10.6	-65	-25
over 10.6	-85	-45

Table 13: Draft Decision for use of frequency bands for UWB systems in Europe [41]

In this specification, no regulation of duty cycle may be found. It is mentioned that it might be possible to run some frequency bands at higher output power until 2010.

[47] describes the current discussion on the regulatory situation, where the ECC and the Japanese regulatory authorities are working towards UWB regulations [48] [49]. Differently from the regulations made by the FCC [50] in the USA, in Europe and in Japan a detect and avoid (DAA) mechanism is envisaged that mitigates interference to existing wireless services.

The DAA mechanism allows a UWB receiver to detect the frequency spectrum in its vicinity and modify its reception parameters. This helps to avoid interference caused by other radio technologies such as WiMax. If a UWB device detects that the frequency spectrum is occupied, it can move to a sub-band or avoid specific frequency ranges [45].

MB-OFDM is particularly well suited to implement DAA, because the FFT can be used as a channelised radiometer, and the IFFT can be used to sculpt the transmit spectrum [51].

3.8.1.3. Standardisation

There are various activities in the field of standardisation of UWB technologies. The most important of them are:

- The IEEE established the IEEE802.15.3a study group to define a new physical layer concept for short range, high-data-rate applications, as an extension to the existing IEEE802.15.3-2004 standard. With a minimum data rate of 110 Mbps at a distance of 10 m, the study group intended to develop a standard to address such applications as video or multimedia links, or cable replacements [34].

  However, the activities of the study group were terminated, after the competition of two alternative technical solutions led to a deadlock.

  One side was taken by the multi band OFDM approach of the Multiband OFDM Alliance (MBOA, cf. ch. 3.8.2.3), which unified with the WiMedia Alliance (WMA) [39] in 2005. MBOA, and later WMA, are backed by Intel and many more suppliers.

  The other side took a pulse-based approach (cf. ch. 3.8.2.2) and is mainly supported by the UWB forum [38] around Freescale Semiconductor. This approach is very similar to the Direct Sequence Spread Spectrum (DSSS).

- The IEEE802.15.4a study group is an extension to the IEEE802.15.4 low-rate WPAN task group. It addresses new applications that require only moderate data throughput, but long battery life such as low-rate wireless personal area networks, sensors, and small networks [34]. However, it is not yet clear, when the results of this work group will be available [37].

- In early 2006, the WiMedia Alliance (WMA) and the Bluetooth Special Interest Group (BSIG) signed an agreement for a joint development for a UWB-based high-speed Bluetooth [127].

3.8.2. Physical Layer

3.8.2.1. Introduction

Many different techniques may be used to satisfy the requirements of an UWB signal. UWB systems have historically been based on impulse radio concepts. Those are described in ch. 3.8.2.2. However, recently more and more attention was attributed to OFDM-based multiband approaches, which are presented in ch. 3.8.2.3.

3.8.2.2. Impulse Radio Schemes

Impulse radio (IR) refers to the generation of series of very short duration pulses, of the order of hundreds of picoseconds. Each pulse has a very wide spectrum, which must adhere to the spectral mask requirements. Any given pulse will have very low energy because of the very low power limits permitted for UWB transmission. Therefore, many pulses will typically be combined to carry the information for one bit (continuous pulse transmission) [34].
IR has the significant advantage of being essentially a baseband technology, which potentially lead to very simple, homodyne transceiver design, as it is compared to a typical narrowband transceiver structure in Figure 51 and Figure 52.

This project has been co-funded by the European Commission DG-Information Society and Media in the 6th Framework Programme. The content of this publication is the sole responsibility of the project partners listed herein and does not necessarily represent the view of the European Commission or its services.

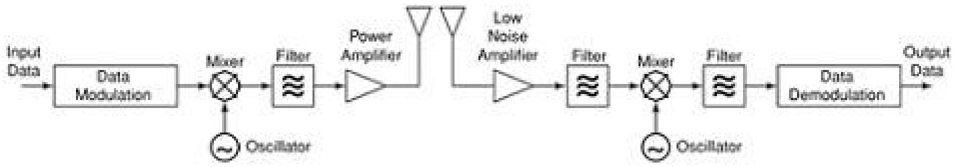

Figure 51: A typical narrowband transceiver architecture [36]

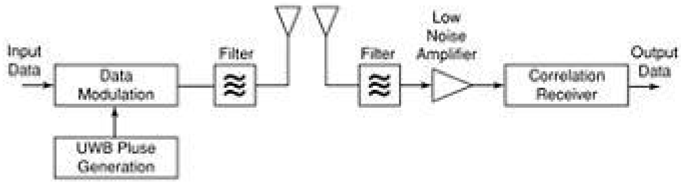

Figure 52: An example of an UWB transceiver architecture [36]

3.8.2.3. *Multiband OFDM Schemes*

Another approach is to extend the techniques utilised for direct sequence spread spectrum (DSSS) or Code Division Multiple Access (CDMA) schemes, as they are used for modern wireless communication systems, e.g. WLAN (IEEE802.11b) or third-generation mobile communication.

There are three main techniques for generating a spread-spectrum multicarrier (SS-MC) transmission [34]:

- In a *multi-carrier CDMA* system, the original data stream is spread in the frequency over the different sub-carriers f_i with each chip of pseudo-random chip c_i. A block diagram is shown in Figure 53.
- Within a *multi-carrier direct-sequence (DS)-CDMA* system, the original data is spread in the time domain after serial-to-parallel conversion of the data stream [34].
- The *multi-tone (MT) CDMA* comes with a much smaller carrier spacing, and therefore is the closest to the original UWB idea. The original data is spread in the time domain, as in the case of MC-DS-CDMA systems. However, it causes the highest self-interference due to the overlapping spectra.

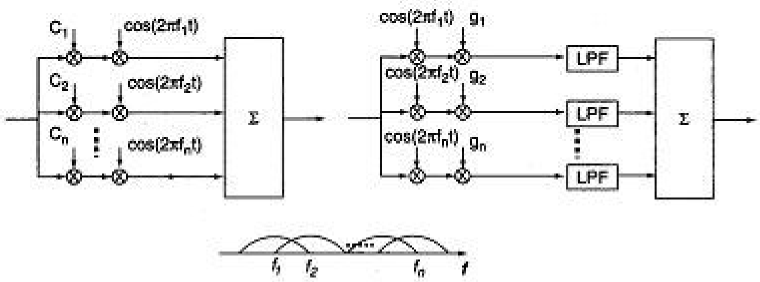

Figure 53: Block diagram and spectrum for multi-carrier CDMA system [36]

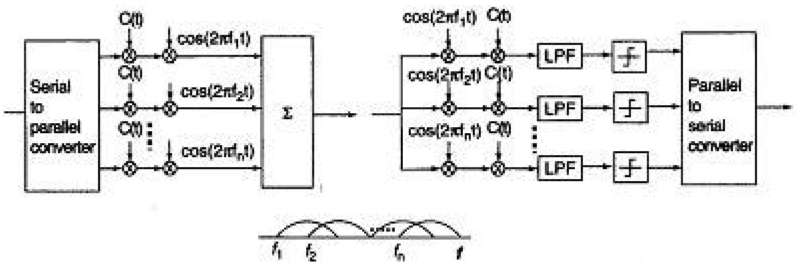

Figure 54: Block diagram and spectrum for multi-carrier DS-CDMA system [36]

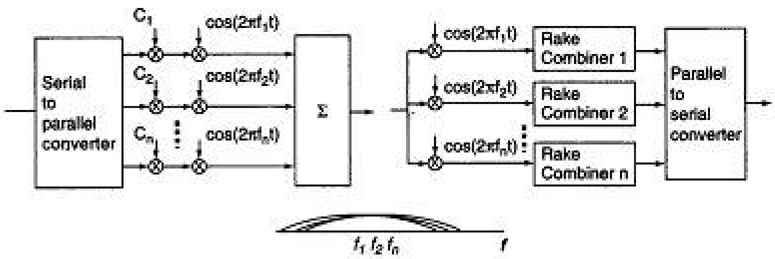

Figure 55: Block diagram and spectrum for multi-tone CDMA system [36]

The MBOA proposal is based on a MC-CDMA system. It is defined for the frequency band from 3.1 GHz to 4.8 GHz, being divided into three sub-bands of 500 MHz each, as illustrated in Figure 56.

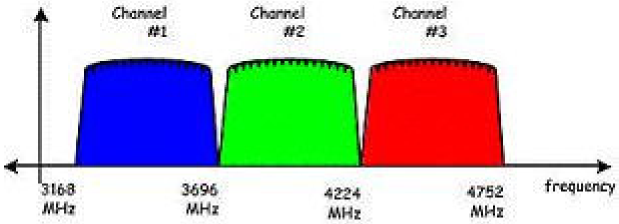

Figure 56: Frequency allocation of sub-bands for a multi-band OFDM system [33]

3.8.2.4. Standardised PHY (ECMA-368)

This section focuses on one of the standardised PHY service and protocol for a UWB system [73]. It describes a frame structure, which is depicted in Figure 57.

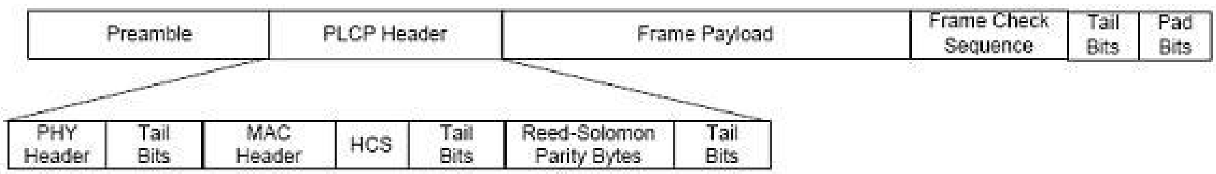

Figure 57: UWB PHY frame structure according to ECMA-368 [73]

The preamble contains either a preamble sequence which indicates a standard frame or a burst frame. Furthermore the Physical Layer Convergence Protocol (PLCP) header is including the MAC and PHY headers which are further protected by a header checksum (HCS). The payload for each frame is always followed by a frame checksum (FCS).

3.8.3. Data Link Layer

3.8.3.1. General architecture

Functions within the MAC should be executed regardless of the underlying Physical Layer (PHY). Restricting the view to these points the novel transmission technique of UWB does not affect the design of the MAC and existing solutions typically designed for wireless networks can be directly incorporated into the design of an UWB network. For that reason, one is able to use MAC implementations from existing networks as IEEE 802.11b [1], Bluetooth [25], and the IEEE 802.15.3 [72]. The last one was originally developed for narrowband systems in the ISM band at 2.4GHz, but given the current physical layer proposals that focus on UWB, it should also serve in the UWB case.
Despite the general independence from the physical layer, it should be highlighted that in reality the design of an efficient MAC often requires an accurate knowledge of the underlying physical layer. In case of UWB this is a crucial issue because of the distinct features of UWB systems such as low-power constraints versus rather precise ranging capability. These specific features may enable the definition of novel MAC-functionality which requires different MAC implementations.

3.8.3.2. Standardised MAC (ECMA-368)

In this section we want to focus on one standardised MAC service and protocol for a UWB system [73]. Within the standardisation it was specified that each device should have an individual MAC address called DevAddr (device address), which identifies a single MAC sublayer. Each address is a 16-bit value which is generated locally, without central coordination. Consequently it is possible for a single value to ambiguously identify two or more MAC entities. The standard provides mechanisms to resolve ambiguous DevAddrs.

The addressing scheme includes multicast and broadcast address values. A multicast address identifies a group of MAC entities, and the broadcast address identifies all entities. Furthermore the MAC relies on special functionality from the underlying PHY, i.e.

- Frame transmission in both single frame and burst mode
- Frame reception for both single frame and burst mode transmission
- PLCP header error indication for both PHY and MAC header structures.
- Clear channel assessment for estimation of medium activity
- Range measurements in timestamps if MAC range measurement is supported.

The frame transmission and reception are supported by the exchange of parameters between the MAC and the PHY layer. These parameters allow the MAC sub layer to control, and be informed of, the frame transmission mode/data rate/length and the frame preamble. In single frame transmission, the MAC sub layer has full control of the frame timing. In burst mode transmission the MAC sub layer has control of the first frame timing and the PHY provides accurate timing for the remaining frames in the burst.

Additionally, to the required service functionality of the PHY (cf. ch. 3.8.2.4) there are also some requirements on the MAC service functionality. These functionalities are

- Communication between cooperating devices within radio range on a single channel using the PHY
- A distributed, reservation-based channel access mechanism
- A prioritis, contention-based channel access mechanism
- A synchronisation facility for coordinated applications
- Mechanisms for handling mobility and interference situations
- Device power management by scheduling of frame transmission and reception
- Secure communications with data authentication and encryption using cryptographic algorithms
- A mechanism for measuring distances between two devices.

Each of the used devices should support all necessary MAC functions which are required for the targeted application. No central coordinator for the MAC is available. Coordination between devices within reach is achieved by beacon frames. The beacon signal is transmitted periodically which allows to discover devices and organise devices dynamically. The beacon signals provide also basic timing for the network. Additionally, reservation and scheduling is possible when accessing the medium by following the beacon mechanism.

In a network formed with fully distributed medium access coordination, logical groups are formed. This helps to facilitate contention-free frame exchanges while exploring medium reuse over different spatial regions. For the current Standard, two logical groups have been specified. They are called the beacon group and extended beacon group and are determined with respect to an individual device.

The specified MAC protocol algorithms try to achieve that no member of an extended beacon group transmits a beacon frame at the same time as a device. If a device is enabled, it scans one or more channels for beacons and selects a channel. When no beacon signal was detected an own beacon period (BP) is created and sent. Conversely, if there are beacon signals detected, the device synchronises to them. Data is exchanged with members of the same beacon group over the same channel as used for the beacons.

Due to the unlicensed use of spectrum in UWB systems each device operates in a dynamic environment. Interference to this underlying technology is possible from many licensed services and networks. Thus sometimes a more reliable transmission would be possible in another channel. Thus, the devices should be able to dynamically change the channel in which they are operating without requiring disruption of links with its peers. The procedure to change the channel is defined in more detail in [73].

From the previous description it is essential for the beacon protocol that each participating device protects the BPs. Furthermore, if another BP from a different group is detected which is usually unaligned with the current BP, the device should try to protect the alien BP by announcing a reservation to cover it in its beacon.

The basic structure for the frame exchange is a superframe. The superframe is composed of 256 medium access slots (MASs). Each superframe starts with a BP which extends over one or more contiguous MASs. The start of the firs MAS in the BP, and the superframe, is called the beacon period start time (BPST). A superframe is shown in Figure 58.

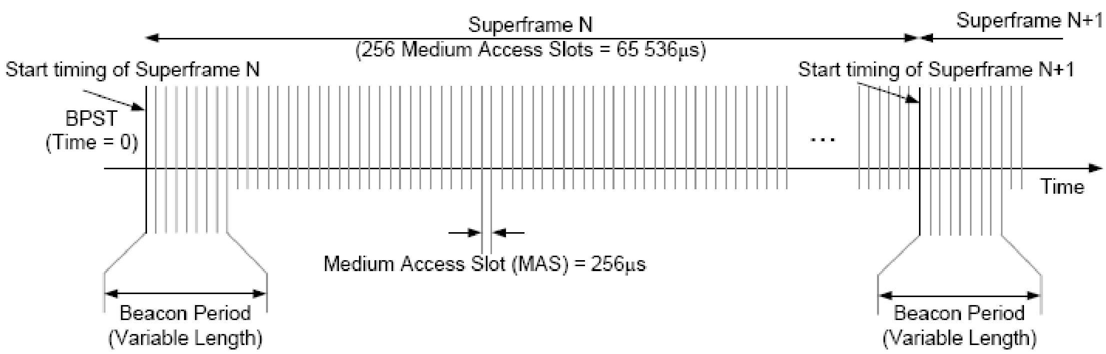

Figure 58: UWB MAC superframe structure according to ECMA-368 [73]

Each superframe consists of the previously introduced BP followed by medium Access slots. The whole superframe contains 256 MASs where a variable amount is used for the BP.

The medium is accessed in one of the three ways:

- During the BP: This is the most obvious procedure to get access to the medium. In this scenario a device tries to get access to the medium only by reservation during the BP. However, still this reservation during the BP might cover some scenarios which are not easy to handle for the MAC protocol which are for instance overlapping BPs from different devices.
- During reservations: The Distributed Reservation Protocol (DRP) allows devices to reserve MASs to communicate with neighbors. All devices which are using DRP have to announce their reservations with the according DRP Information Elements (IEs) within their beacons. The reservation is the set of MACs identified by the DRP IEs.
- Outside the BP and reservations: The Prioritized Contention Access (PCA) provides differentiated, distributed contention access to the medium for four different access categories (ACs). A device employs a prioritis contention procedure for each AC to get access to the medium. The AC is resolved by the user priorities defined in the standard and can be found in [73]. Unless, this access method is exceptional, there are scenarios where the medium is still unavailable, for example within the BP or within reserved blocks.

Data is passed between the MAC sub layer and its client in MAC Service Data Units (MSDUs) qualified by certain parameters. MSDUs are transported between devices in data frames. To reduce the frame error rate of a marginal link, data frames can be fragmented and reassembled.

If the source device wishes to verify the delivery of a frame, then one of following three acknowledgement policies is used.

- The No-ACK policy, is appropriate for frames that do not require guaranteed delivery, or are delay sensitive and a retransmitted frame would arrive too late.
- The Imm-ACK (Immediate) policy, provides an acknowledgement process in which each frame is individually acknowledged following the reception of the frame.
- The B-ACK policy, lets the source send multiple frames without intervening ACK frames. Instead, the acknowledgements of the individual frames are grouped into a single response frame that is sent when requested by the source device.

The B-ACK process decreases the overhead of the Imm-ACK process while allowing the source device to verify the delivery of frames to the destination. If the source device does not receive the requested acknowledgement, then it may retransmit the frame, or it may discard the frame. The decision to retransmit or discard the frame depends on the type of data or command that is being sent.

Furthermore the MAC layer has to fulfill some other basic tasks. One very important task, especially in wireless networks, is security. Since the signal is propagated on air, anybody who has the possibilities to capture the signal is able to read the transmitted information or at least replay the recorded data and cause damage to the data transmission. For that reason two security levels are defined within the MAC, i.e. no security or strong security. The used security protection includes data encryption, message integrity, and replay attack protection. Replay attacks are taken care of by securing frame counters and replay counters. For data encryption, 128bit symmetric temporal keys are employed based on AES-128 with CCM (Counter with CBC-MAC). However, specific mechanisms to address denial of service attacks are not discussed in this standard.

Another important feature of the used MAC layer is the support for higher-layer timer synchronisation. Depending on the application it is required, that the timers at different devices are synchronised. Thus, the used UWB-MAC is able to provide optional MAC facilities to achieve accurate synchronisation in higher layers not only for one application at a time. A related feature of the MAC is the possibility to adapt the frame rate. This may become suitable when increased throughput is desired or increased frame error rate is detected.

Since UWB devices are intended to be mobile devices, the MAC should also provide power management capabilities. One effective method to extend the lifetime of battery powered devices is to allow complete shutdown of the devices or reduce power during long idle periods with respect to the size of the superframe. The two management modes used here are active and hibernation. Devices in active mode transmit and receive beacons in every superframe. Hibernated devices do not receive and transmit within the superframes.

3.8.4. eSafety relevant issues

Ultra-Wide Band solutions promise a very good suitability to eSafety applications. This is due to two major reasons:

- They come with an inherent high data rate, which allows the efficient exchange of information between distributed systems.
- The theoretical accuracy of ranging increases with the bandwidth, as described in ch. 4.1.2. This is also the reason that the ECMA-368 conformant MAC supports additional one-dimensional ranging measurements based on two-way time transfer techniques.

However, no activities are known to authors, which apply UWB technologies for eSafety applications.

4. Investigation on Localisation Techniques

4.1. Physical Background

4.1.1. Basic Principles

Mainly, three different measurement principles are used today: angle-of-arrival (AOA), received-signal strength (RSS), and propagation-time based systems that can further be divided into three different subclasses: time-of-arrival (TOA), roundtrip-time-of-flight (RTOF) and time-difference-of-arrival (TDOA).
An overview of the principles is shown in Figure 59.

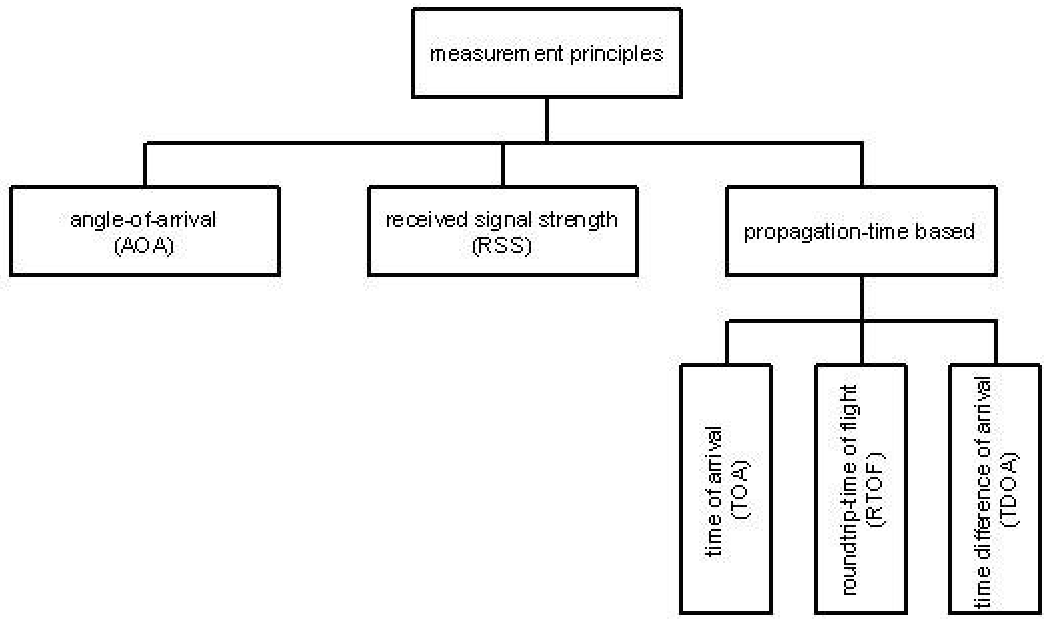

Figure 59: Measurement Principles for Localisation Techniques [16]

This project has been co-funded by the European Commission DG-Information Society and Media in the 6th Framework Programme. The content of this publication is the sole responsibility of the project partners listed herein and does not necessarily represent the view of the European Commission or its services.

4.1.2. Accuracy

From radar theory, it is known that the accuracy of a EM-based measurement increases with increasing bandwidth. In [22], the theoretical root-mean-square-(rms)-error δM of a radar measurement M is calculated to

$$\delta M = \frac{kM}{\sqrt{2E/N_0}}, \qquad \text{(Eq. 19)}$$

where k is a constant whose value is in the vicinity of unity,
E is the received signal energy, and
N_0 is the noise power per unit bandwidth.

For a time-delay (range) measurement (cf. ch. 4.4), k depends on the shape of the frequency spectrum $S(f)$. M is the rise time of the pulse, which is inversely proportional to bandwidth.

For an angle measurement (cf. ch. 4.3), k depends on the shape of the aperture illumination $A(x)$, and M is the beamwidth.

4.1.3. Triangulation

Given the locations of anchor transmitter devices in a reference coordinate system and the respective ranges between those devices and a mobile receiver device, the ranges can be triangulated through simple geometry to render the location of the latter in the same coordinate system: each stationary, or anchor, device sits at the center of a circle whose radius is equal to the range. The intersection of these circles resolves the mobile location.

4.2. RSS

RSS systems are based on propagation-loss equations. As long as $r > \lambda$, the free-space transmission loss, LB, is proportional to $1/r^2$. This case holds true for EM-waves. For smaller r or larger λ, the propagation works inductively, and the LB is proportional to $1/r^3$. This propagation model shall be applied for lower-frequency RFID applications.
However, these simple equations are in most cases unsuitable to calculate the distance value from the difference of transmitted and received power under real conditions [67], as additional mechanisms such as reflection, diffraction and scattering affect wave propagation and causing “small-scale” slow and fast fading components [68]. To overcome this problem, advanced propagation models or site-specific path loss models are required, or the actual field distribution in the area of interest has to be learned from measurements. Based on these a-priori measurements and interpolation, a significant improvement of accuracy can be achieved, as long as a sufficient number of anchor points is available [66].
The major advantage of RSS systems is the fact that most modern radio modules already provide a received signal strength indicator (RSSI). Also, the bit error rate (BER) can be used to estimate the signal attenuation. Consequently, implementing a RSSI-based local-positioning system within a wireless-communication system is more or less a software topic, and proprietary hardware is not required. This is in contrast to most of the alternatives described below.

This project has been co-funded by the European Commission DG-Information Society and Media in the 6th Framework Programme. The content of this publication is the sole responsibility of the project partners listed herein and does not necessarily represent the view of the European Commission or its services.

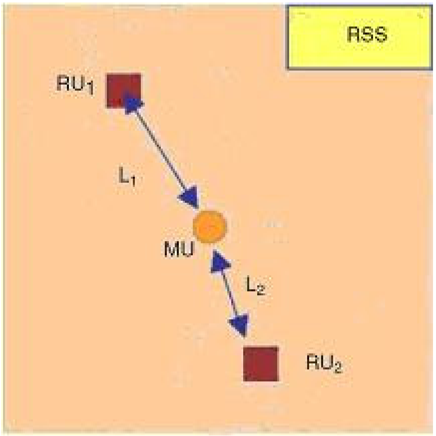

Figure 60: Measurement Principles for Received Signal Strength (RSS) [16]
L_1 and L_2 denote the measured path loss

4.3. AOA

In AOA systems, the position is calculated via goniometry. With the use of directional antennas or antenna arrays, the angle or bearing relative to points located at known positions is measured. The intersection of several measured direction pointers then yields the position value. The accuracy of this approach is limited by the possible directivity of the measuring aperture, by shadowing, and/or by multipath reflections arriving from misleading directions [16].
The basic principle is shown in Figure 61.

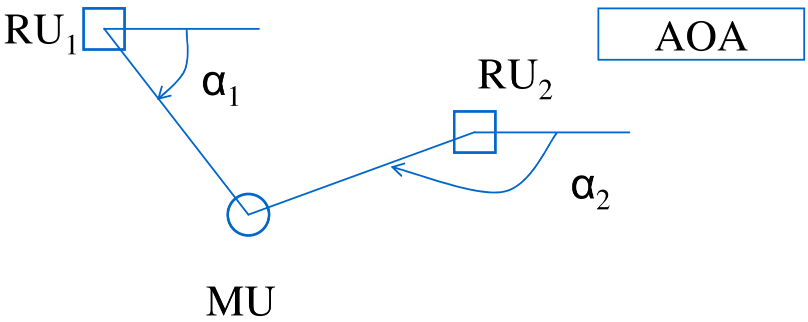

Figure 61: Measurement Principles for Angle-of-Arrival (AOA) [16]
RU and MU denote remote and mobile unit, α_1 and α_2 are the measured direction angles

4.4. Propagation Time Based Techniques

4.4.1. Introductory Remarks

Due to their physical restraints, AOA and RSS systems only deliver moderate position accuracy. The perhaps most intuitive and accurate approach for local position measurement is to measure the time-of-flight of the signal travelling from the transmitter to the measuring unit. This can be done in different approaches:

- Time-of-Arrival (TOA), described in ch. 4.4.2,
- Roundtrip-Time-of-Flight (RTOF) described in ch. 4.4.3, and
- Time-Difference of Arrival (TDOA) described in ch. 4.4.4

4.4.2. Time-of-Arrival (TOA)

In Time-of-Arrival (TOA) systems, the one-way propagation time is measured. Given this time and the speed of propagation, the distance, or range, between the two devices can be estimated. This concept requires precise time synchronisation of all involved fixed and mobile units. In this case, the absolute time synchronisation must have at least a precision related to the desired positioning accuracy.
For example, a positioning accuracy in the decimetre range requires absolute time synchronisation significantly below 1 ns. Since the clock information has to be distributed to and kept in the mobile unit, this approach either leads to a very expensive or less accurate system [16].

4.4.3. Roundtrip-Time-of-Flight (RTOF)

The absolute synchronisation requirement can be replaced by a more moderate relative clock synchronisation requirement if a Roundtrip-Time-of-Flight (RTOF) approach is chosen. Here, the measuring unit more or less acts as common radar. A transponder responds to the interrogating radar signal, and the complete round-trip propagation time is measured. In this case, the synchronisation challenge is that the measuring unit has to know the exact delay/processing time caused by the responder.
A simple calculation shows that this requirement is also difficult to meet. Provided that both the measuring unit and the transponder have a fairly good crystal clock source with 25 ppm accuracy, a processing time of 1 ms in the transponder can lead to a measurement deviation of several meters [16].

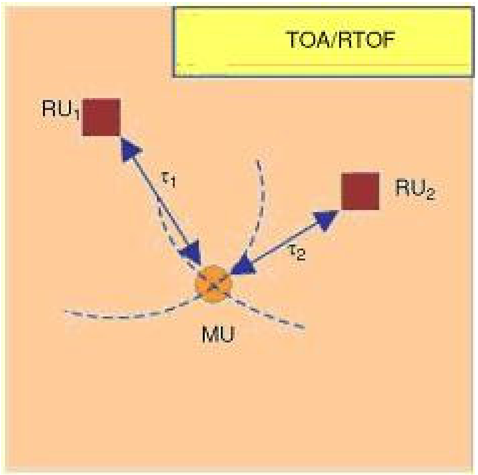

Figure 62: Measurement Principles for Time-of-Arrival (TOA) [16]
This method uses with Roundtrip-Time-of-Flight (RTOF), where τ_1 and τ_2 denote the measured one way or the roundtrip signal propagation time, the spatial position is given by the intersection of circles centred at the RUs

4.4.4. Time-Difference of Arrival (TDOA)

In TDOA systems, the time-difference of arrival of the signals received in several pairs of measuring units is evaluated. The benefit of TDOA systems is that it is only necessary to synchronise the measuring units. This synchronisation can be performed with the help of a backbone network or a reference transponder in a known position.
The TDOA is traditionally obtained through OWR transactions [68].

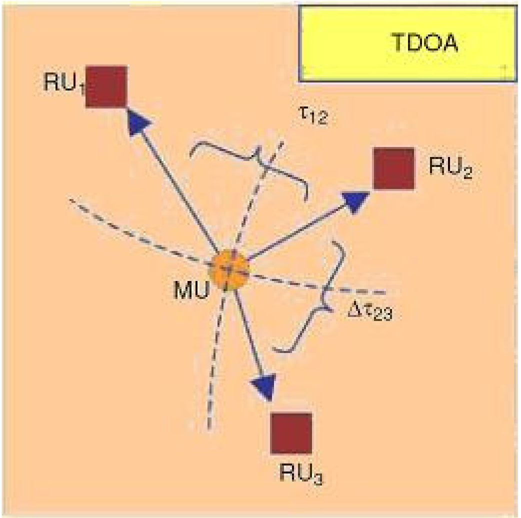

Figure 63: Measurement Principles for Time-Difference-of-Arrival (TDOA) [16]
$\Delta\tau_{12}$ and $\Delta\tau_{23}$ denote the measured propagation time difference from a signal travelling from the MU to two different RUs and the position is given by the intersection of hyperbola with foci at the RUs.

4.4.5. Measurement Principles

4.4.5.1. One Way Ranging (OWR)

The one-way ranging scheme operates under the assumption that the two ranging devices are synchronised a-priori to a common clock. This enables the receiver device to easily correlate the received signal with the known transmitted sequence to estimate the TOA as the time of maximum correlation [68].

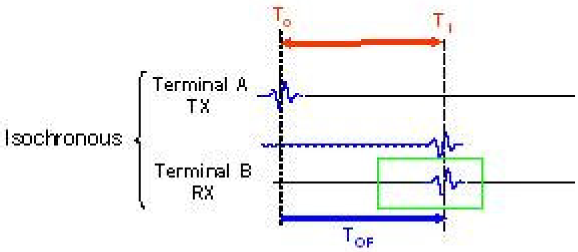

Figure 64: One Way Ranging [19]

The time of flight can be estimated to

$$\tilde{T}_{OF\,B} = (T_1 - T_0), \qquad \text{(Eq. 20)}$$

The distance between both nodes can consequently be estimated to

$$\tilde{d}_{AB} = \tilde{T}_{OF\,B}.c\ . \qquad \text{(Eq. 21)}$$

4.4.5.2. Two-Way Ranging (TWR)

Two-way ranging enables measuring the signal round-trip propagation time t_p between two asynchronous transceivers through a classical two-way remote synchronisation technique. A pair of terminals is time multiplexed with half-duplex packet exchanges. This procedure relies on a typical mechanism for fused location and communication: a transmitter (TX) sends a packet to a receiver (Rx) which replies after waiting a nominal period T_{Reply} delay necessary for synchronising with packets containing synchronous timing information [68].
In the context of RF-based RTL, only half-duplex channels are regarded. A half-duplex channel is a one-way system that is “turned around” to retransmit a signal in the opposite direction. In this

This project has been co-funded by the European Commission DG-Information Society and Media in the 6th Framework Programme. The content of this publication is the sole responsibility of the project partners listed herein and does not necessarily represent the view of the European Commission or its services.

method, the one-way delay between the transmitter and receiver is estimated as one-half of the measured round trip delay [18]. The half-duplex system has the advantage of only requiring "reflecting" hardware at one station, but it is susceptible to fluctuations in the delay.
There are several approaches for two-way ranging. The most important of them are described within this chapter.

Asymmetric Two-Way Ranging

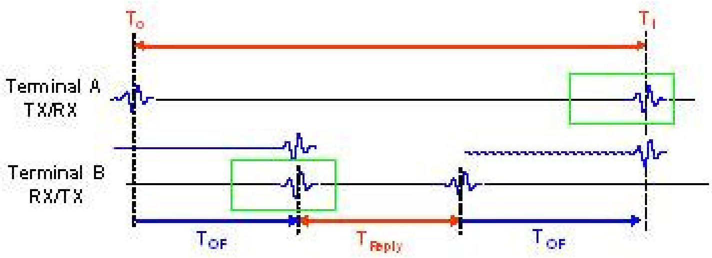

Figure 65: Asymmetric Two Way Ranging [19]

The delay estimate can be sent to the user and applied as a correction, or the transmitter can advance the signal so that it arrives at the user's site on time.
The time of flight can be estimated to

$$\tilde{T}_{OF\,A} = \frac{1}{2}\left[(T_1 - T_0) - T_{\text{Reply}}\right]. \qquad \text{(Eq. 22)}$$

The distance between both nodes can consequently be estimated to

$$\tilde{d}_{AB} = \tilde{T}_{OF\,A}.c\,. \qquad \text{(Eq. 23)}$$

However, it has to be taken into account that the clock drift has an impact on the perceived time. With Δf_A and Δf_B being the frequency offset relative to the nominal ideal frequency, the estimation can be written as

$$\tilde{T}_{OF\,A} = T_{OF\,A}(1+\Delta f_A) + \frac{T_{\text{Reply}}}{2}\frac{(\Delta f_A - \Delta f_B)}{(1+\Delta f_B)}\,. \qquad \text{(Eq. 24)}$$

Symmetric Two-Way Ranging with synchronisation
[20] describes a two-way ranging as it is commonly used in satellite-based systems. The measurements are shown in Figure 66 with
T_{1AT} being the time, when Device A transmits message 1.
T_{1BR} being the time, when Device B receives message 1.
T_{2AR} is the time, when Device A receives message 2.
T_{1BR} is the time, when Device B receives message 1.
t_0 is the unknown clock offset
t_P is the unknown propagation delay

Figure 66: Two Way Ranging with synchronisation [20]

This project has been co-funded by the European Commission DG-Information Society and Media in the 6th Framework Programme. The content of this publication is the sole responsibility of the project partners listed herein and does not necessarily represent the view of the European Commission or its services.

Based on the measurements, the two unknowns can be calculated

$$\begin{aligned} t_p &= \tfrac{1}{2}\left[\left(T_{2AR} - T_{1AT}\right) - \left(T_{2BT} - T_{1BR}\right) \right] \\ &= \tfrac{1}{2}\left(T_{RTT,A} - T_{REPLY,B} \right) \\ t_o &= \tfrac{1}{2}\left[\left(T_{2BT} + T_{1BR}\right) - \left(T_{2AR} + T_{1AT}\right) \right] \end{aligned} \quad \text{(Eq. 25)}$$

Multiple measurements yield finer precision and accuracy, including frequency offset correction.

In [21], a problem for this approach is highlighted. Usually, the reply time $T_{RTT,A}$ and the round trip time $T_{REPLY,B}$ will be significantly larger than the propagation delay. If there is a clock drift between clock A and clock B, this will lead to a significant error, as $T_{RTT,A}$ is measured with clock A and $T_{REPLY,B}$ with clock B.
Therefore, this “straightforward TWR” requires very low crystal tolerances, e.g. smaller 10 ppm or precise phase tracking.

Symmetric Double Sided – Two Way Ranging
In order to avoid the effect of high inaccuracy after subtracting two large numbers measured with different clocks, [21] proposes the Symmetric Double Sided – Two Way Ranging (SDS-TWR) approach. It is shown in Figure 67. This approach allows an improvement to the two-way ranging scheme described in the previous, however at the price of an additional message in the exchange between two ranging devices [69].

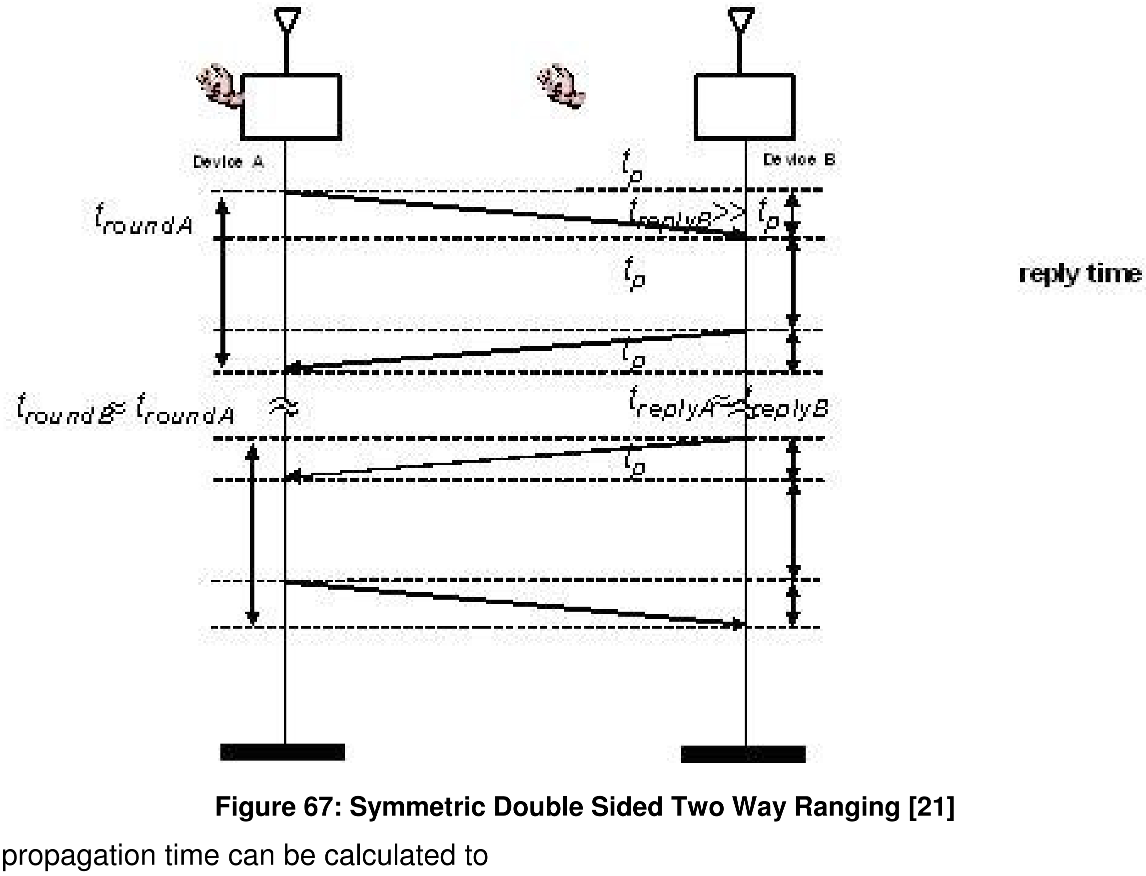

Figure 67: Symmetric Double Sided Two Way Ranging [21]

The propagation time can be calculated to

$$t_p = \frac{t_{roundA} - t_{replyA} + t_{roundB} - t_{replyB}}{4}. \quad \text{(Eq. 26)}$$

SDS-TWR comes up as an enhancement on “Straightforward TWR” which eliminates the need of phase tracking, which can work with standard tolerances (up to 40 ppm or more) [21].

4.4.6. Accuracy

Eq. 19 can be simplified for time-delay measurements, when using the effective bandwidth B_{eff}. It is the calculated to

$$\delta M = \frac{1}{B_{eff}\sqrt{2E/N_0}}, \qquad \text{(Eq. 27)}$$

where the effective bandwidth calculates to

$$B_{eff} = \frac{1}{E}\int_{-\infty}^{\infty}(2\pi f)^2 |S(f)|^2 df, \qquad \text{(Eq. 28)}$$

Table 14 gives an overview on the theoretically achievable accuracy in dependence of the effective bandwidth and the signal to noise ratio derived from radar theory.

BEFF [MHZ]	E/N0 [DB]							
	15		20		25		30	
4	5,15E-08	s	4,90E-08	s	4,73E-08	s	4,60E-08	s
	15,46	m	14,70	m	14,18	m	13,80	m
20	1,03E-08	s	9,80E-09	s	9,46E-09	s	9,20E-09	s
	3,09	m	2,94	m	2,84	m	2,76	m
40	5,15E-09	s	4,90E-09	s	4,73E-09	s	4,60E-09	s
	1,55	m	1,47	m	1,42	m	1,38	m
200	1,03E-09	s	9,80E-10	s	9,46E-10	s	9,20E-10	s
	0,31	m	0,29	m	0,28	m	0,28	m
400	5,15E-10	s	4,90E-10	s	4,73E-10	s	4,60E-10	s
	0,15	m	0,15	m	0,14	m	0,14	m

Table 14: Theoretically achievable accuracy with time of flight measurements

4.5. Self-Localisation

4.5.1. Introduction

Self localisation is understood as the process of localisation, which is performed by the object itself. In most cases, it is based upon time-of-flight or time-difference-of-flight measurements of RF-signals emitted from satellites. Current systems are based upon the satellite-based Global Positioning System GPS. In future, the improved European system GALILEO can be used, which functions according to the same principles, but shall allow improved quality.
The Global Positioning System (GPS) is controlled and maintained by the U.S. Government. For civil users the Standard Positioning Service (SPS) provides a less accurate positioning capability than the Precise Positioning Service (PPS), which is available only for U.S. military and other authorized users. It should be noted that GPS can temporarily be switched off by US without notice which reduces availability, reliability and safety of systems relying (mainly) on GPS. This should not be the case for Galileo.
[71] defines levels of performance the U.S. Government commits to provide to civil users. This section shall give an overview of the errors of GPS measurements. Beside inaccuracies of the system itself, errors caused by contributions of ionosphere, troposphere, receiver, multipath, or

This project has been co-funded by the European Commission DG-Information Society and Media in the 6th Framework Programme. The content of this publication is the sole responsibility of the project partners listed herein and does not necessarily represent the view of the European Commission or its services.

interference have to be added. These sources of error will be discussed more in detail below. Generally the GPS performance is described by the parameters

- Accuracy,
- Availability,
- Continuity of function, and
- Integrity.

Regarding to the need of a cheap system we will talk about the capabilities of mass-market GPS receiver only. These receivers have up to 20 channels and evaluate the Coarse/Acquisition (C/A) code, what is transmitted with the L1 signal by all GPS satellites. The accuracy of GPS is improved with a Satellite Based Augmentation System (SBAS). For that, WAAS (Wide Area Augmentation System)/EGNOS (European Geostationary Navigation Overlay Service) support is integrated. These features are the state of the art in today's automotive navigation systems. Other available systems induce additional costs and/or bigger and unusable antenna sizes. Also post-processing methods will not be taken into account.

4.5.2. Accuracy

The 24 GPS satellites are spaced so that from any point on earth, at least four satellites will be in view above a 5° mask angle with respect to the local horizon (no local obscures are considered). Each satellite continually broadcasts its changing position and time. With *trilateration* a GPS receiver calculates its own position (Longitude and Latitude, *2D-fix*) by getting signals from three satellites. With the signal of a fourth satellite, the receiver can also figure out the altitude (*3D-fix*). To calculate the position in space (3-dimensional) four satellites are necessary, because the time of the receiver has to be synchronised with the GPS time. The importance of synchronisation shows the following: A time inaccuracy of ten nanoseconds (10^{-8} sec) leads to a position error of three meters.

This shows the importance of an exact determination of the travelling time between satellite and ground receiver. The accuracy of positioning is strongly influenced by this. However, several "real world" effects make it difficult to measure the exact travelling time and degrade the accuracy of the system. These are outlined in the following descriptions.

4.5.3. Atmospheric effects

4.5.3.1. Ionosphere single-frequency model error (± 7 meter)

Changing atmospheric conditions change the speed of the GPS signals unpredictably as they pass through the ionosphere. The high ionisation in this sphere is mainly caused by UV-radiation and X-ray and reduces the velocity of propagation of the signal. Therefore this effect is stronger during daytimes than during the night. If the satellite is directly overhead the error is minimised and becomes greater toward the horizon, since the satellite signals must travel through the greater "thickness" of the ionosphere.

4.5.3.2. Troposphere model error (± 0.25 meter)

The amount of humidity in the air also has a delaying effect on the signal, resulting in errors similar to those generated in the ionosphere but located much closer to the ground in the troposphere. The areas affected by these problems tend to be smaller in size and to move faster than the billows in the ionosphere.

4.5.3.3. Multipath effects (± 0.5 meter)

GPS signals reach the receiver not only in a direct way. The signal reflects off surrounding terrain, buildings etc. These multipath issues cause inaccuracy. A variety of receiver techniques, most notably narrow correlator spacing, have been developed to mitigate multipath errors. An opinion is that multipath effects are much less severe in dynamic applications such as cars and planes. When the GPS antenna is moving, the false solutions using reflected signals quickly fail to converge and only the direct signals result in stable solutions.

This project has been co-funded by the European Commission DG-Information Society and Media in the 6th Framework Programme. The content of this publication is the sole responsibility of the project partners listed herein and does not necessarily represent the view of the European Commission or its services.

4.5.3.4. Ephemeris errors (± 2.5 meter)

Considering the case when a GPS satellite is boosted back into a proper orbit, for some time following the manoeuvres, the receiver's calculation of the satellite's position will be incorrect until it receives another ephemeris update. Additionally, the amount of accuracy sent in the ephemeris is limited by the bandwidth; using the data from the satellites alone limits its accuracy.

4.5.3.5. Clock errors (± 2 meter)

It is a prerequisite that the clocks within the different satellites are synchronised. However, every synchronisation comes up with a timing deviation, which may account for measurement errors in the range of up to two meters.

4.5.3.6. Numerical errors of the receiver (± 1 meter)

GPS receivers of course are digital systems. All operations are performed with a digital processor. Numerical errors due to systematic errors in analog-digital conversion and limited word length may lead to measurement errors in the range of up to one meter.

4.5.4. Definition of Accuracy

The specified errors of the previous effects have to be seen as "typical" values. For the user it is important to know the accuracy of the whole system. When all of these effects are added up, GPS should typically be accurate to about 15 meters. But we need a value for the probability that a measurement lies within a given accuracy. The manufacturers of GPS receivers normally give a value for the Circular Error Probable (CEP). Typical for the mentioned low cost receiver is a 2.5m CEP. This means that 50% of all measurements are within a radius of 2.5 meters. Other definitions are

- LEP (Linear Error Probable)
- SEP (Spherical Error Probable)
- DOP (Dilution of Precision)

The accuracy also depends from the geometrical configuration of the satellites used. The larger the region in the sky covered by the satellites in sight the smaller the DOP value.
A smaller DOP value indicates a higher accuracy. More accurately, if the DOP value doubles, the error in determining a position increases by a factor of two. There are different DOP notations

- HDOP (Horizontal Dilution of Precision)
- VDOP (Vertical Dilution of Precision)
- PDOP (Position Dilution of Precision) – Position in 3-D space

4.5.5. Increasing Accuracy

The most of the above mentioned GPS receivers provide a "pseudo" Differential-GPS (DGPS). A Satellite Based Augmentation System (SBAS) mainly broadcasts differential corrections regarding the ionospheric error. Additionally, the SBAS satellites provide integrity data and can be used as normal GPS satellites. If a GPS receiver has SBAS support, then mostly for both, the European system EGNOS (European Geostationary Navigation Overlay Service) and the U.S. system WAAS (Wide Area Augmentation System) is used.
Commonly, accuracy increases with the number of satellites in sight. The DOP value decreases with more satellites in view, because it naturally leads to a more stretched distribution of the satellites in the sky. In urban areas the view is often obscured by buildings, tunnels etc. These difficult receiving conditions are the main reasons for inaccuracies. Similar problems occur with SBAS. As SBAS is considered intentionally for aviation purposes, SBAS satellites are often just a bit above the local horizon.
Onboard automotive navigation systems use GPS in combination with a gyroscope and tachometer pickup, allowing a continuous navigation solution by dead reckoning when buildings, terrain, or tunnels or other obstacles block the satellite signals.

5. Investigated Approaches

5.1. Approach 1: UWB emulator

5.1.1. General Description

5.1.1.1. Technology background

This approach deals using broadband signals from 4MHz to 400MHz. Two different measurement principles are used in combination:

- a propagation-time based method, which uses time-of-arrival (TOA) respectively Roundtrip-Time-of-Flight (RTOF) and
- a method evaluating the angle-of-arrival (AOA).

The method of measuring the received-signal strength (RSS) is not taken into account because there might be obstacles in the line of sight (LOS), which attenuate the signal strength additionally.

5.1.1.2. Propagation Time Based approach

The idea of the propagation time based approach is to measure the two-way propagation time between the car and the VRU using a repeater carried by the VRU. With the knowledge of the processing delay in the VRU system the distance can be calculated by:

$$\tilde{d}_1 = \frac{1}{2}\left[\Delta t_{1,1} - t_{\mathrm{Rep\_del}}\right]c\,, \qquad \text{(Eq. 29)}$$

$$\tilde{d}_2 = \left[\Delta t_{1,2} - t_{\mathrm{Rep\_del}}\right]c - \tilde{d}_1\,, \qquad \text{(Eq. 30)}$$

where t_{Rep_del} denotes the delay in the repeater and c the velocity of light. If two measurement points on the car are available, the position of the VRU can be estimated using triangulation. With the knowledge of the two measured distances d_1, d_2 and the known distance of measuring points on the car $d_{1,2}$ the position of the VRU relative to the car can be estimated by angle γ and distance d_1 (cf. Figure 68):

$$\gamma = ar\cos\left[\frac{d_{1,2}{}^2 + d_1{}^2 - d_2{}^2}{2.d_{1,2}.d_1}\right], \qquad \text{(Eq. 31)}$$

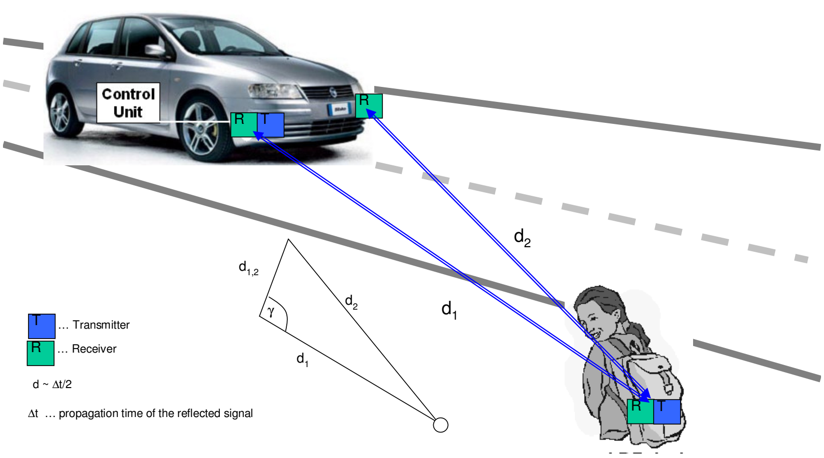

Figure 68: Propagation time based approach with Roundtrip-Time-of-Flight (RTOF)

This project has been co-funded by the European Commission DG-Information Society and Media in the 6th Framework Programme. The content of this publication is the sole responsibility of the project partners listed herein and does not necessarily represent the view of the European Commission or its services.

5.1.1.3. Angle-of-arrival (AOA) based approach

For the AOA approach antenna arrays (two or more closely spaced antennas) are needed. If there are two such antenna arrays mounted on the car the position of the VRU can be estimated by the point of intersection of the two directions estimated by the two antenna arrays. Due to the very flat crossing angle of the two direction vectors, the error of the estimated position can be very high. Therefore a combination of one direction and one distance will lead to better results. The basic principle is shown in Figure 69.

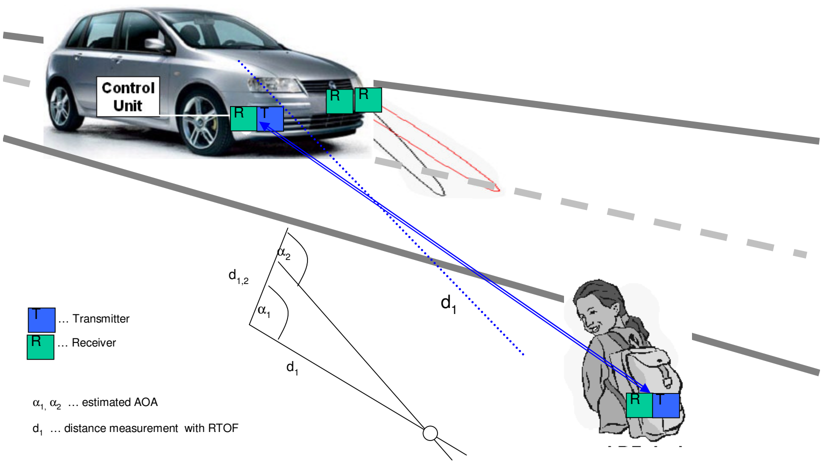

**Figure 69: Angle-of-arrival (AOA) based approach with two estimation methods
Estimation by the intersection of the two directions and estimation with one direction und one distance measurement.**

5.1.2. Simulation for Localisation

5.1.2.1. Simulation Model

In order to identify the best localisation method for a VRU within the WATCH-OVER project, a simulation tool was developed. The simulation results provide a useful base of information to make a good decision for the method best suited to the special application in WATCH-OVER. The simulation takes into account the two most important use cases described in the user requirements ("WATCH-OVER_D2.1-Requirements and use cases", Table 29).

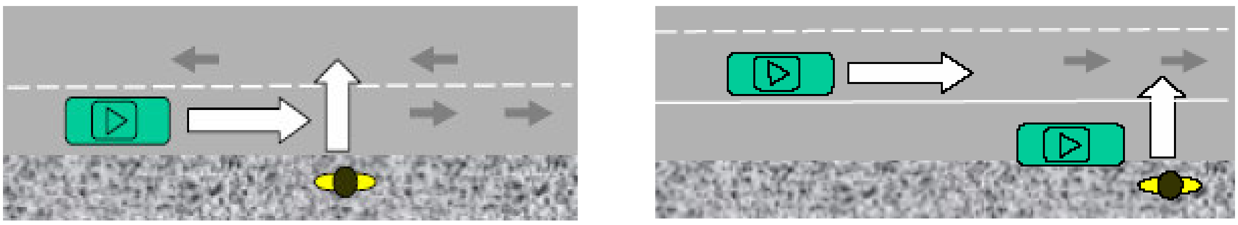

**Figure 70: The two most important scenarios
This information was taken from the WATCH-OVER_D2.1-Requirements and use cases.**

5.1.2.2. Simulation Scenarios

The first scenario describes a pedestrian crossing the road from the right to the left. In the second picture we have the same scenario but the pedestrian is occluded by a parked car. This scenario is of high interest because the driver or a video system cannot detect or recognise the pedestrian. A localisation system using radio communication can however help in this situation. The scenarios 3 and 4 are similar but from the opposite road side.

This project has been co-funded by the European Commission DG-Information Society and Media in the 6th Framework Programme. The content of this publication is the sole responsibility of the project partners listed herein and does not necessarily represent the view of the European Commission or its services.

In technical terms a simulation model was developed which can reproduce a car driving along a road with a selectable velocity vector. The VRU can also be placed in the scenario with its velocity vector. The following simulations are all done with a car velocity of 13 m/s (almost 50 km/h) and a VRU velocity of 2 m/s crossing the road. To allow relative localisation a radio communication system is assumed with one transmit antenna and three receive antennas on the car side. The spacing of the receive antenna is 1,6 m from Rx1 to Rx2 and 0,1 m from Rx2 to Rx3. The VRU is equipped with a repeater which reflects the transmitted signal back to the receiving antennas on the car. To make the simulation realistic a geometric stochastic radio channel model is used which allows placing scatterer areas (representing e.g. buildings) and obstacles occluding the VRU. Figure 71 shows the two scenarios which are analysed below. The first scenario has no obstacle in the line of sight (LOS) path and the second scenario shows an obstacle attenuating the LOS path.

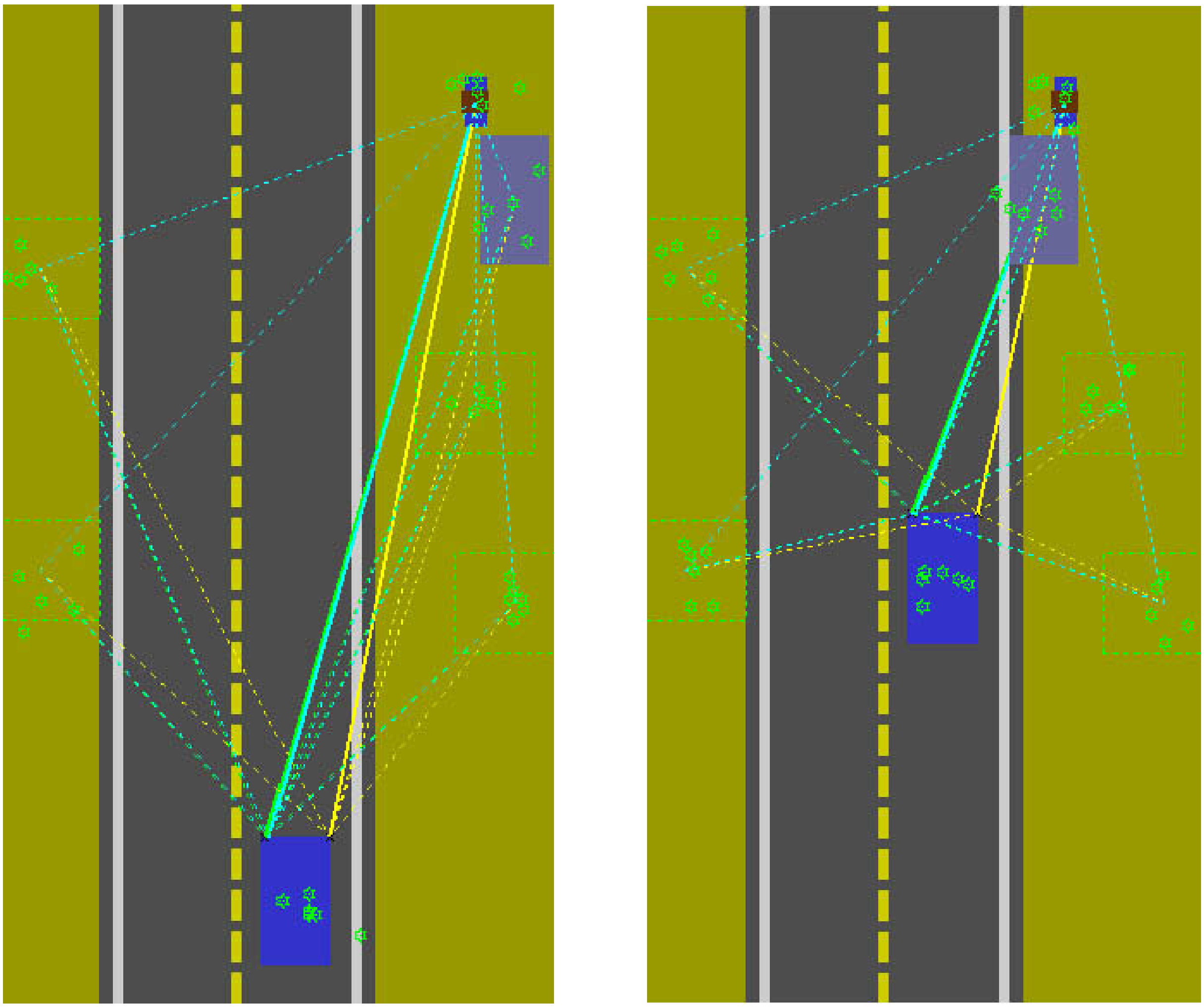

Figure 71: The figure shows the geometrical situation of the scenarios left: LOS without obstacles; right: NLOS with an obstacle

This project has been co-funded by the European Commission DG-Information Society and Media in the 6th Framework Programme. The content of this publication is the sole responsibility of the project partners listed herein and does not necessarily represent the view of the European Commission or its services.

5.1.2.3. Simulation Parameters

The parameters shown in Table 15 are selected for the simulation.

	X	Y	units
Car position	7.5	5	m
Car velocity	0	13	m/s
Rx1 Antenna	0.8	0	m
Rx2 Antenna	-0.8	0	m
Rx3 Antenna	-0.7	0	m
VRU position	12	27	m
VRU velocity	-2	0	m/s
Scatterer cluster 1	1	22	m
Scatterer cluster 2	1	13	m
Scatterer cluster 3	12	18	m
Scatterer cluster 4	13	12	m
Obstacle	10	26	m

Table 15: Parameters for the simulation scenario

5.1.2.4. Channel Model

For the modelling of the radio channel a COST 259 / COST 273 like channel model was developed.

COST (COperation européenne dans le domaine de la recherche Scientifique et Technique) is a European Union Forum for cooperative scientfic research [86]. Several European COST projects deal with the topics of wave propagation and radio network planning. Among the most important are “COST 259: Wireless Flexible Personalised Communications” with a duration from December 1996 to April 2000 [87] and “COST 273: Towards Mobile Broadband Multimedia Networks” with a duration from 2001 to 2005 [88].

This channel model is a geometric stochastic channel model, where one part of the radio channel is calculated geometrically (e.g. small scale fading) and the other part varies stochastically with a certain distribution function to fulfil the large scale fading behaviour and the long term statistic of realistic scenarios. The model consists of several scatterer clusters (representing scattering objects like buildings) with a certain distribution of varying point scatterers. Around the antennas there is a near cluster. The received signal is the superposition of the line of sight (LOS) signal and the reflected signals from the scatterers of near cluster and far clusters.

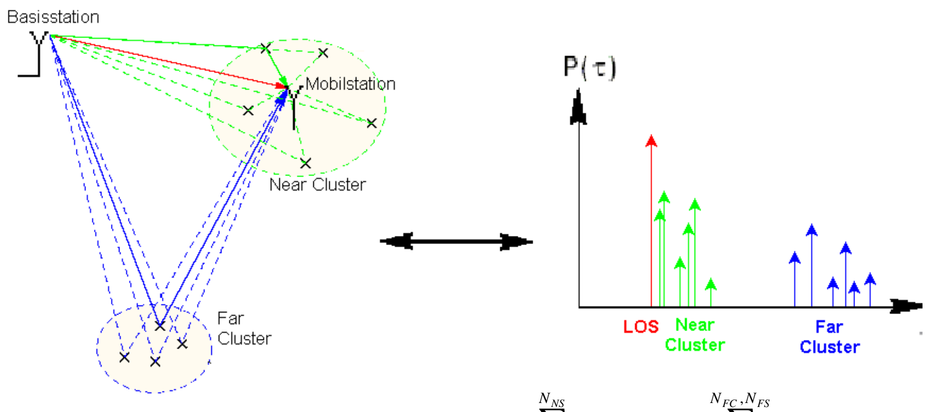

$$Y = H_{LOS} \cdot X + \sum_{k=0}^{N_{NS}} H_{NS}(k) \cdot X + \sum_{n,m}^{N_{FC}, N_{FS}} H_{FS}(n,m) \cdot X$$

Figure 72: geometrical situation with near and far cluster (left) and resulting power delay profile (right). The formula gives the superposition of several signals.

This project has been co-funded by the European Commission DG-Information Society and Media in the 6th Framework Programme. The content of this publication is the sole responsibility of the project partners listed herein and does not necessarily represent the view of the European Commission or its services.

5.1.2.5. Estimation algorithm

For the estimation of the distance between each antenna on the car and the reflector carried by the VRU a correlation algorithm and a special maximum likelihood algorithm was used. The calculation of the VRU's position on the road was done in two different ways. The first method was the triangulation using two estimated distances (d_1 distance to Rx1 and d_2 distance to Rx2). The second method includes the estimation of the angle of arrival (AOA) using the closely spaced antennas Rx2 and Rx3 with a smart antenna algorithm in addition to an estimation of the distance d_1 to Rx1.

Furthermore a post processing algorithm using constrains of the VRU trajectory was performed. The performance of both algorithms with and without post processing is evaluated by comparing the estimated VRU position in respect to the real VRU position. Only the distance of the VRU to the roadside was taken into account.

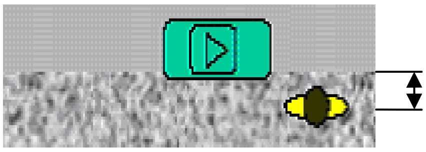

Figure 73: VRU position relative to the road side

5.1.3. Simulation Results

5.1.3.1. General comments

We shall now show the results obtained from our simulation. First we shall analyse the performance of the distance estimation algorithms, that are based on correlation with a special maximum likelihood estimation. Then we shall discuss the accuracy of the VRU localisation algorithms using triangulation based on two distances or based on an angle of arrival and a distance. Finally the best results using post processing are discussed. All these results are discussed both for scenarios without and with an obstacle in the line of sight.

Another parameter of the simulations is the signal to interference ratio (SIR). The SIR is used as proportion of the LOS power to the sum of power received from the scatterers. The simulations were done with various SIR values as follows: 0dB, 2dB, 4dB, 8dB and 14dB. Based on experience made in the past it looks as if the 2dB scenario would be the most important case. It needs measurements for verification, as already suggested.

5.1.3.2. Simulation of distance measurements using RTOF without an obstacle

This chapter describes the simulation results for the estimation of the distance between car and VRU using RTOF without an obstacle.

The simulation was done with different bandwidths between 4 and 400 MHz and different power of the scatterers, SIR between 0 and 14 dB. The SNR depends on the distance and is in the range between 0 and 20 dB.

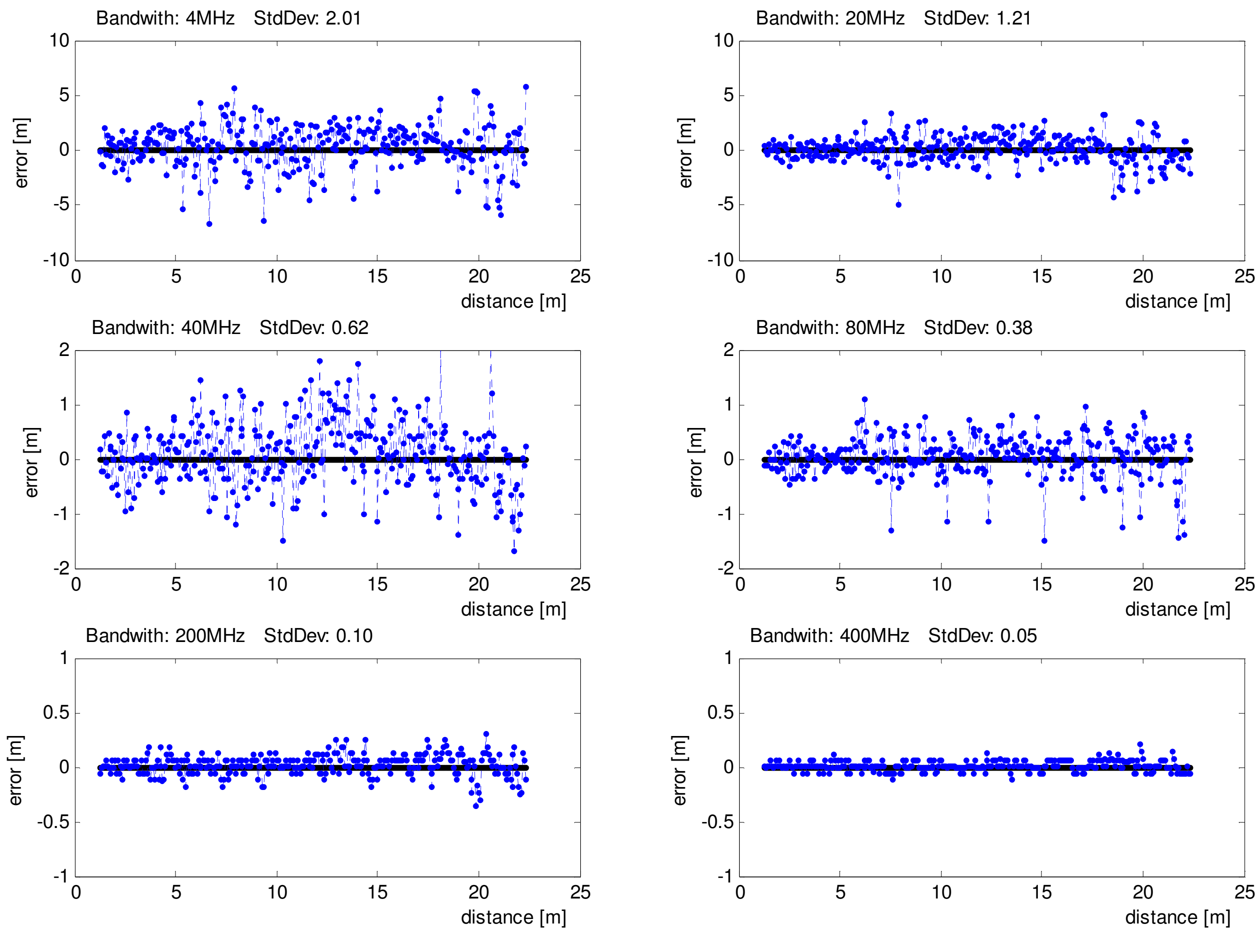

Figure 74: Estimation error of the distance between car and VRU without an obstacle
The simulation was done with different bandwidth (BW 4-400MHz) and a SIR of 2dB. The SNR depends on the distance and is in the range of 0 – 20 dB.

	SIR [dB]				
BW [MHz]	**0**	**2**	**4**	**8**	**14**
4	3,76	2,01	1,48	1,12	0,60
20	1,46	1,21	0,88	0,53	0,29
40	0,82	0,62	0,64	0,28	0,14
80	0,47	0,38	0,21	0,15	0,09
200	0,15	0,10	0,07	0,05	0,03
400	0,06	0,05	0,04	0,05	0,03

Table 16: Standard deviation of the estimated distance car <-> VRU without an obstacle [m]

The accuracy of the distance estimation is strongly related to bandwidth (BW): The higher the bandwidth, the better the resolution. Whereas the error is in the range of up to 6 m for a bandwidth of 4 MHz, it goes down to below 0,2 m in the case of 400 MHz.

5.1.3.3. Simulation of distance measurements using RTOF with an obstacle

This chapter describes the simulation results for the estimation of the distance between car and VRU using RTOF with an obstacle in the LOS.

The simulation was done with different bandwidths between 4 and 400 MHz and different power of the scatterers, SIR between 0 and 14 dB. As the obstacle causes an attenuation of the LOS these results in a further reduction of the SIR. The SNR depends on the distance and is in the range between 0 and 20 dB.

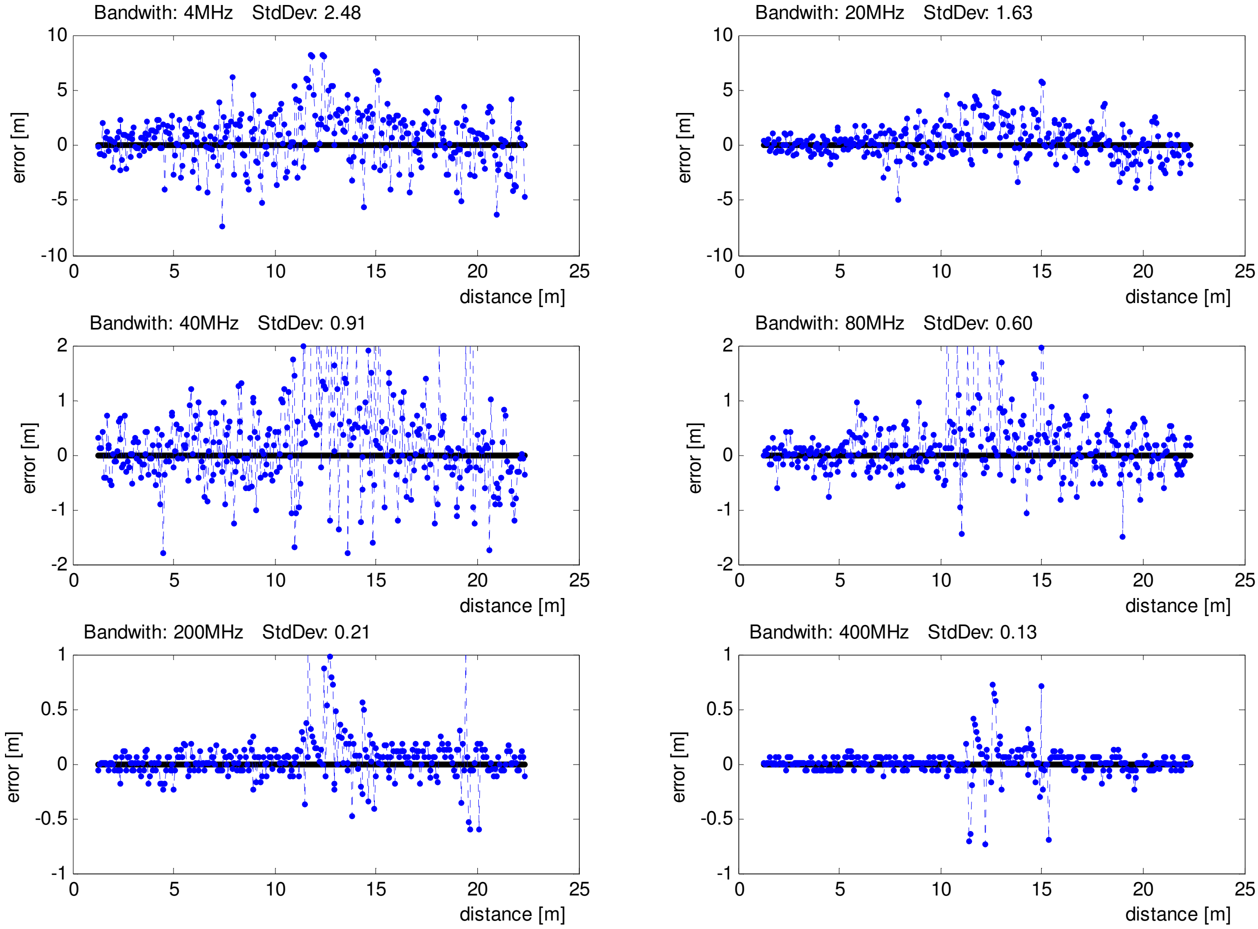

Figure 75: Estimation error of the distance between car and VRU with an obstacle The simulation was done with different bandwidth (BW 4-400MHz) and a SIR of 2dB. The SNR depends on the distance and is in the range of 0 – 20 dB.

	SIR [dB]				
BW [MHz]	**0**	**2**	**4**	**8**	**14**
4	3,08	2,48	2,03	1,64	1,60
20	2,07	1,63	1,31	0,96	0,71
40	1,00	0,91	0,70	0,64	0,50
80	0,81	0,60	0,62	0,52	0,46
200	0,40	0,21	0,22	0,41	0,24
400	0,20	0,13	0,17	0,40	0,28

Table 17: Standard deviation of the estimated distance car <-> VRU with an obstacle [m] The simulation was done with different bandwidth (BW 4-400MHz) and different power of the scatterers (SIR 0 – 14dB). The SNR depends on the distance and is in the range of 0 – 20 dB.

This project has been co-funded by the European Commission DG-Information Society and Media in the 6th Framework Programme. The content of this publication is the sole responsibility of the project partners listed herein and does not necessarily represent the view of the European Commission or its services.

The accuracy of the distance estimation is strongly related to bandwidth (BW): The higher the bandwidth, the better the resolution. Whereas the error is in the range of up to 8 m for a bandwidth of 4 MHz, it goes down to below 0,8 m in the case of 400 MHz.

In comparison with ch. 5.1.3.2, the figure above shows an increased error in distance measurements when the LOS component is occluded by an obstacle. In these cases a post processing algorithm using information from the undisturbed past can reduce the errors.

5.1.3.4. RTOF-based triangulation without an obstacle

This chapter describes the simulation results for the estimation of the position relative to the road using triangulation without an obstacle using two distance measurements obtained using RTOF.

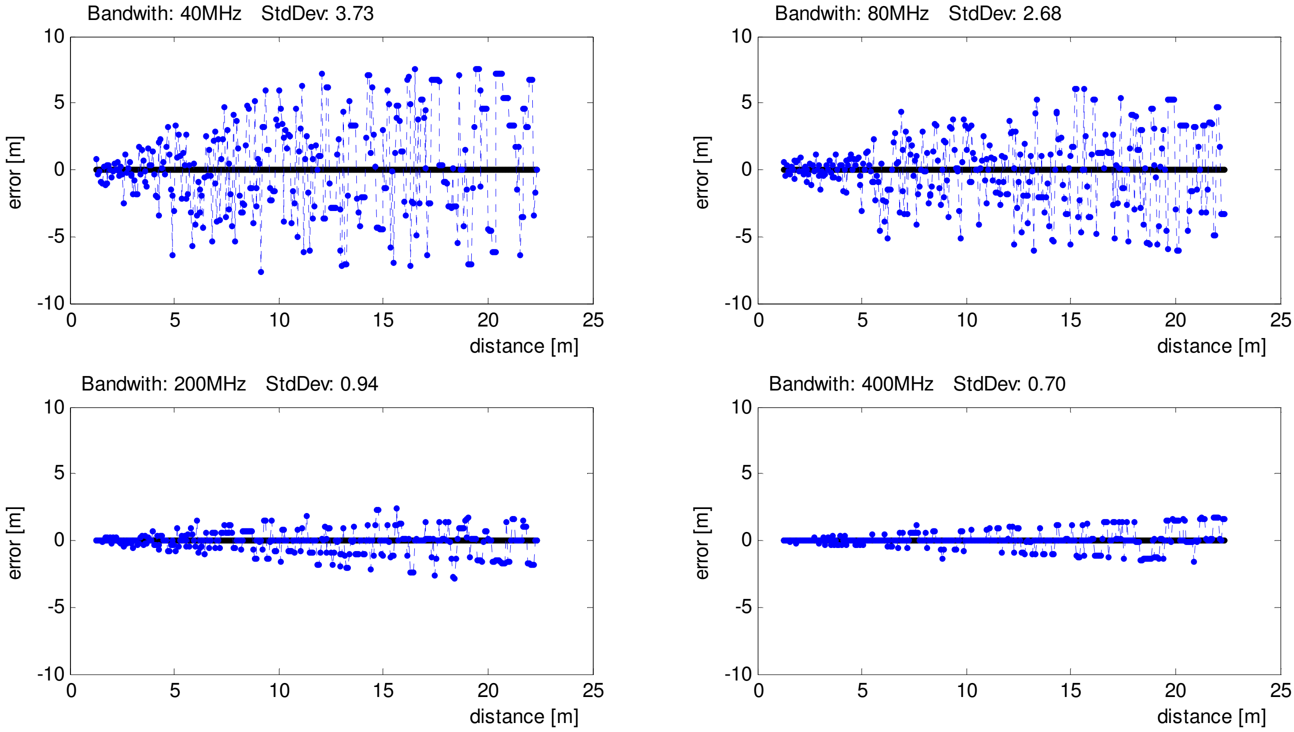

Figure 76: Estimation error of the VRU position relative to the road using triangulation without an obstacle
The simulation was done with different bandwidth (BW 4-400MHz) and a SIR of 2dB. The SNR depends on the distance and is in the range of 0 – 20 dB.

	SIR [dB]				
BW [MHz]	**0**	**2**	**4**	**8**	**14**
40	3,43	3,73	3,00	3,05	2,05
80	2,85	2,68	2,34	1,76	1,06
200	1,34	0,94	0,77	0,71	0,38
400	0,73	0,70	0,49	0,21	0,03

Table 18: Standard deviation of estimated position relative to the road using triangulation without an obstacle [m]
The simulation was done with different bandwidtsh (BW 4-400MHz) and different powers of the scatterers (SIR 0 – 14dB). The SNR depends on the distance and is in the range of 0 – 20 dB.

The accuracy of the distance estimation is strongly related to bandwidth (BW): The higher the bandwidth, the better the resolution. Whereas the error is in the range of up to 6 m for a bandwidth of 4 MHz, it goes down to below 2 m in the case of 400 MHz.

This project has been co-funded by the European Commission DG-Information Society and Media in the 6th Framework Programme. The content of this publication is the sole responsibility of the project partners listed herein and does not necessarily represent the view of the European Commission or its services.

5.1.3.5. RTOF-based triangulation with an obstacle

This chapter describes the simulation results for the estimation of the position relative to the road using triangulation with an obstacle using two distance measurements obtained using RTOF.

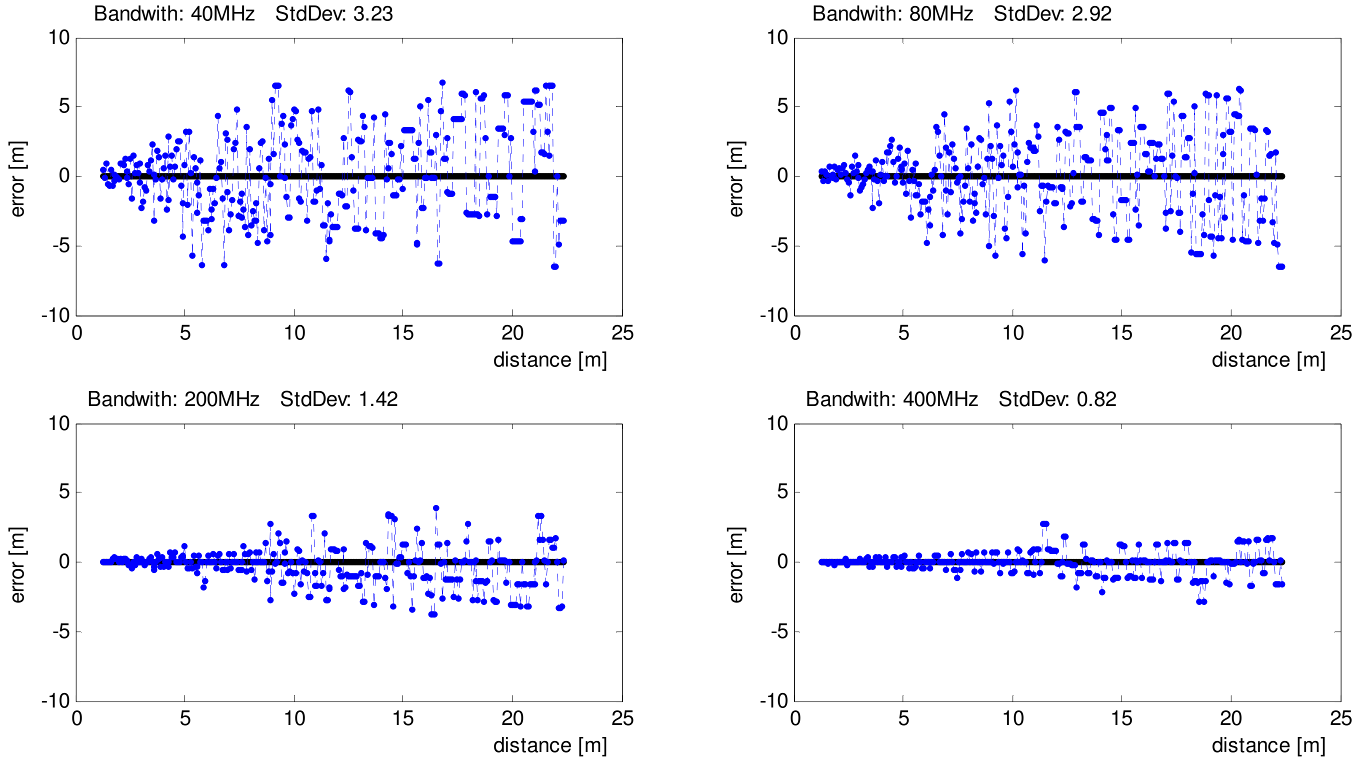

Figure 77: Estimation error of the VRU position relative to the road using triangulation with an obstacle
The simulation was done with different bandwidths (BW 4-400MHz) and a SIR of 2dB. The SNR depends on the distance and is in the range of 0 – 20 dB.

	SIR [dB]				
BW [MHz]	**0**	**2**	**4**	**8**	**14**
40	3,80	3,23	3,19	3,23	2,10
80	3,40	2,92	2,64	2,04	1,77
200	1,68	1,42	1,12	0,94	0,96
400	1,11	0,82	0,82	0,66	0,66

Table 19: Standard deviation of the estimation position relative to the road using triangulation with an obstacle [m]
The simulation was done with different bandwidths (BW 4-400MHz) and different powers of the scatterers (SIR 0 – 14dB). The SNR depends on the distance and is in the range of 0 – 20 dB.

The accuracy of the distance estimation is strongly related to bandwidth (BW): The higher the bandwidth, the better the resolution. Whereas the error is in the range of up to 6 m for a bandwidth of 4 MHz, it goes down to below 2 m in the case of 400 MHz.

In comparison with ch. 5.1.3.4, the figure above shows a comparable error in distance measurements when the LOS component is occluded by an obstacle.

This project has been co-funded by the European Commission DG-Information Society and Media in the 6th Framework Programme. The content of this publication is the sole responsibility of the project partners listed herein and does not necessarily represent the view of the European Commission or its services.

5.1.3.6. AOA- and distance based estimation without an obstacle

This chapter describes the simulation results for the estimation of the position relative to the road using one AoA measurement and one distance measurement without an obstacle in the LOS.

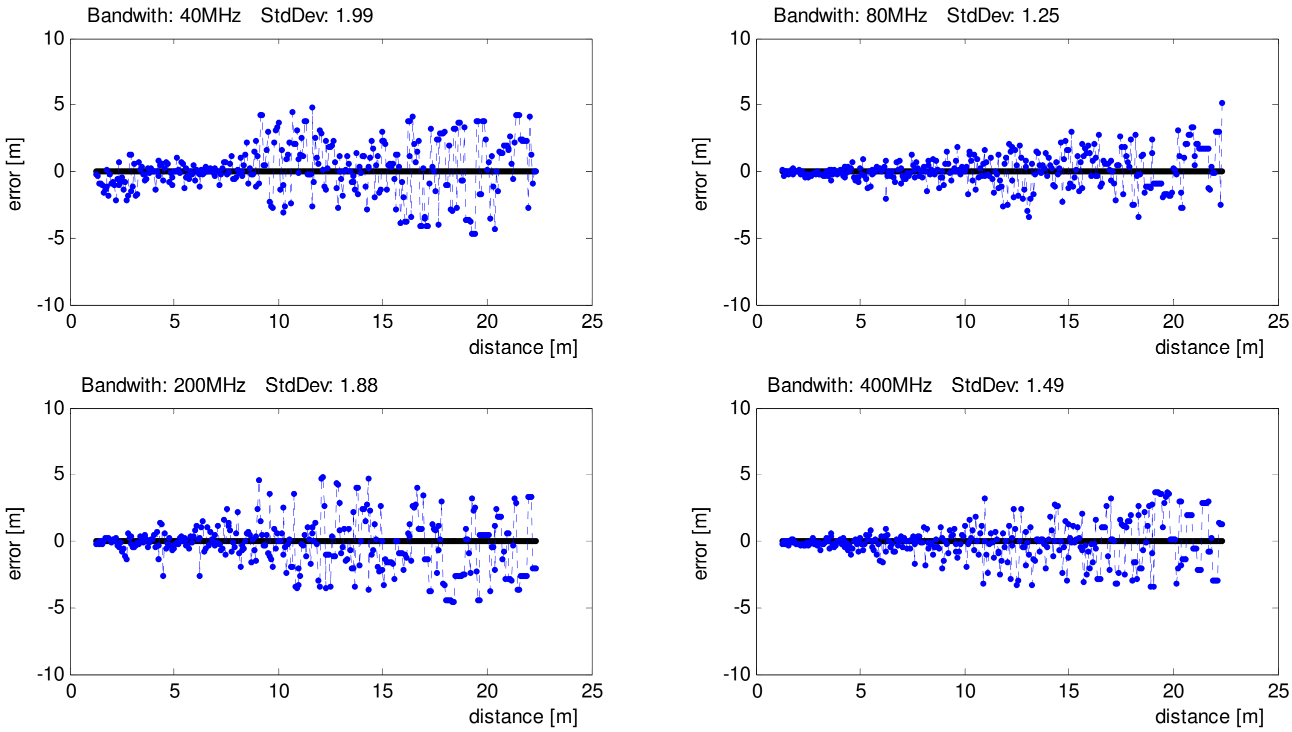

Figure 78: Simulation results of the scenario depicted above without an obstacle. The simulation was done with different bandwidths (BW 40-400MHz) and a SIR of 2dB. The SNR depends on the distance and is in the range of 0 – 20 dB.

	SIR [dB]				
BW [MHz]	**0**	**2**	**4**	**8**	**14**
40	1,79	1,99	2,12	1,82	1,93
80	1,45	1,25	1,49	1,40	1,45
200	1,98	1,88	1,89	2,13	1,90
400	1,34	1,49	1,38	1,28	1,50

Table 20: Simulation results of the scenario depicted above without an obstacle [m] The simulation was done with different bandwidths (BW 4-400MHz) and different powers of the scatterers (SIR 0 – 14dB). The SNR depends on the distance and is in the range of 0 – 20 dB.

In this case, the accuracy of the distance estimation is hardly related to bandwidth (BW): The higher the bandwidth, the better the resolution. Whereas the error is in the range of up to 6 m for a bandwidth of 4 MHz, it goes down to approx. 4 m in the case of 400 MHz.

This project has been co-funded by the European Commission DG-Information Society and Media in the 6th Framework Programme. The content of this publication is the sole responsibility of the project partners listed herein and does not necessarily represent the view of the European Commission or its services.

5.1.3.7. AOA- and distance based estimation with an obstacle

This chapter describes the simulation results for the estimation of the position relative to the road using one AoA measurement and one distance measurement when the LOS is occluded by an obstacle.

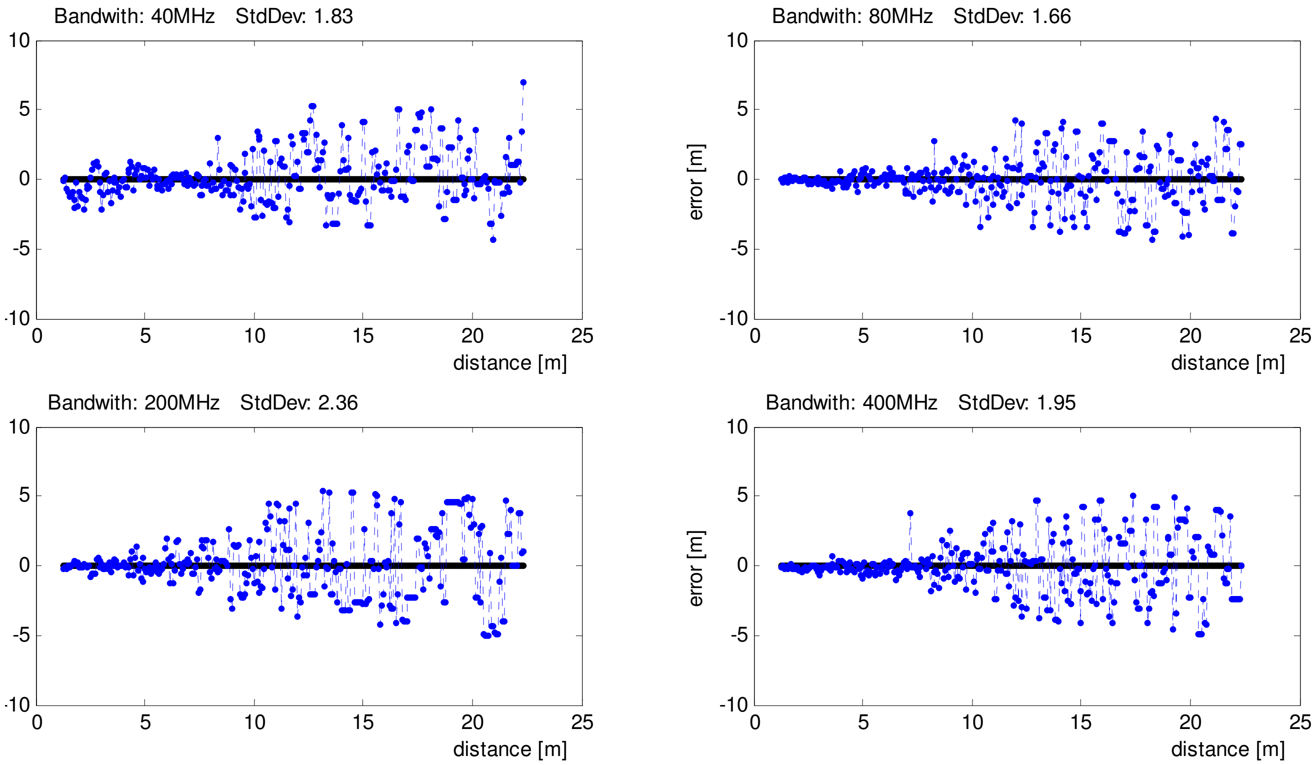

Figure 79: Simulation results of the scenario depicted above with an obstacle. The simulation was done with different bandwidths (BW 40-400MHz) and a SIR of 2dB. The SNR depends on the distance and is in the range of 0 – 20 dB.

	SIR [dB]				
BW [MHz]	**0**	**2**	**4**	**8**	**14**
40	2,20	1,83	2,26	2,10	2,30
80	1,77	1,66	1,76	1,74	1,75
200	2,09	2,36	2,25	2,42	2,73
400	1,96	1,95	1,97	1,97	2,26

Table 21: Simulation results of the scenario depicted above without an obstacle [m] The simulation was done with different bandwidths (BW 4-400MHz) and different powers of the scatterers (SIR 0 – 14dB). The SNR depends on the distance and is in the range of 0 – 20 dB.

In this case, the accuracy of the distance estimation is hardly related to bandwidth (BW): The higher the bandwidth, the better the resolution. Whereas the error is in the range of up to 6 m for a bandwidth of 4 MHz, it goes down to approx. 5 m in the case of 400 MHz.

In comparison with ch. 5.1.3.6, the figure above shows a comparable error in distance measurements when the LOS component is occluded by an obstacle.

This project has been co-funded by the European Commission DG-Information Society and Media in the 6th Framework Programme. The content of this publication is the sole responsibility of the project partners listed herein and does not necessarily represent the view of the European Commission or its services.

5.1.3.8. AOA- and distance based triangulation with post processing without an obstacle

This chapter describes the benefits of post processing for the simulation results for triangulation relative to the road using one AoA measurement and one distance measurement without an obstacle in the LOS.

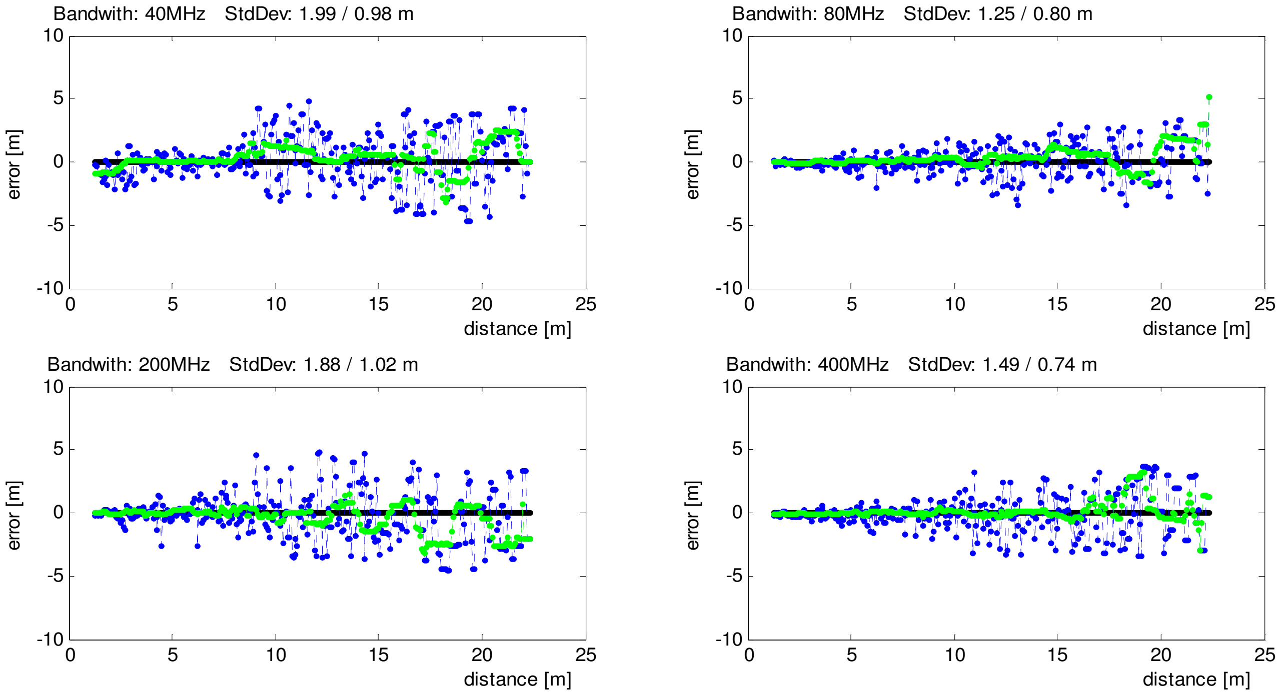

Figure 80: Simulation results of the scenario depicted above with an obstacle. Parameters are BW 40-400MHz, SIR 2dB, SNR 0 – 20 dB. The green curve is the result of a post processing taking into account the trajectory of VRU.

5.1.4. Summary of the results

Table 22 shows an overview over possible methods for localisation in WATCH-OVER. If triangulation is chosen, the bandwidth of 40 MHz seems to be a minimum to get helpful information for the driver. Higher bandwidths provide better resolution.

In the case of estimation of the AoA and the distance, the result is mainly dependent on the accuracy of the AoA because the angle is close to 90° so that an error in distance from the car to the VRU leads to a small error in the distance to the roadside. The estimation of the AoA again is dependent on the carrier frequency and not on the bandwidth. So the results do not vary much in relation to the bandwidth.

	triangulation		AoA+distance	
BW [MHz]	**estimated**	**+post proc.**	**estimated**	**+post proc.**
40	3,73	1,87	1,99	0,98
80	2,68	1,20	1,25	0,80
200	0,94	0,49	1,88	1,02
400	0,70	0,43	1,49	0,74

Table 22: Simulation results of the scenario without an obstacle with and without post processing The simulation was done with different bandwidths (BW 40-400MHz) and a SIR of 2dB. The SNR depends on the distance and is in the range of 0 – 20 dB.

5.1.5. Suitability to WATCH-OVER

The WATCH-OVER system requires an estimated accuracy of the VRU distance to the road of about one meter. If the VRU is still quite far away an accuracy of two meters could also be helpful.

This project has been co-funded by the European Commission DG-Information Society and Media in the 6th Framework Programme. The content of this publication is the sole responsibility of the project partners listed herein and does not necessarily represent the view of the European Commission or its services.

As it can be seen in the simulation results above, an accuracy of one meter seems to be possible using the method of estimation AOA in addition to the estimation of the distance. If the method of triangulation with two estimated distances is used the accuracy is very dependent to the used bandwidth. The minimum required bandwidth seems to be 40 MHz. In this case the scatterer power should be relatively low (SIR > 8dB). This is fulfilled in open places and rural areas where only a few scatterer areas exist.

BW [MHz]	Triangulation SIR: 2 dB	Triangulation SIR: 8 dB	AoA+distance SIR: 2 dB
40	1,87	1,35	0,98
80	1,20	0,69	0,80
200	0,49	0,33	1,02
400	0,43	0,16	0,74

Table 23: Simulation results with post processing without an obstacle [m]
The simulation was done with different bandwidth (BW 4-400MHz) and a SIR of 2dB (8dB). The SNR depends on the distance and is in the range of 0 – 20 dB.

5.2. Approach 2: UWB-system using AOA

5.2.1. General Description

Today, several UWB systems for communication purposes are already available on the market or under development. A selection of those companies was approached in order to identify the suitability for ranging applications. However, it was found out that the larger companies, i.e. Freescale and Infineon, concentrate on the market for consumer electronics and thus, showed no further interest in ranging applications. Consequently, no access to low-level information from the physical layer was provided.

Therefore, closer contact was set-up to IMST [75], who has developed a low data rate localisation system based on UWB.

The development was partially supported within the PULS-ON project with funds from the state government in Nordrhein-Westfalen (Germany) and the European Commission (FKZ 005-0210-0005) [75].

One typical application scenario is shown in Figure 81. Base stations are dislocated around a building at known positions. They are connected to a control station via standard wireless communication (IEEE802.11h). Communication to mobile stations within the building is based on a 2.4 GHz UWB-transmission, which can be used for localisation as well. It is based on the AOA-approach, described in ch. 4.3.

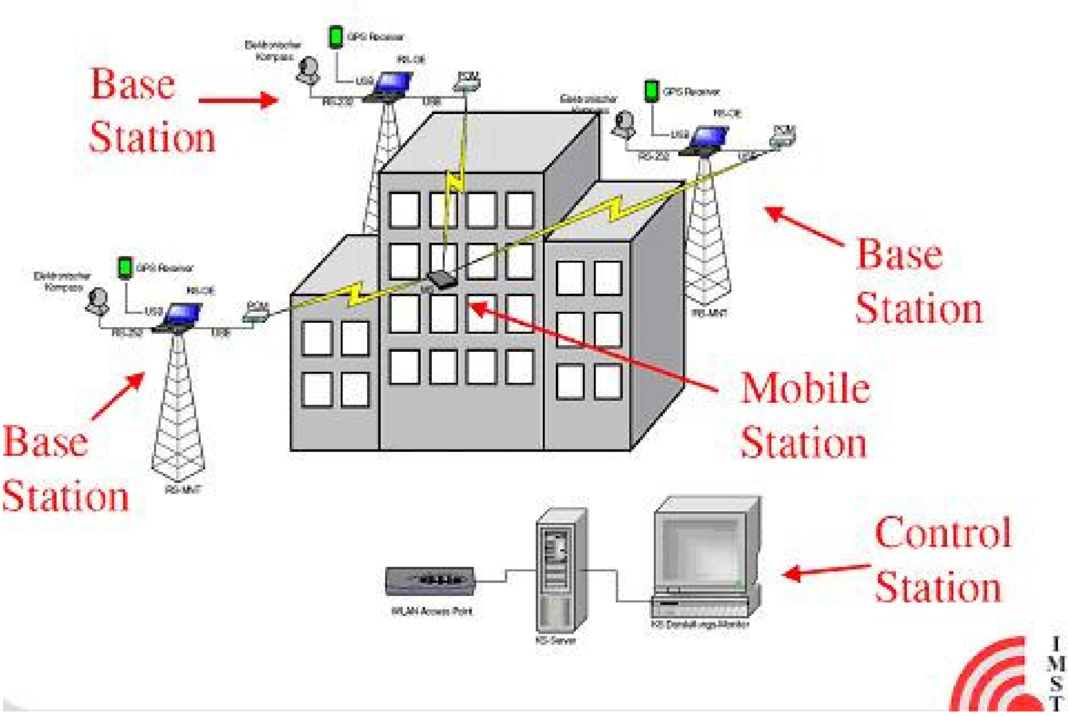

Figure 81: System architecture of Puls-On project [75]

5.2.2. System Description

5.2.2.1. Mobile station

The mobile station mainly consists of a transmitter. It is based on a packet wise transmission, with a packet length of 2000 symbols. Out of those, 500 symbols are used for acquisition and training, and 1500 symbols for data transmission. Single pulses have a duration of 10 ns. Every two pulses form a frame within a QPSK-TR signalling. The frame duration is 220 ns, which leads to a packet length of 0.44 ms.

The basic packet rate is 2.5 Hz. It can be reconfigured.

Figure 82 shows photos of the 1st and 2nd generation mobile stations. Figure 83 shows their internal architecture.

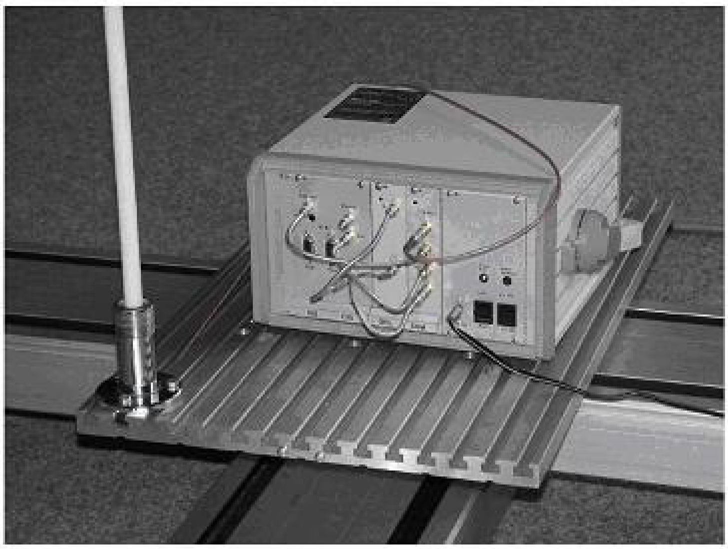

Figure 82: Iltis mobile stations from IMST: 1st generation (left) and 2nd generation (right) [76]

This project has been co-funded by the European Commission DG-Information Society and Media in the 6th Framework Programme. The content of this publication is the sole responsibility of the project partners listed herein and does not necessarily represent the view of the European Commission or its services.

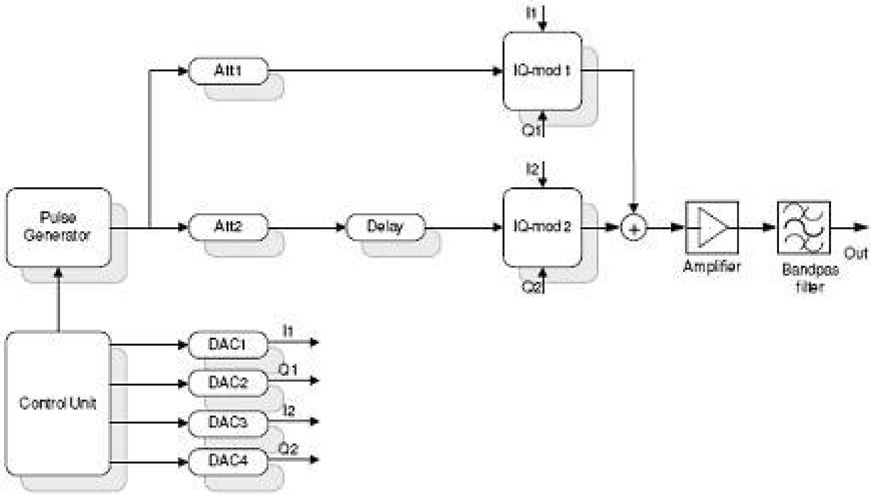

Figure 83: Internal architecture of Iltis mobile stations [75]

5.2.2.2. Base station

The base station receives the data packets from the mobile stations and demodulates it. In addition, it determines the angle of arrival (AOA). Pictures of the base station are shown in Figure 84. In order to achieve this, the phase differences of signal measured at the different ports of the antenna system are evaluated, as shown in Figure 85. The internal architecture of a base station in depicted in Figure 86.

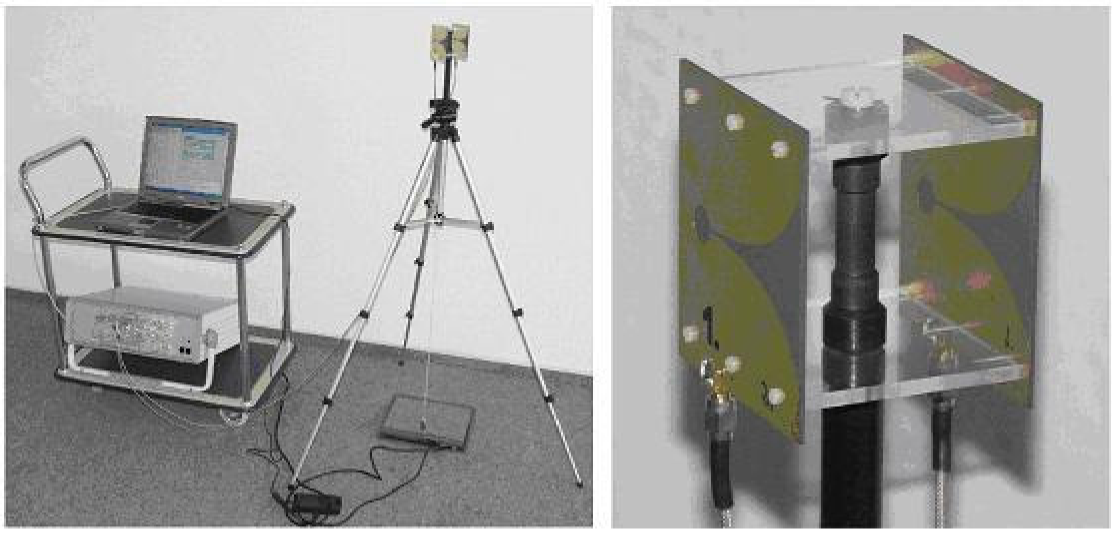

Figure 84: Iltis base stations from IMST [75]

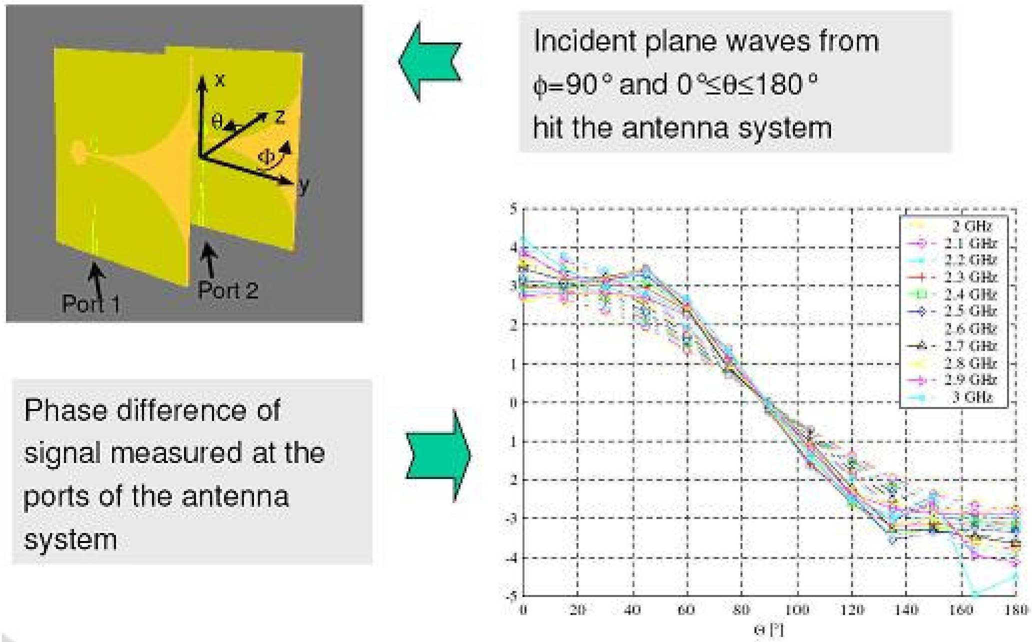

Figure 85: Determining the angle of arrival in an Iltis base station from IMST [75]

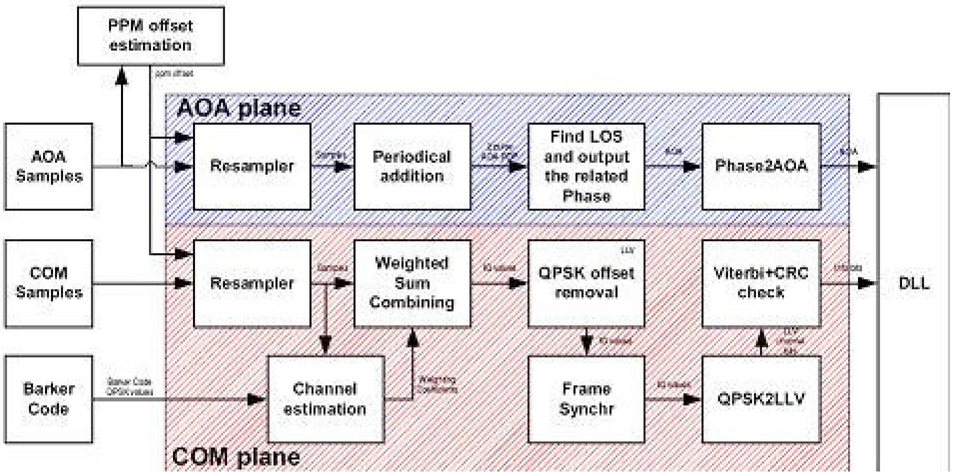

Figure 86: Internal architecture of Iltis base stations [75]

5.2.3. Measurements

Two measurement days were performed with the Iltis system. Due to IMST internal reasons, the results of these measurements are under NDA. Therefore, it is not possible to publish the results within this report. It is possible however to highlight some general notes in the following paragraph.

5.2.4. Suitability to WATCH-OVER

The results from the measurements show a reasonable suitability for eSafety applications in general. Main aspects that can be derived from the measurements are:

- The system shows good accuracy for smaller angles. Due to the fact that the antenna design was optimised for original target application, the accuracy deteriorated at larger angles due to reflections at one of the antennas.
- The system shows a reasonable range when used without obstacles. When metallic obstacles, e.g. cars, are in between mobile and base stations, severe degradation of the signal could be observed.
- Hardware is available with mobile stations at a reasonable size being on the short-term roadmap.

5.3. Approach 3: CSS based systems

5.3.1. General Description

The following basic characteristics promise good results for localisation from chirp based systems.

- The chirp waveform of the chirp signals is flat in time and frequency domain simultaneously.
- The chirp waveform has a sharp correlation peak
- The chirp waveform has a flat cross correlation floor

Therefore, the time shift between overlapping chirp signals can be transformed into a continuous frequency signal. In doing so, very good ranging accuracy seems to be achievable, even with reduced bandwidth. A pure correlation peak detection may deliver reasonable results even in multipath environment.

5.3.2. Measurements

Extensive measurements were performed with one CSS-based system, dubbed nanoLOC [85]. They can be found in the attachment A to this report.

5.3.3. Suitability to WATCH-OVER

Based on the experiences with the nanoLOC system [85] in the above mentioned measurements, it can be stated that it shows a good suitability for eSafety applications in general and promises a very good fit for the WATCH-OVER use case. This is due to the following characteristics:

- It shows good stability of communication also under adverse conditions and larger ranges.
- It shows a reasonable accuracy also for the extrapolation use case of WATCH-OVER.
- It is available as an ASIC from a European based company with excellent support delivered in the phase of this scouting activity.

5.4. Approach 4: Self Localisation

5.4.1. Achievable Accuracy with SBAS

Some measurements were performed to figure out the achievable accuracy under real life conditions, two at a fixed point and four in a moving car. A u-blox Antaris EvalKit GPS receiver [90] was used with 16 channels, 4 Hz update rate, and potential EGNOS/WAAS support.

5.4.2. Measurement #1: static measurement scenario, good conditions

The conditions of this first measurement are described as follows:

- Fixed place
- Good conditions (no buildings etc. close to the receiver)
- In average 9 satellites in view (range from 7 to 11 satellites)

After one hour with 1 hour with 14239 measurements, the results shown in Table 24 could be observed.

Std deviation horizontal [m]	0.86
Std deviation vertical [m]	2.35
Std deviation circular [m]	2.50

Table 24: Accuracy of results for self-localisation (measurement #1) static measurement scenario, good conditions)

Obviously, the horizontal accuracy is better than the vertical one. The reason for that is in the general geometrical configuration of the satellites.
The plots in Figure 87 show LEP/CEP values and the maximum distances for 95 % of the measurements.

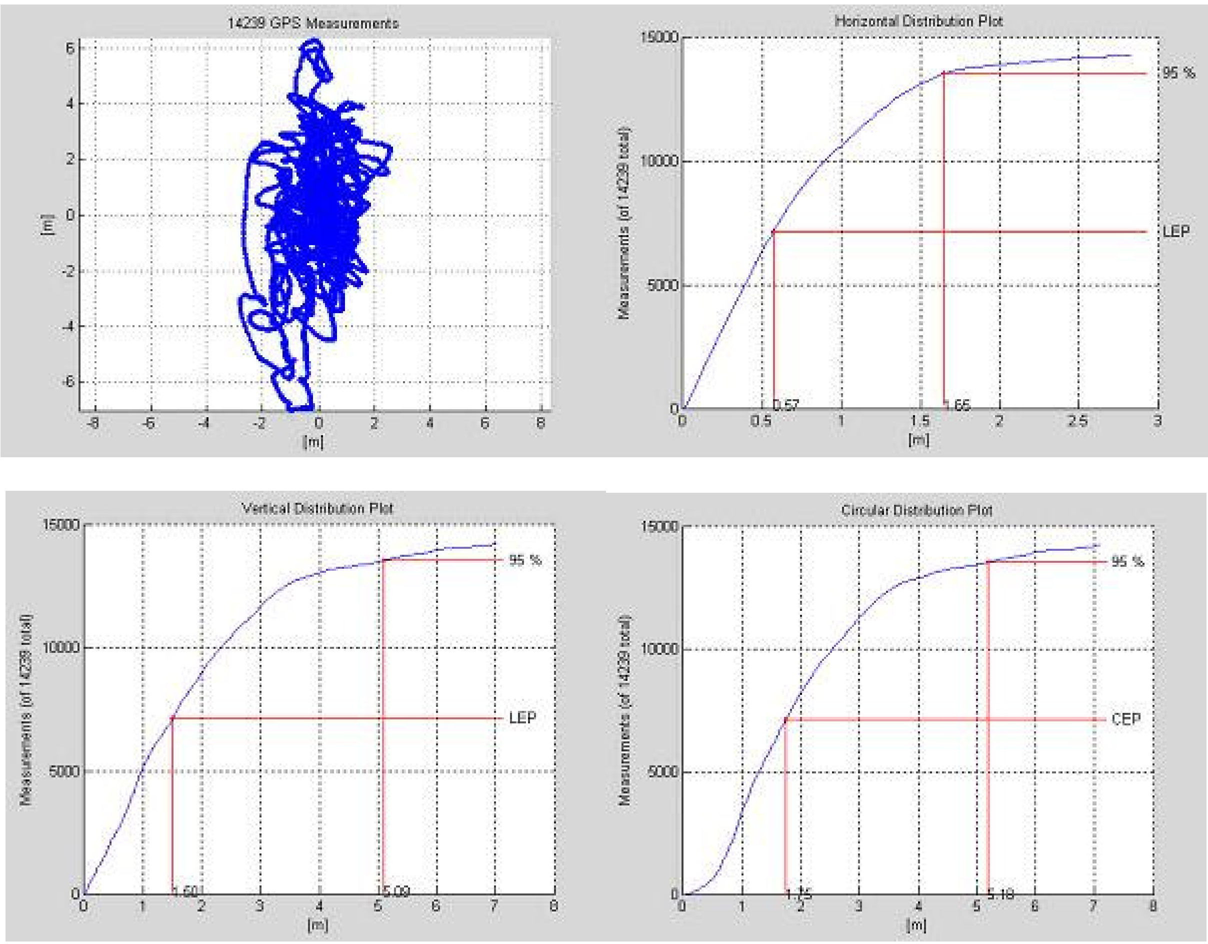

Figure 87: Accuracy of results for self-localisation (measurement #1) static measurement scenario, good conditions)

5.4.3. Measurement #2: static measurement scenario, bad conditions

The conditions of this second measurement are described as follows:

- Fixed place
- Bad conditions (close to a 25 m high building, sometimes not enough satellites (<3) in view)
- In average 4 satellites in view (range from <3 to 5 satellites)

After one hour with 1 hour with 12868 measurements, the results shown in Table 25 could be observed.

Std deviation horizontal [m]	23.59
Std deviation vertical [m]	11.29
Std deviation circular [m]	26.15

Table 25: Accuracy of results for self-localisation (measurement #2) static measurement scenario, bad conditions

In Figure 88, we see a significant deterioration of the measurement results by an enlargement of the standard deviation of about factor 10.

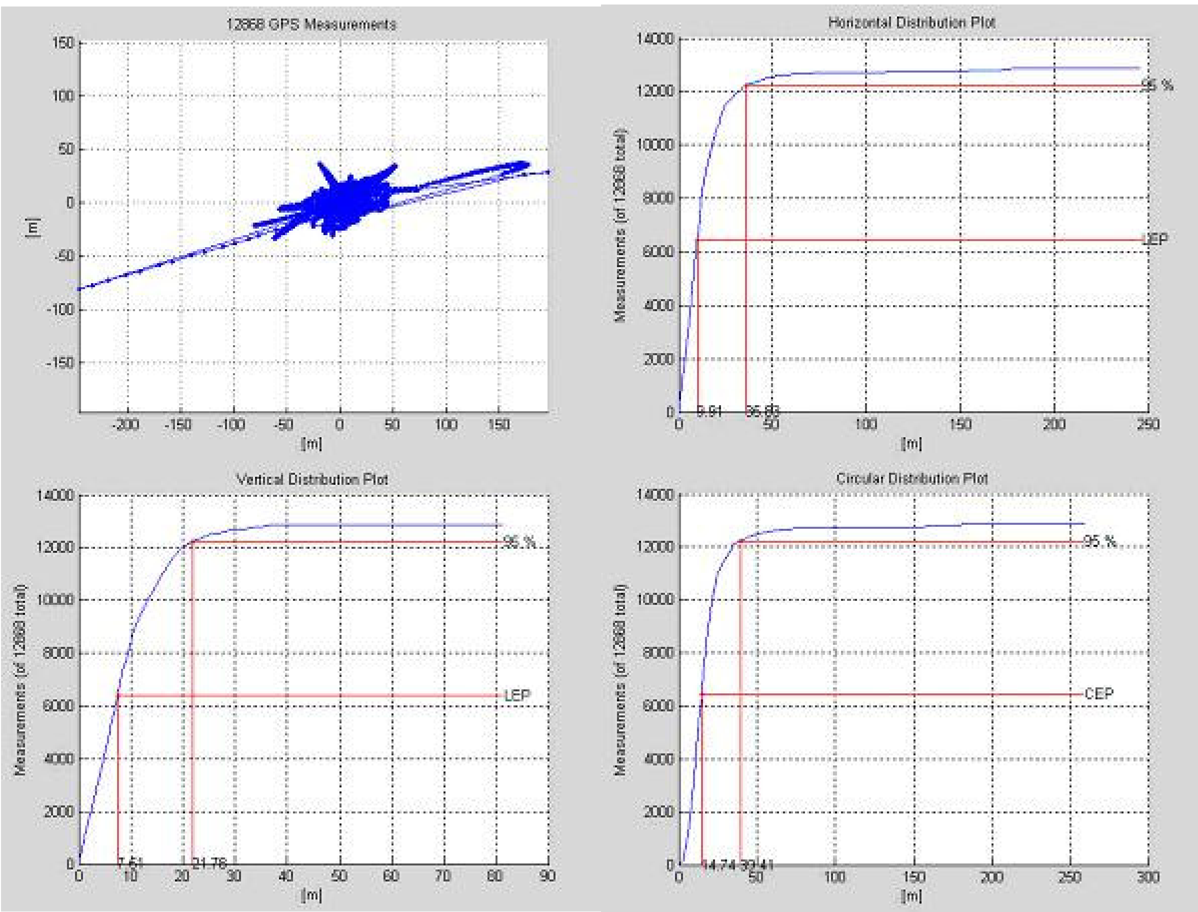

Figure 88: Accuracy of results for self-localisation (measurement #2) static measurement scenario, bad conditions)

5.4.4. Measurement #3: dynamic measurement scenario

The conditions of this third measurement are described as follows:

- The GPS receiver was mounted on a moving car
- The car drove 4 times the same road
- It was tried to drive on the roads at the same lateral position. So it can be assumed that the maximum variation for the lateral position does not exceed 1 m in reality.
- The time distance between two track logs are approx. 30 min

Figure 89 illustrates the difficulties in urban areas with different accuracy and missing measurements (the different logs are marked with white, red, green and blue dots).

This project has been co-funded by the European Commission DG-Information Society and Media in the 6th Framework Programme. The content of this publication is the sole responsibility of the project partners listed herein and does not necessarily represent the view of the European Commission or its services.

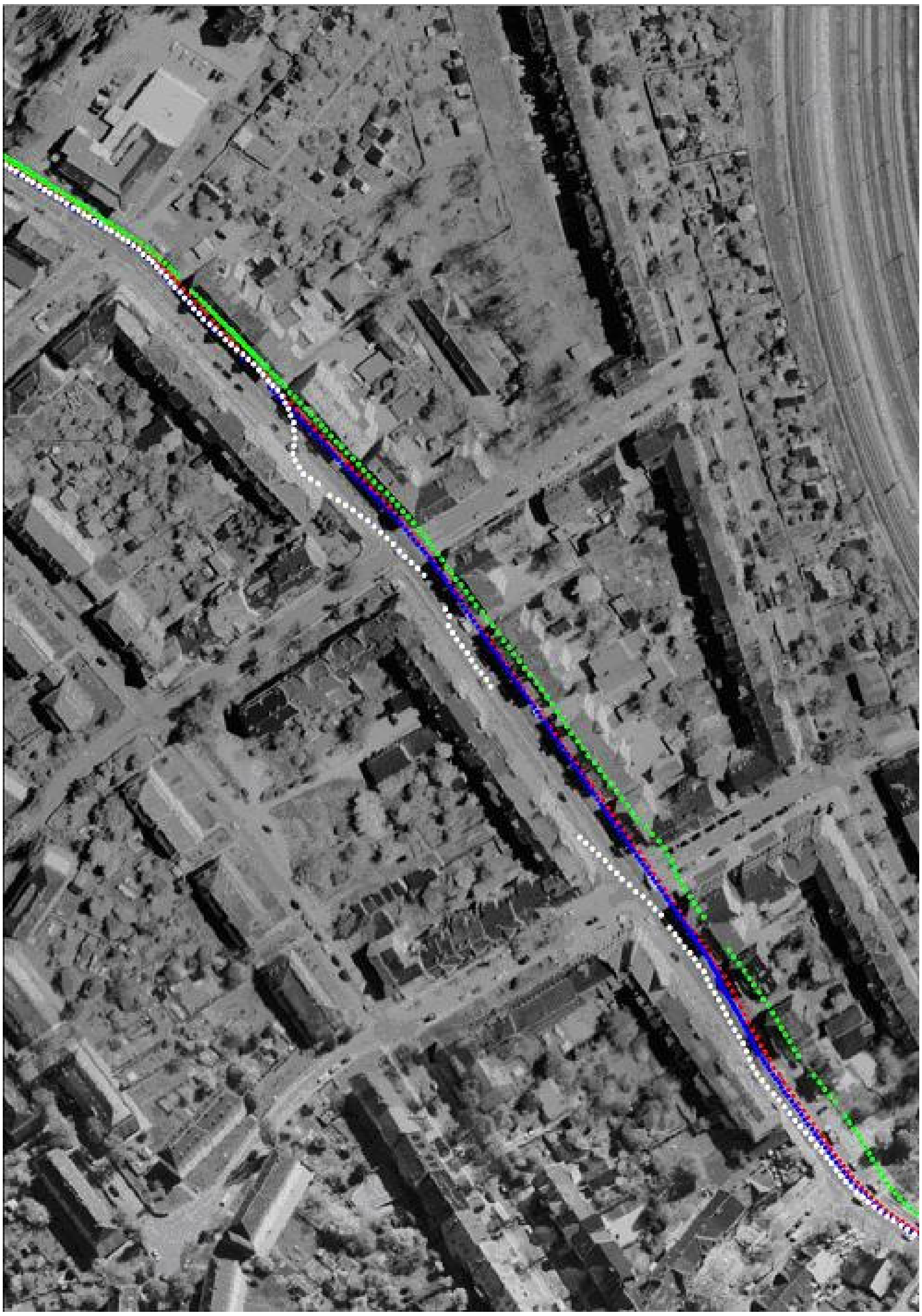

Figure 89: Accuracy of results for self-localisation (measurement #3) dynamic measurement scenario

5.4.5. Suitability to WATCH-OVER

The results from the measurements are ambiguous with regard to the suitability for eSafety applications.

- It is negative that the absolute accuracy is in the range of only a couple of meters, which is, far below the required accuracy (cf. ch. 2.1.2.6 ff).
- However, two positive aspects can be identified:
    - It can be assumed that the relative accuracy between two identical GPS receivers is much better that the absolute accuracy shown above, when both receivers work

simultaneously in very close distances. However, this supposition should be verified in further measurements.

- In addition, it can be assumed that not only an increasing number of vehicles, but also a rapidly increasing number of portable devices come with integrated GPS receivers. This is especially anticipated for mobile phones.

If the latter assumption will hold true, it makes very good sense to include the additional GPS-based information into the sensor fusion, when it comes virtually for free.

5.5. Approach 5: RFID

5.5.1. General Description

Within the WATCH-OVER project, a demonstrator was built for illustration purposes that employs a set of readers to be attached to the side of a vehicle, and a tag to be attached to a VRU (see Figure 90). Attaching more than one radio-receiver to a given vehicle provides a means to inform the vehicle's driver about the relative position of the VRU. Based on this, the driver can take appropriate action. The demonstrator revolves around the scenario in which a VRU (bicyclist) is travelling alongside the vehicle, which is about to take a turn.

5.5.2. Measurements

The radius of the reader's proximity zone is 2 meters. To achieve the desired pronounced proximity effect, the wavelength has to be larger than the zone's radius. Hence the signal frequency must be less than 150 MHz. In this case, a frequency of 27 MHz was employed.

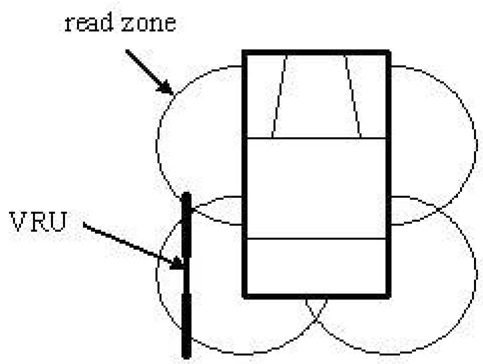

Figure 90: Demonstrator scenario

An example of a succession of indications is given in Figure 91. Because of the presence of the vehicle's body, the signal strength was seen to vary by a factor of two which affects the extent of the proximity zone and even its shape. By setting the transmission power, the zone's extent can be adjusted.

Figure 91: Left-rear, left-front indication

5.5.3. Suitability to WATCH-OVER

During the measurements, it quickly became clear that RFID based systems are not suitable to the range of WATCH-OVER use cases. As mentioned, its range is limited to only a couple of meters. Consequently, only those use cases where VRU and vehicle are in very close proximity, can be covered by RFID.

In addition, the accuracy of the RSSI-based RFID-detectors is strongly dependant from the actual environment. Especially attenuators and reflectors must be taken into account.

6. Recommendations

The goal of the WATCH-OVER project is the design and development of a cooperative system for the prevention of accidents involving vulnerable road users in urban and extra-urban areas. The innovative concept is represented by an on board platform and by a vulnerable user module. The system is based on short range wireless communication and vision sensors.
In the first phase of this project Project (Task 4.1: "Communication technologies scouting and selection" within the Work Package WP4: "Communication and Sensing Technologies"), a technology scouting for the selection of the communication technology was performed. The outcome of these efforts is collected within this document.

From the scouting activities with the WATCH-OVER project, the following overall situation could be derived:

- It is assessed that communication based localisation and information flow between VRU and vehicle provide an additional means to increase the accuracy of detection, ranging, and localisation.
- A broad variety of technologies exist. Due to cost, size, energy consumption and availability reasons, Short Range Wireless Communication (SRWN) are a major candidate to provide communication and localisation.
- Technologies and products for SRWN rapidly evolve. A broad choice is available for communication purposes.
- From this large choice, only selected technologies are inherently suitable to offer ranging and localisation.
- The number of technologies can be further reduced when two additional parameters are regarded:
  - The accuracy of many of the inherently location-capable systems is at a low level, so that the use cases of the WATCH-OVER project cannot be covered.
  - Practically all RF-systems working in the Gigahertz-range are theoretically capable to support ranging. However, for doing this they must be equipped with additional circuitry, which accesses the low-level, high-accuracy timing information at the signal input. As the design of an integrated circuit (IC) is far beyond the objectives and the means of the WATCH-OVER project. Therefore, it is only realistic to use existing hardware.

    Many of the ranging-capable systems are either only prototypes, or are addressing a different market.
    - This could be observed for most of the UWB-based products, where contacts to the manufacturers showed their meagre interest in applications beyond consumer electronics.
    - Unfortunately the same situation was encountered during the examination of other eSafety-related communication protocols and products.

Taking into account the above mentioned parameters and the requirements defined in ch. 2.1, the following technological solutions are ruled out.

- All RSSI-based systems are ruled out, as the achievable accuracy is far below the required levels. This is true for
  - pure IEEE802.15.4, as described in ch. 3.2.
  - current narrow-band Bluetooth-based systems, as described in ch. 3.4.
  - IEEE802.11 in both its native specification, but also in its eSafety-related version. I.e. the activities of DSRC and IEEE802.11p, which theoretically promise to be a major candidate also for the WATCH-OVER project, have no support for ranging and localisation, except the integrated RSSI-measurements. IEEE802.11 was examined in ch. 3.5.
  - RFID-based systems. Apart from the insufficient accuracy, RFID additionally suffers from the very limited range, as discussed in ch. 5.5.

- Angle-of-Arrival-(AOA)-based systems are ruled out, as they showed insufficient stability under non-line-of-sight-(NLOS)-conditions. Unfortunately this was also observed with Ultra-Wide-Band-(UWB)-transceivers (cf. ch. 5.2). As the detection of obstructed VRUs is one of the use cases described for the WATCH-OVER project, this approach also had to be ruled out.

Based on the evaluation done above, it is decided to further proceed with the following approaches:

- The CSS-based system, described in IEEE802.15.4a (cf. ch. 3.3), turns out to provide a good trade-off between bandwidth consumption, hardware efforts and achievable accuracy. This was evaluated under real-life conditions in extensive measurement sessions, reported in Annex I of this document.
  CSS-based systems are already available as an integrated circuit (IC), allowing low power, low footprint and flexible designs at reasonable cost. This IC is developed and produced by the Berlin-based company Nanotron [81]. Already during this first phase of technology scouting within the WATCH-OVER project, good support was delivered by this company, despite the fact there is no direct involvement in the project.
- UWB-systems promise a good accuracy, if time-of-flight measurements are used. This could be affirmed through various simulations, described in ch. 5.1).
  The simulation was oriented towards an UWB-emulator provided by ARCS. This system comes with a very generic approach and promises a very high flexibility. Furthermore, it is under direct support from one of the WATCH-OVER project partners.
- Systems for self-localisation allow an accuracy well below the level of the two relative ranging systems selected above (cf. ch. 5.4). However, due to their absolute positioning, they allow consistency checks and maps. As GPS / Galileo based systems for are assumed to come for free in future product generations, it makes good sense to include their information into the sensor fusion, as well.
  Product support from u-blox is envisaged.

During all the future efforts, the aspects of security and privacy must be considered.

7. References

[1] http://grouper.ieee.org/groups/802/11/index.html

[2] http://grouper.ieee.org/groups/802/15/

[3] http://grouper.ieee.org/groups/802/16/

[4] http://standards.ieee.org/

[5] http://standards.ieee.org/getieee802/

[6] A. Sikora, D. Lill, V.F. Groza, "Comparison of Internet and Dedicated Communication Protocols for Instrumentation and Measurement Systems using Short Range Wireless Networks", IMTC 2006 – Instrumentation and Measurement Technology Conference, Sorrento (Italy), April 2006.

[7] G. Montenegro, N. Kushalnagar: Transmission of IPv6 Packets over IEEE 802.15.4 Networks, http://www.ietf.org/internet-drafts/draft-ietf-6lowpan-format-01.txt.

[8] A. Klapproth, "TCP/IP über IEEE 802.15.4", Design & Elektronik Developer Forum "ZigBee & Co", Munich (Germany), 4. April 2006.

[9] D. Rahusen, "IPv6 über 802.15.4 – Status und Trends", Design & Elektronik Developer Forum "ZigBee & Co", Munich (Germany), 4. April 2006.

[10] A. Sikora, "Deploying IPv6 over IEEE802.15.4 Short Range Wireless Networks – Status and Trends", IFAC Workshop on Programmable Devices and Embedded Systems PDeS 2006, Brno (Czech Republic), 14.-16.2.2006.

[11] IEEE Std. 802.15.4 – 2003: Standard for Telecommunications and Information Exchange Between Systems – Local Area Metropolitan Area Networks – Specific Requirements - Wireless Medium Access Control (MAC) and Physical Layer (PHY) Specifications for Low Rate Wireless Personal Area Networks (WPAN), http://www.ieee802.org/15/pub/TG4.html.

[12] "Advanced Encryption Standard (AES)", available at: http://csrc.nist.gov/publications/fips/fips197/fips-197.pdf

[13] Nanotron Technologies GmbH, "nanoNET Chirp-based Wireless Networks", White Paper, Version 1.02, available at (21.7.2006): http://www.nanotron.de/nanotron_intern/de/ ... … downloads/whitepaper/White_Paper_nanoNET.pdf

[14] C. Buck, R. Hach, „Chirp-basiertes Funkverfahren", Funkschau 22/2005, pp.45-46 (in German), available at (21.7.2006): http://www.funkschau.de/heftarchiv/pdf/2005/fs22/fs_0522_s45.pdf

[15] Nanotron Technologies GmbH, "nanoLOC Ranging Demonstrator: User Guide", Version 1.01, NA-06-0721-0377-1.01

[16] M. Vossiek, L. Wiebking, P. Gulden, J. Wieghardt, C. Hoffmann, P. Heide, „Wireless Local Positioning", IEEE microwave magazine, December 2003.

[17] NIST „Two Way Time Transfer",m available at (21.7.2006): http://tf.nist.gov/time/twoway.htm

[18] D. W. Hanson, "Fundamentals of Two-Way Time Transfer by Satellite", 43rd Annual Frequency Control Symposium, pp. 174-178, 1989, available at (21.7.2006): http://www.boulder.nist.gov/timefreq/general/pdf/836.pdf

[19] Benoit Denis, "UWB Localisation Techniques", IEEE 802.15-04/418r0, 10 August 2004.

[20] R. Roberts, "Ranging Subcommittee Final Report", IEEE P802.15.04-0581r0, 18.10.2004, available at (21.7.2006): http://grouper.ieee.org/groups/802/15/pub/04/15-04-0581-00-004a-ranging-subcommittee-final-report.doc

[21] R. Hach, "Symmetric Double Sided – Two Way Ranging", IEEE-15-05-0334-00-004a, available at (21.7.2006): http://www.ieee802.org/15/pub/2005/15-05-0334-00-004a-symetric-double-sided-two-way-ranging.ppt.

[22] M.I. Skolnik, "Introduction to Radar Systems", McGraw Hill, 2001.

[23] A. Sikora "wireless personal and local area networks", J.Wiley & Sons, 2003.

[24] A. Sikora, Lecture Notes "Wireless Communication Technologies", UCE Loerrach, 2006.

[25] http://www.bluetooth.org

[26] "Scatternet - Part 1: Baseband vs. Host Stack Implementation", White paper, available at: https://www.bluetooth.org/foundry/sitecontent/document/... Scatternet_Part_1-_Baseband_vs_Host_Stack_Implementation.

[27] "Specification of the Bluetooth System", available at: http://www.bluetooth.org/foundry/adopters/document/Core_v2.0_EDR/en/1/Core_v2.0_EDR.zip
[28] T.G.Xydis, "Security Comparison: Bluetooth Communications vs. 802.11", Bluetooth Security Experts Group, revised version 2-1-2002.
[29] "Vehicle Safety Communications Project", available at (29.7.2006): http://www-nrd.nhtsa.dot.gov/pdf/nrd-12/060419-0843/
[30] R. Roebuck, "DSRC Technology and the DSRC Industry Consortium (DIC) Prototype Team", available at (29.7.2006): www.itsa.org/itsa/files/pdf/DSRCICWhitePaper.pdf
[31] available at (30.7.2006): http://standards.ieee.org/cgi-bin/status?intelligent%20transportation
[32] FCC, "New Public Safety Applications and Broadband Internet Access among Uses Envisioned by FCC Authorisation of Ultra-Wideband Technology", Press Release, February 14, 2002, available at (30.7.2006): http://www.fcc.gov/Bureaus/Engineering_Technology/News_Releases/2002/nret0203.html
[33] MBOA, "Ultrawideband: High-speed, short-range technology with far-reaching effects", MBOA-SIG White Paper, September 1, 2004
[34] I. Oppermann, M. Hämäläinen, J. Iinatti, "UWB: Theory and Applications", J. Wiley & Sons, 2004.
[35] M. Wolf, J. Sachs, R. Zetik, „Ultra-Breitband: Highspeed für Funknetzwerke", available at (30.7.2006): http://www.tecchannel.de/entwicklung/grundlagen/429761
[36] F. Nekoogar, "Ultra-Wideband Communications: Fundamentals and Applications", Prentice Hall, 2005, sample chapter available at (30.7.2006): http://www.phptr.com/articles/article.asp?p=433381&rl=1
[37] Sikora, A., "ZigBee startet durch", Elektronik Wireless 1/2006, S.24-28.
[38] http://www.uwbforum.org/
[39] http://www.wimedia.org
[40] W. Ongena, "Bluetooth soll breitbandig warden", Markt & Technik Nr. 16/21.4.2006, pp.40-43 (in German).
[41] N. Schmidt, „Indoor Location Tracking and Information System: Ein System zur Lokalisierung und Kommunikation mittels Ultrabreitbandfunk", 11. ITG-Fachtagung Mobilfunk in Osnabrück, 17./18. Mai 2006, available at (1.8.2006): http://www.mobilfunktagung.de/fileadmin/users/65/upload/Mobilfunktagung/Vortraege/ … 16_schmidt.pdf
[42] http://www.wimaxforum.org
[43] http://grouper.ieee.org/groups/802/16 and http://www.ieee802.org/16
[44] http://www.wina.org
[45] http://networks.siemens.com/communications/lexicon/5/f018995.htm
[46] http://www.wisair.com/wp-content/542_502.pdf
[47] T. Zasowski, A. Wittneben, "Performance of UWB Systems using a Temporal Detect-and-Avoid Mechanism", IEEE International Conference on Ultra-Wideband, ICUWB 2006, Waltham, Massachusetts, USA, Sept. 2006.
[48] ECC (Electronic Communications Commitee), "Draft of the ECC decision on the harmonised conditions for devices using UWB technology in bands below 10.6 GHz, (ECC/DEC/(06)AA)," November 2005.
[49] R. Kohno, "Progress and schedule of japanese regulation for UWB", IEEE 802.15-06-0023-00-004a, January 2006.
[50] FCC, "Revision of part 15 of the commission's rules regarding ultrawideband transmission systems," First Report and Order, ET Docket 98-153, FCC 02-48, adopted/released Feb. 14/ Apr. 22 2002.
[51] J. Lansford, "Detect and Avoid for MB-OFDM", IEEE 802.19-05/0034r0, Sep. 2005, available at (14.10.06): http://www.ieee802.org/19/pub/2005/19-05-0034-00-0000-DAA_for_MB-OFDM.ppt
[52] „RFID White Paper: Technology, Systems, and Applications", August 2005, http://www.bitkom.de

[53] K. Finkenzeller, „RFID-Handbook - Fundamentals and Applications in Contactless Smart Cards and Identification”, Wiley & Sons, 2nd edition, 2003.
[54] Tanenbaum, A.S., “Computer Networks”, 4th edition, Prentice Hall, 2003, ISBN 0-13-066102-3
[55] A. Sikora, "Mesh-Netze mit W-LAN", chip-Professional March/April 2/2005, S.114-116.
[56] http://pdos.csail.mit.edu/roofnet/doku.php
[57] http://standards.ieee.org/regauth/oui/oui.txt
[58] A. Sikora, "Sicherheit in Wireless LANs", Elektronik, 18/2002, S.44-52.
[59] A. Sikora, "Grundlagen WiMAX - Anwendung, Architektur und Aufbau", tecchannel 9.12.2005, http://www.tecchannel.de/netzwerk/grundlagen/433538/
[60] E. Agis et. al., "Global, Interoperable Broadband Wireless Networks: Extending WiMAX Technology to Mobility", Intel Technology Journal, Volume 8, Issue 3, 2004, pp.173-188.
[61] D. Renaudeau, D. Boettle, H. Steyaert, "WIMAX: From Fixed Wireless Access to Internet in the Pocket”, Alcatel Telecommunications Review - 2nd Quarter 2005, http://www.alcatel.com/atr
[62] http://grouper.ieee.org/groups/802/15/pub/TG4a.html
[63] http://grouper.ieee.org/groups/802/15/pub/TG4b.html
[64] D. Taubenheim, S. Kyperountas, N. Correal, “Distributed Radiolocation Hardware Core for IEEE 802.15.4”, Motorola Labs, Plantation, Florida, USA, White Paper, 8. Dec 2005, available at (15.10.2006): www.chipcon.com/files/Radiolocation_Engine_WP.pdf.
[65] Chipcon AS SmartRF® CC2431 PRELIMINARY Data Sheet (Rev. 1.0)
[66] U. Großmann, “WLAN Indoor Positioning based on euclidian distance and interpolation (isobars)”, in: Wollert, J.., “Wireless Technologies 8. Kongress, 27.-28. September 2006, Dortmund”, VDI Fortschrittsberichte, 2006.
[67] J. Latvala, J. Syrjärinne, H. Ikonen, and J. Niittylahti, “Evaluation of RSSI-based human tracking,” in Proc. 2000 European Signal Processing Conf., Sept. 2000, vol. 4, p. 2273–2276.
[68] R. Roberts, “Ranging Subcommittee Final Report”, IEEE P802.15 Working Group for Wireless Personal Area Networks (WPANs), IEEE P802.15-04-0581r0, Oct. 2004.
[69] V. Brethour, “Crystal Offsets and UWB”, IEEE P802.15 Working Group for Wireless Personal Area Networks (WPANs), IEEE 802.15-05-0335-01-004a, June 2005.
[70] U. Hiegert, “Analyse der Anwendungsmöglichkeiten von WiMAX“, Diploma Thesis, Department Information Technology, UCE Loerrach, Oct 2006.
[71] U.S. Department of Defence: “Global Positioning System, Standard Positioning Service, Performance Standard”, 2001
[72] IEEE 802.15.3-2003, “IEEE standard for information technology – telecommunications and information exchange between systems – local and metropolitan area networks – specific requirements part 15.3: wireless medium access control (MAC) and physical layer (PHY) specifications for high-rate wireless personal area networks (WPANs)” Sept. 2003.
[73] Standard ECMA-368, High Rate Ultra Wideband PHY and MAC Standard, 1st Edition, Dec. 2005.
[74] http://www.imst.de
[75] J. Romme, „A Low Datarate Localisation System“, 4.11.2005, EFPL Lausanne, available at: http://icawww1.epfl.ch/uwb4sn/slides/RommeUWB4SN041105.pdf.
[76] N. Schmidt, “ILTIS: Indoor Location Tracking and Information System Ein System zur Lokalisierung und Kommunikation mittels Ultrabreitbandfunk“, 11.05.2006.
[77] http://www.esafetysupport.org/
[78] US Department of Transportation, National Highway Traffic Safety Administration, “Final Report: Vehicle Safety Communications Project, DOT HS 810 591, April 2006, http://www.nthsa.dot.gov.
[79] J. Hightower, G. Borrielllo, „A Survey and Taxonomy of Location Systems for Ubiquitous Computing“; Technical Report UW-CSE 01-08-03, August 2001, available at: http://citeseer.ist.psu.edu/cache/papers/cs/27008/ftp:zSzzSzftp.cs.washington.eduzSztrzSz2 … 001zSz08zSzUW-CSE-01-08-03.pdf/hightower01survey.pdf
[80] http://www.vdi-nachrichten.com/ce-richtlinien/default.asp?mp-pvid=1-1Y500j-96x-1GvoU6

[81] Nanotron Technologies GmbH, "nanoLOC TRX High Performance Transceiver Enabling Location Awareness", available at http://nanotron.com/EN/PR_nanoLOC.php
[82] Nanotron Technologies GmbH, "Living in a Crowded Neighbourhood - Coexistence in the 2.4 GHz ISM Band", White Paper, available at http://www.nanotron.com/EN/ … docs/Coexistence/whitepaper/nanoNET_Coexistance_WP_Draft_V1.00_2006-05-19.pdf
[83] Nanotron Technologies GmbH, "Chirp Modulation confirmed for IEEE Standard", available at http://www.nanotron.com/EN/NE_releases_2006-10-09.php
[84] Nanotron Technologies GmbH, "EBM (Energy Budget Management)", available at http://www.nanotron.com/EN/CO_techn-ebm.php
[85] Nanotron Technologies GmbH, "nanoNET TRX Transceiver (NA1TR8)", available at http://nanotron.com/EN/docs/ nanoNET-TRX/NA1TR8/datasheet/nanoNET_TRX_Transceiver_NA1TR8_DS_Ver2.08.pdf
[86] http://www.awe-communications.com/Links/COST.html
[87] http://www.lx.it.pt/cost259/
[88] http://www.lx.it.pt/cost273/
[89] W. Lohmann, R. Meyfarth, „Standardisierungsbestrebungen im Bereich der Car-2-Car Kommunikation", 8. Wireless Technologies Kongress 2006, Dortmund, 27./29. September 2006, published in: J. Wollert, Fortschritt-Berichte VDI, Reihe 10 Nr. 772, VDI Verlag Düsseldorf 2006.
[90] http://www.u-blox.de/
[91] A. Lübke, „Wireless Communication for Automotive Applications", 8. Wireless Technologies Kongress 2006, Dortmund, 27./29. September 2006, published in: J. Wollert, Fortschritt-Berichte VDI, Reihe 10 Nr. 772, VDI Verlag Düsseldorf 2006.

ANNEXES

Annex A: CSS measurement report

Measurement Report

- Real-Time Ranging -

nanotron TECHNOLOGIES

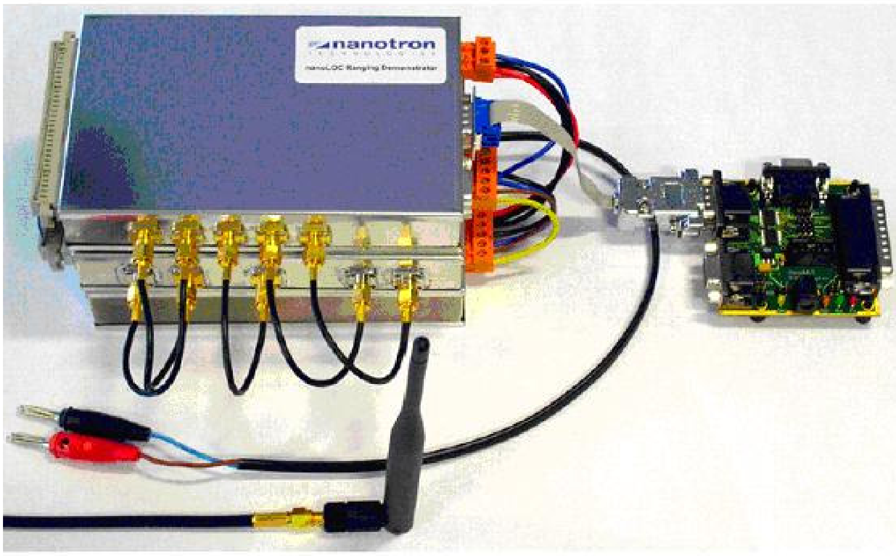

Steinbeis-Research Institute Wireless Communication,
University of Cooperative Education Loerrach

Datum: 13.1.2007
V0.3

1. Revision History

Revision	Date	Author	Changes
0.3	13.1.2007	AS	Results of nanoLOC based measurements added
0.2	21.10.2006	AS	Description of measurement scenario 2 with and results of measurement session 19th Oct 2006
0.11	3.9.2006	AS	Description of frame formats added
0.1	27.8.2006	AS	First draft with scenario 1

2. Introduction

This report describes the measurement results from two measurement sessions based on the discrete hardware prototype of the nanoLOC Ranging demonstrator from the Berlin based company Nanotron Technologies GmbH.
The major focus on the measurements was on the ranging capabilities of the system under various circumstances, which reflect the major use cases of the WATCH-OVER project.

Contents

3. System description

Hardware

<u>Overview</u>

The measurements for his report were performed between July 2006 and January 2007. Due to the status of the development, the first measurements were performed with a Discrete Hardware Prototype (DHP), whereas the later measurements could already use the nanoLOC ASIC.

Both systems are based on equal circuitry and functionality. The transmission of the device utilizes Chirp Spread Spectrum (CSS) that transmits signals with frequencies that are linearly increasing or decreasing. These frequency modulated pulses are called chirps.

<u>DHP</u>

The nanoLOC Ranging Demonstrator is a Discrete Hardware Prototype (DHP) and accompanying software that allows the measuring and testing of the RF link and ranging capabilities of nanoLOC.

The hardware includes

- a Power Supply Board,
- an analogue TX/RX board, and
- a digital Board.

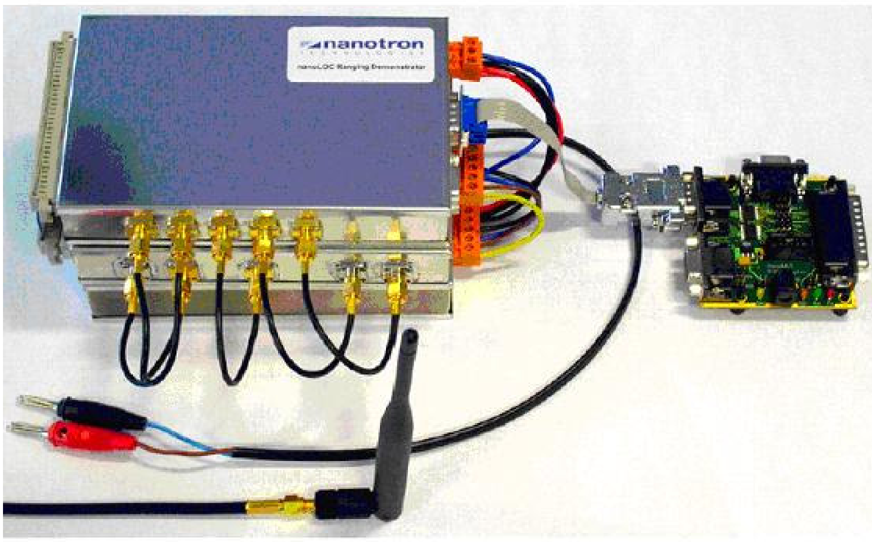

Fig. 1: nanoLOC DHP Ranging Demonstrator components

<u>ASIC</u>

The nanoLOC ASIC (TRX transceiver) is a highly integrated mixed signal chip. nanoLOC supports 7 frequency channels with 3 non-overlapping channels. Data rates are selectable between 31,25 kbps and 2 Mbps. The transceiver includes a MAC controller with SMA/CA and TDMA support as well as Forward Error Correction (FEC) and 128 bit hardware encryption. It provides scrambling, automatic address matching, and packet retransmission

It can work with almost every microcontroller. The development board, which is depicted in Fig. 2, uses a ATmega-microcontroller from Atmel.

Fig. 2: nanoLOC ASIC Ranging Demonstrator components

Software

In addition, a GUI-based software is included, which helps to visualize and save the measurement results. The measurement itself is based on the Symmetric Double Sided – Two Way Ranging described in [1] [2].

The following preconditions are met for the measurements with this DHP:

- The measurements are done in the 2.4 GHz-band with a raw bandwidth of 80 MHz and an effective bandwidth of 64 MHz.
- All measurements are performed with 24 up- and 24 down-chirps per measurement point, respectively. The control and the summing up of these values are performed in hardware.
- Consequently, each measurement consumes approximately 2 ms.

The software is also adapted to the ASIC-based version.

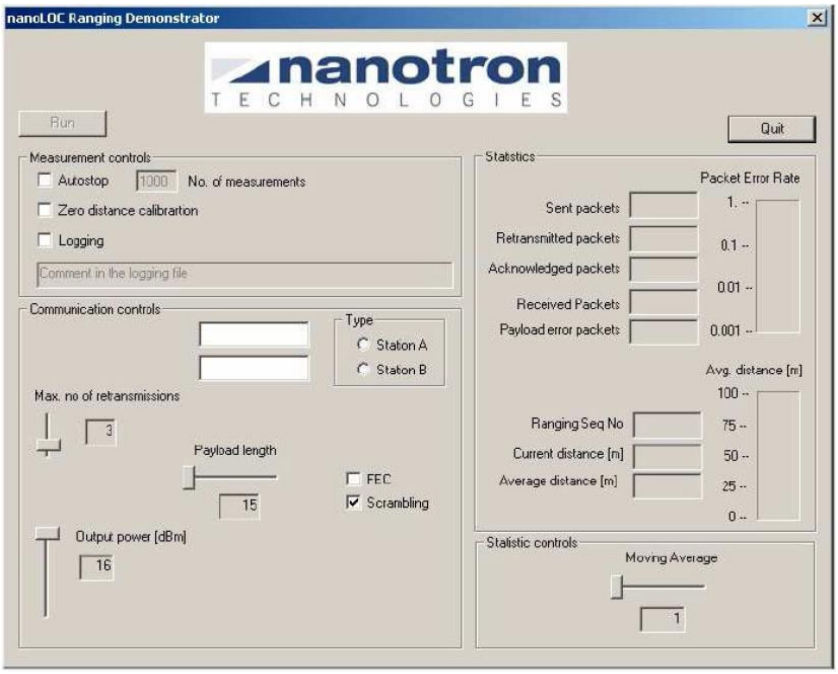

Fig. 3: nanoLOC Ranging Demonstrator software

Timing behaviour

PHY frame format
On the physical layer (layer 1), a frame comes with the format shown in Table 1.

30 Bit	64 Bit		4 Bit
Preamble	Sync Word	Data	Tail

Table 1: Frame format on physical layer

MAC frame format
On the MAC layer (layer 2), a data frame comes with the format shown in Table 2.

16 Byte	2 Byte	≥ 1 Byte	2 / 4 Byte
Header	Header CRC	Data	Data CRC

Table 2: Data frame format on MAC layer

An acknowledgement frame comes with a reduced length, as shown in Table 3.

8 Byte	2 Byte
Header	Header CRC

Table 3: Acknowledgement frame format on MAC layer

Interframe space
The acknowledgement is transferred 8 µs after successful reception of the data frame.

Data rate
The data rate is 1 MBit / s, which is transmitted as 1 MSymbol / s.

4. Measurement setup

Remarks

All measurement setups were selected as real life environment. It was the idea of the performed measurement sessions to achieve results, which represent the performance of the system under real-life conditions.

Measurement setup 1 (Suburban area)

The first measurement session was performed in a suburban area in an environment with few cars and other metallic objects. Fig.4 gives an impression of the conditions.
The measurements were done with two nodes, which were denominated A and B. For the WATCH-OVER scenarios, node A was selected as the vehicle based nodes with x-distance of 2.5 m. Node B was selected to represent the vulnerable road user (VRU) in different locations in y-distance between 5 m and 40 m from the vehicle-based nodes (cf. Fig. 5).
The absolute distances between the nodes are shown in Table 4.

	1,25	2,5
40	40,0195265	40,0780489
35	35,0223143	35,0891721
30	30,0260304	30,1039864
25	25,0312305	25,1246891
20	20,0390244	20,1556444

15	15,0519932	15,2069063
10	10,0778222	10,3077641
5	5,15388203	5,59016994

Table 4: Absolute distances in the test setup 1

Node A was placed on a wooden table (with some metal fixes) at a height of 1 m, node B was placed on a wooden chair at a height of 0.7 m.
Whereas in the first measurements, no obstacles were between the both nodes, further measurements included obstacles, i.e. a mid-size passenger car (cf. Fig. 18) or a larger van (cf. Fig. 19).

Fig. 4: Test conditions of test setup 1 without obstacles

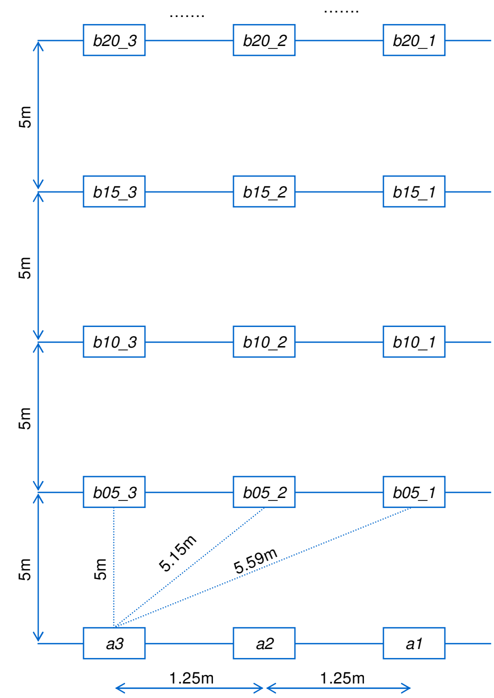

Fig. 5: Test points of test setup 1

Measurement setup 2 (Residential Area)

In a second session measurements were performed in a residential area with a queue of parking cars. Fig.6 gives an overall impression of the conditions. One station was placed either on a table (cf. Fig. 7) or on a rig (cf. Fig. 8). The other station was put into a car, with one antenna mounted on the car's roof at a height of approx. 2 m.

Fig. 6: General conditions of test setup 2

The measurements were performed for static and dynamic use cases. For both use cases, two scenarios were examined: The first scenario is based on line of sigth (LOS) connection between mobile node and base station. In the second scenario the base station is located on the curb with obstructed line of sight.

Fig. 7: Base station positioned on a rig

Fig. 8: Base station positioned on a table

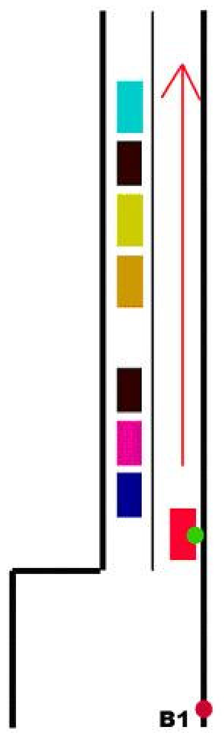

Fig. 9: Test conditions of test setup 2 without obstacles

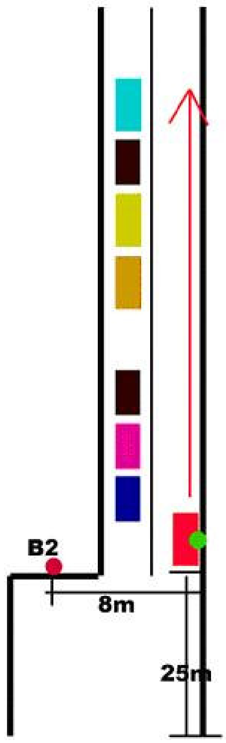

Fig. 10: Test conditions of test setup 2 with obstacles

Further measurement setups

Further setups should be taken into account, i.e.

- Impact of reflecting objects (cars, glassed house fronts)
- Impact of larger opening angles of the measurement field
- More cars, pedestrians and other objects as obstacles
- Speed of node A and B.

5. Measurement results from setup 1 (Suburban area) with DHP

Obstacle free measurements

Distance estimation

For all locations, 1.000 two-sided measurements were recorded on both nodes, A and B. As they are equivalent, only the records from node A were regarded for the following results.

Table 5 shows the results for all distances b from both points a1 and a3. It can be seen that nearly all results are slightly too large.

y-distance [m]	triangular distance [m]	measurement point a1		measurement point a3	
		mean estimated distance [m]	std deviation [m]	mean estimated distance [m]	std deviation [m]
5	5,154	6,269	0,1917	6,033	0,2457
10	10,078	10,868	1,2651	11,162	0,3104
15	15,052	16,306	2,408	14,766	0,6935
20	20,039	20,757	0,27	22,682	1,731

25	25,031	25,548	0,17	25,347	0,256
30	30,026	30,46	0,341	30,733	0,116
35	35,022	35,599	0,4696	35,553	0,1078
40	40,02	40,704	0,8468	40,876	0,0919

Table 5: Mean estimated distances and standard deviation for both points a1 and a3

Fig. 11 illustrates the results within the layout of the given setup, based on triangulation.

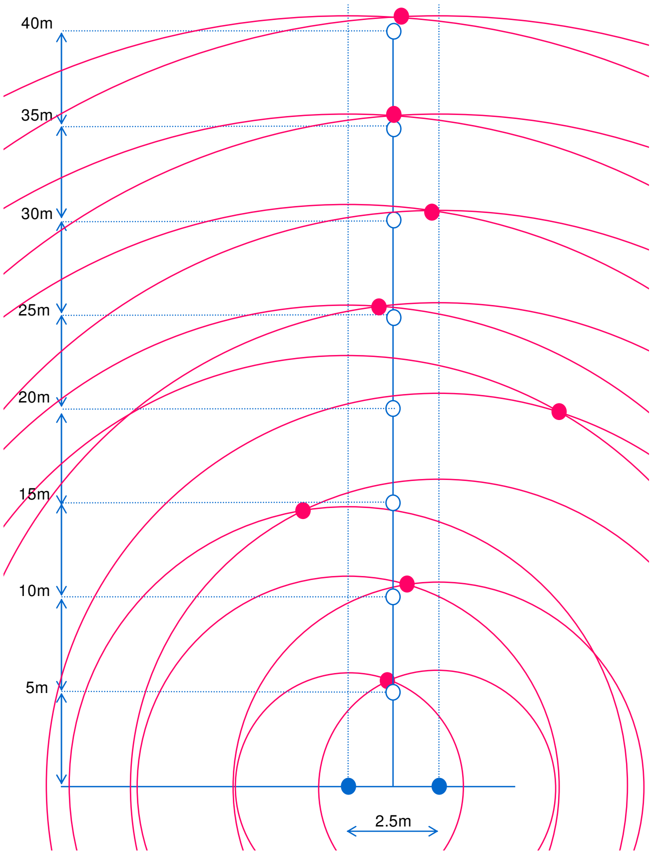

Fig. 11: Illustration of measurement results for test setup 1 without obstacles. The circles show the diameter of the measured distances from both points a1 and a3.

When regarding the measurement results in detail, three different categories can be differentiated. Those are independent from the actual distance.
The first category comes with very homogeneous distance estimation and a very low standard deviation, as they are shown as an example in Fig.12.

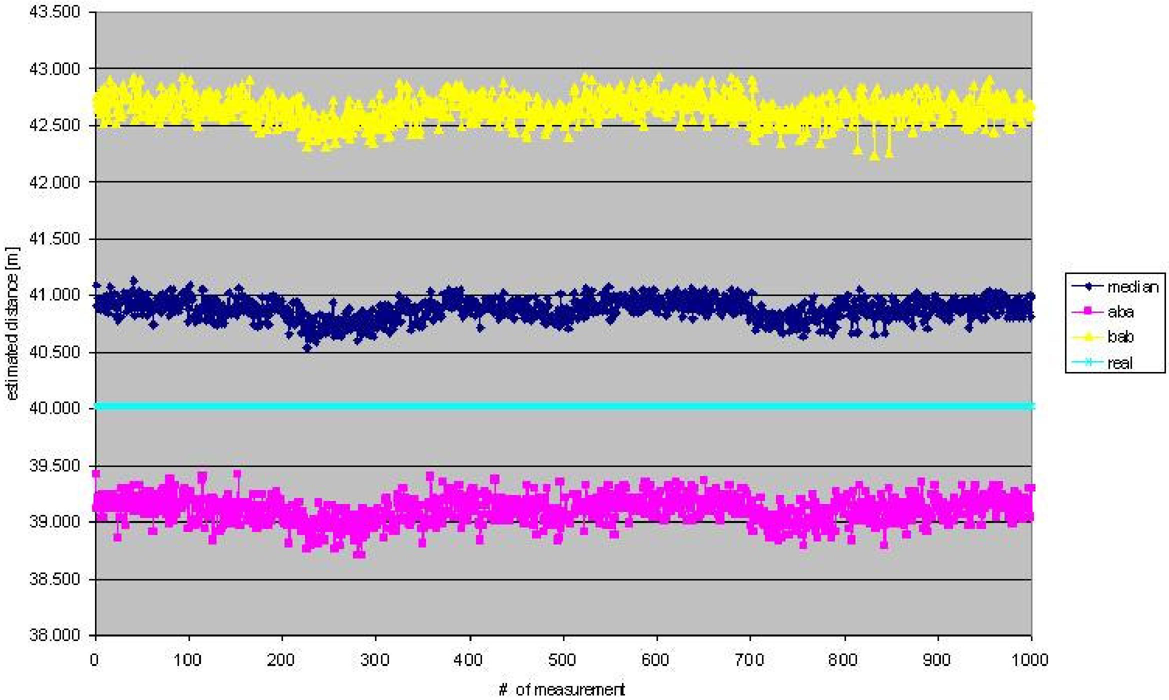

Fig. 12: Measurements with very homogeneous results; point a3, point b2 at a distance of 40 m

The second category shows single measurement points with severe deviation from the original results. Nevertheless, the overall standard deviation remains at a reasonable level. An example is shown in Fig.13.

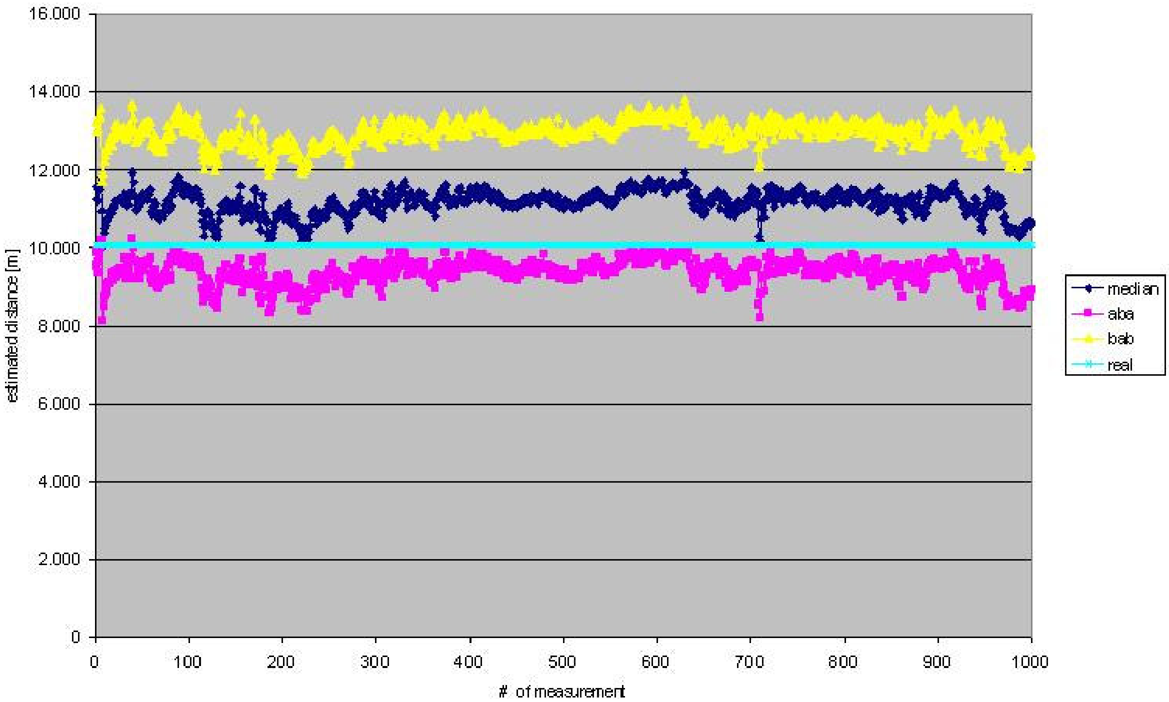

Fig. 13: Measurements with single deviating results; point a3, point b2 at a distance of 10 m

The third and last category comes with a significant number of measurement points with severe deviation from the original results. Consequently, the overall standard deviation deteriorates severely. An example is shown in Fig.14. An explanation for this behaviour may be the real life characteristics of the measurement, where some foot passengers crossed the test field.

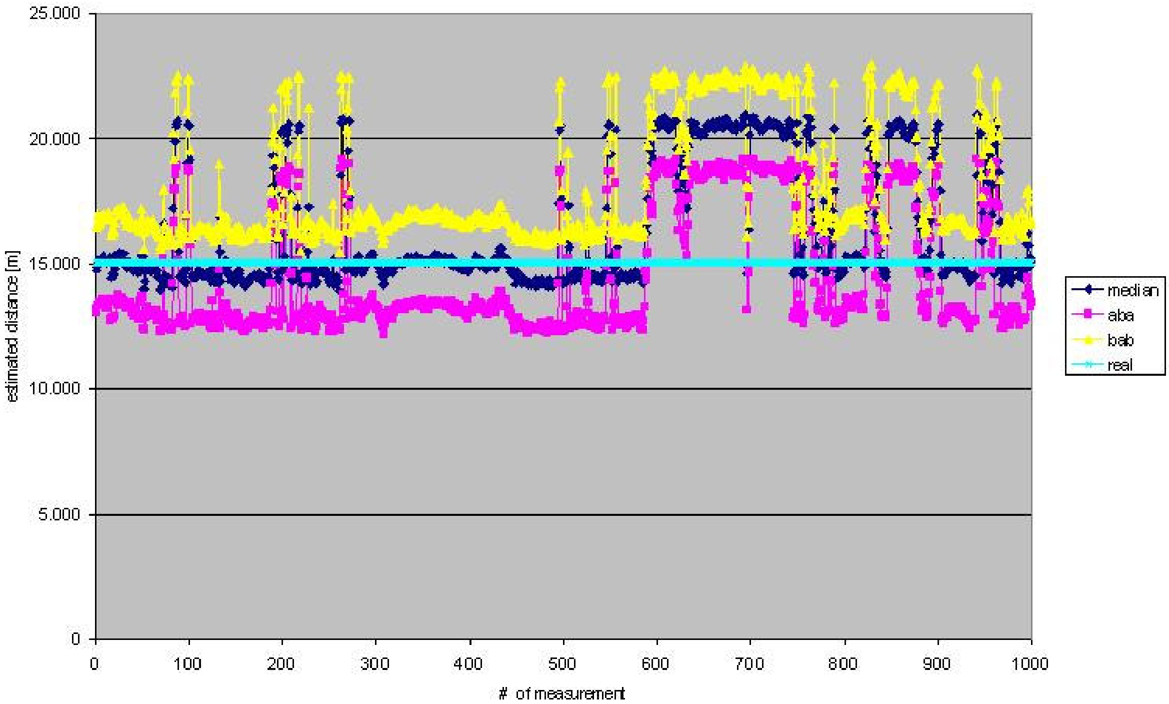

Fig. 14: Measurements with a significant number of deviating results; point a1, point b2 at a distance of 15 m (raw results)

Angle resolution

For the y-distance of 20 m, the three different points b1, b2, b3 were measured in order to gain some more information on the angle resolution. Again, 1.000 two-sided measurements were recorded on both nodes, A and B. As they are equivalent, only the records from node A were regarded for the following results.

Table 6 shows the results for all distances b from both points a1 and a3.

y-distance [m]	b	measurement point a1			measurement point a3		
		triangular distance [m]	mean estimated distance [m]	std deviation [m]	triangular distance [m]	mean estimated distance [m]	std deviation [m]
20	b1	20	21,956	1,84	20,156	21,153	0,114
20	b2	20,039	20,757	0,27	20,039	22,682	1,731
20	b3	21,156	21,195	0,161	20	21,666	0,471

Table 6: Mean estimated distances and standard deviation for both points a1 and a3 and all three point b1, b2, and b3 at a distance of 20m

For the angle resolution, triangulation and the law of cosine has to be applied to the triangle shown in Fig. 15.

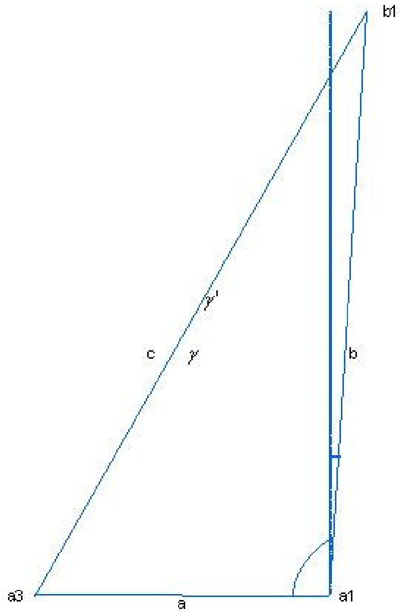

Fig. 15: Triangulation scheme

This delivers

$$c^2 = a^2 + b^2 - 2ab\cos(\gamma)$$
$$\cos(\gamma) = \frac{a^2 + b^2 - c^2}{2ab}$$
$$\gamma = \arccos\left(\frac{a^2 + b^2 - c^2}{2ab}\right)$$
$$\gamma' = \arccos\left(\frac{a^2 + b^2 - c^2}{2ab}\right) - 90°$$

Eg.32

Based on the results from Table 6, the angle γ' can be calculated to the values of Table 7.

y-distance [m]	b	measurement point a1		measurement point a3		angle γ'
		triangular distance [m]	mean estimated distance [m]	triangular distance [m]	mean estimated distance [m]	
20	b1	20	21,956	20,156	21,153	-2,47722496
20	b2	20,039	20,757	20,039	22,682	4,761172063
20	b3	21,156	21,195	20	21,666	0,915617188

Table 7: Calculated angle for the b1, b2, and b3 at a distance of 20m

Data post-processing – (static std deviation)

Especially for the second category of measurement results, one could come up with the idea of post-processing the raw measurement data. The simplest way of this post-processing is based on neglecting the data with a too large deviation from the mean value.
The results of 1000 measurements with node A at position 1 and node B at a distance of 20 m at position 1 with a van parking at the 15 m line are shown in Fig. 16. The corresponding results after all 1000 measurement points are shown in Table 8.
The results with flowing mean and standard deviation values are shown in Fig. 17.

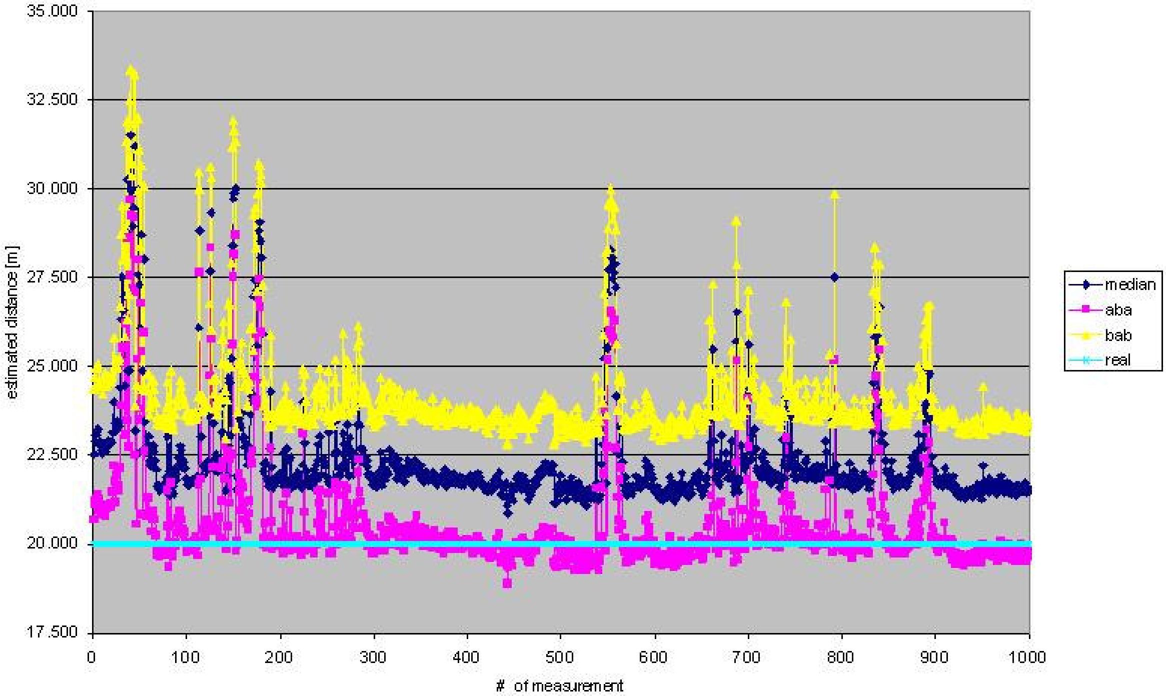

Fig. 16: Measurements with single deviating results; point a1, point b2 at a distance of 20 m with van at 15 m (raw results)

	all values	[mean-1*std_dev; mean+1*std_dev]	[mean-0.5*std_dev; mean+0.5*std_dev]	[mean-0.25*std_dev; mean+0.25*std_dev]
mean estimated distance [m]	22,382	21,975	22,055	22,282
standard deviation	1,516	0,508	0,362	0,205

Table 8: Mean estimated distances and standard deviation after static port processing fot data from Fig. 16

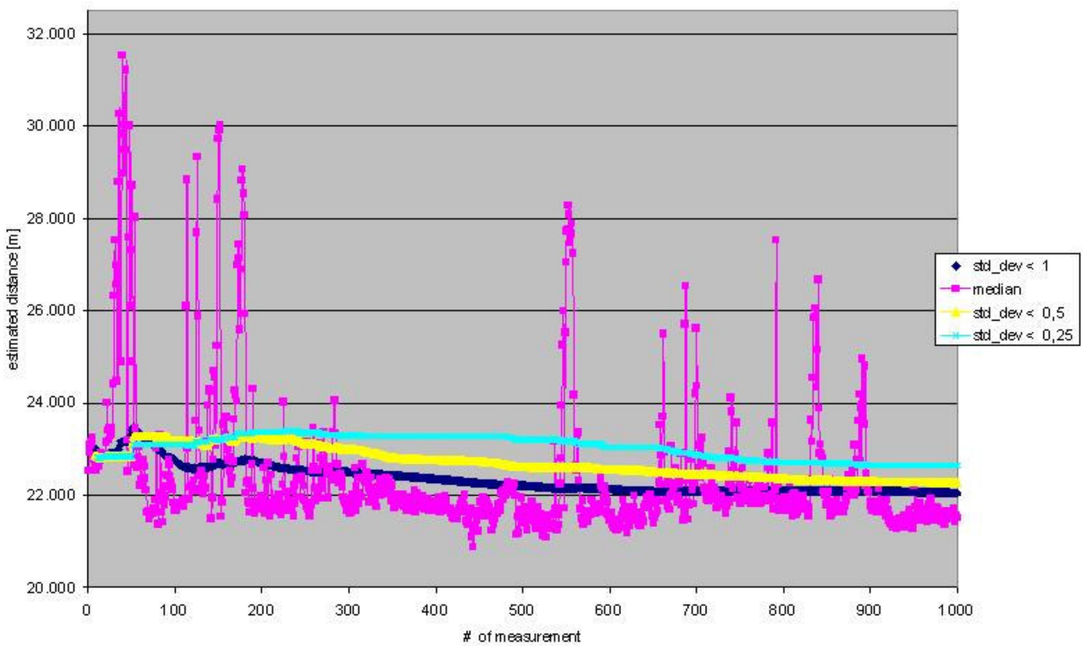

Fig. 17: Mean values excluding results with too large a deviation; mean values and standard deviation are calculated on a flowing basis

Measurements with obstacles

Remarks

For the WATCH-OVER project, setups with obstacles are included into the typical use cases. Therefore, single objects were put in between the measurement points at the vehicle and the vulnerable road user (VRU).

Passenger car

At first, a mid-size passenger car (cf. Fig. 18) was parked at the 15 m line, where the measurement points b were at 20 m.
Apart from measurement point b20_2, which shows the typical behaviour of external deterioration, the results in Table 9 are very satisfactory. I.e. no significant deterioration from the results without obstacles (as shown in Table 6 can be observed. The measurements were not taken for all points.

Fig. 18: Test conditions of test setup 1 with a passenger car in a distance of 15 m and node B in a distance of 20 m

y-distance [m]	b	measurement point a1			measurement point a3		
		triangular distance [m]	mean estimated distance [m]	std deviation [m]	triangular distance [m]	mean estimated distance [m]	std deviation [m]
20	b1	20	20,705	0,6877	20,156	20,794	0,1698
20	b2				20,039	23,885	4,271
20	b3				20	22,3	0,2024

Table 9: Mean estimated distances and standard deviation for both points a1 and a3 and all three point b1, b2, and b3 at a distance of 20m with a passenger car parking at the 15 m line

Van

However, one could argue that in the case of ch. 0, most of the EM waves could either spread around the car or penetrate the windows. Therefore, a larger van with a significantly higher window row was parked at the 15 m line (as shown in Fig. 19). The measurement point of node B are placed directly behind the back of the car, as shown in Fig. 20.
The results from Table 10 show slightly larger distances in comparison with the obstacle free test case (cf. Table 6). However, the estimated distance and localization of the VRU are still very satisfactory in terms of presence detection and distance estimation. However, the angle resolution is still a quite rough level, as it is shown in Fig. 21.

Fig. 19: Test conditions of test setup 1 with a van in a distance of 15 m and node B in a distance of 20 m

Fig. 20: Test conditions of test setup 1 with a van in a distance of 15 m and node B in a distance of 20 m

y-distance [m]	b	measurement point a1			measurement point a3		
		triangular distance [m]	mean estimated distance [m]	std deviation [m]	triangular distance [m]	mean estimated distance [m]	std deviation [m]
20	b1	20	22,382	1,516	20,156	21,082	0,1227
20	b2	20,039	22,856	0,8003	20,039	23,614	0,8442
20	b3	20,156	21,509	0,6461	20	23,955	1,388

Table 10: Mean estimated distances and standard deviation for both points a1 and a3 and all three point b1, b2, and b3 at a distance of 20m with a van parking at the 15 m line

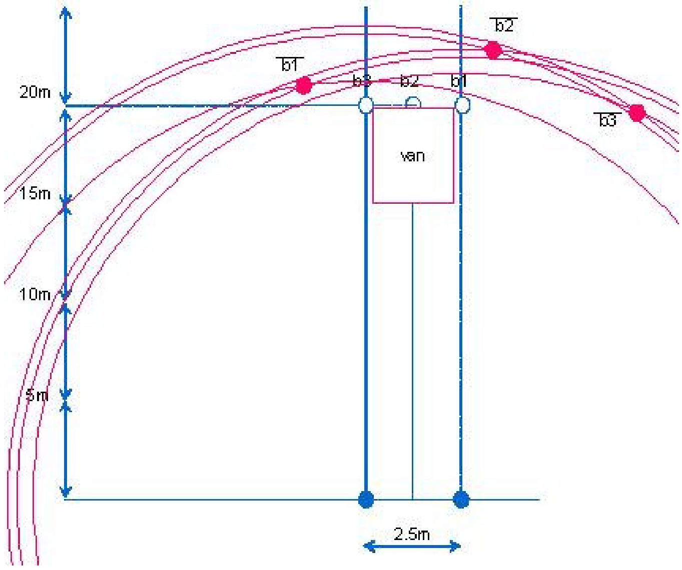

Fig. 21: Illustration of measurement results for test setup 1 with a van parking at the 15 m line. The circles show the diameter of the measured distances from both points a1 and a3.

6. Measurement results from setup 2 (Residential area) with DHP

Static Measurements

Obstacle free measurements

In this second measurement run, nearly all results showed homogenous character, as it is shown in Fig. 22. Only the measurements for a distance of 40 m are worse, with no obvious explanation, and for large distances (e.g. 140 m). It should be highlighted that the range goes up to 130 m with an output power of 0 dBm with a reasonable precision.
The overall results of the measurements without obstacles (as described in ch. 0), are shown in Table 11. The corresponding diagrams are shown in Fig. 23 and 24.
The typical relative error is below 4 %, the typical standard deviation is in the range of 0.1 m.

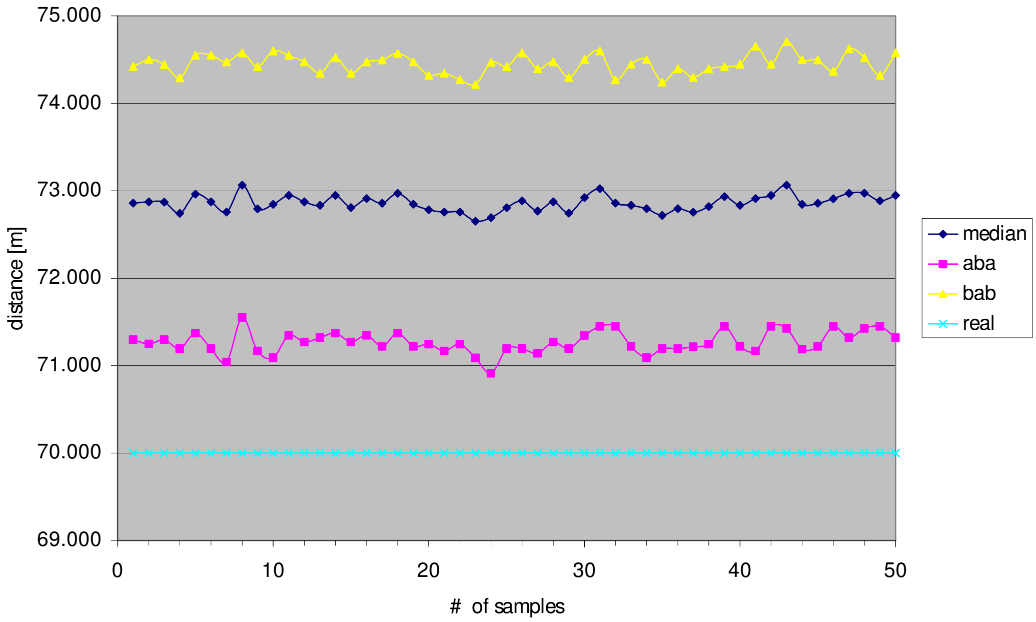

Fig. 22: Measurements with very homogeneous results; static measurement, no obstacles at a distance of 70 m

real distance [m]	measured distance [m]	relative error [%]	standard mean deviation [m]	output power	comments
10	10,642	6,42%	0,081896893	0 dBm	
20	20,335	1,68%	0,115982054	0 dBm	
30	29,913	-0,29%	0,067656772	0 dBm	
40	43,664	9,16%	0,69171883	0 dBm	larger deviation
50	53,1937	6,39%	0,081879267	0 dBm	
60	62,58564	4,31%	0,127681805	0 dBm	
70	72,85874	4,08%	0,091163636	0 dBm	
80	82,69886	3,37%	0,12474742	0 dBm	
90	92,80318	3,11%	0,108168555	0 dBm	
100	102,5657662	2,57%	0,108154239	0 dBm	
110	112,2863	2,08%	0,135248562	0 dBm	
120	121,99864	1,67%	0,163450393	0 dBm	
130	132,6162	2,01%	0,119931953	0 dBm	
140	148,20186	5,86%	1,998768815	16 dBm	larger deviation

Table 11: Mean estimated distances, relative error and standard deviation for static measurements without obstacles in setup 2

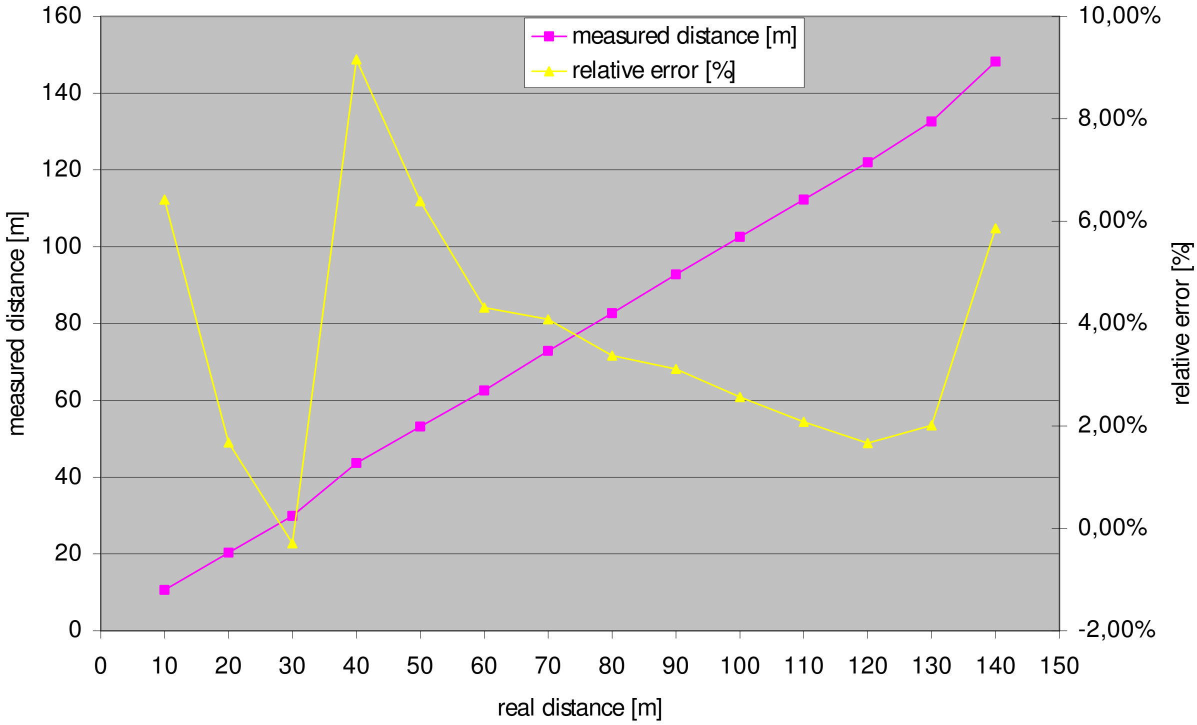

Fig. 23: Mean estimated distances and relative error for static measurements without obstacles in setup 2

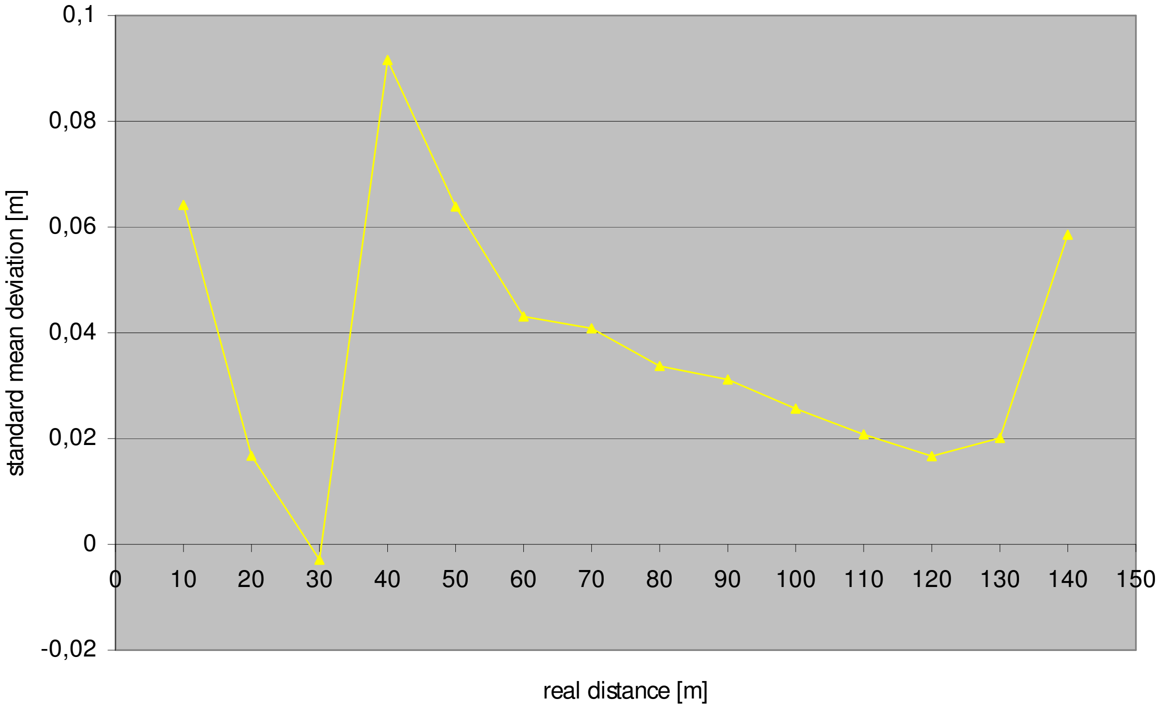

Fig. 24: Standard mean deviation for static measurements without obstacles in setup 2

Measurements with obstacles

Also, for the measurements with obstacles, nearly all results continue to show a homogenous character. The relative errors were quite deteriorated. One exceptional value at 9,43 m might be the result of a process error during the denomination of the result files. For the other cases, the relative error is up to a maximum of 12 %, with typical values below 5 %. The typical standard deviation is in the range of below 0.4 m.
It should be highlighted that the range goes up to 105 m with an output power of 0 dBm and a reasonable precision. The measurements at 115 m failed.
The overall results of the measurements with obstacles (as described in ch. 0), are shown in Table 12. The corresponding diagrams are shown in Fig. 31 and 26.

real distance [m]	measured distance [m]	relative error [%]	standard mean deviation [m]	output power	comments
8	8,649266667	8,12%	0,078913252	0 dBm	
9,433981132	20,43158	116,57%	1,656408028	0 dBm	
17	17,9442	5,55%	0,069377112	0 dBm	
26,2488095	29,39572	11,99%	1,592250724	0 dBm	
35,90264614	36,75434	2,37%	0,230549	0 dBm	
45,70557953	50,87446	11,31%	0,379283977	0 dBm	
55,57877293	58,82968	5,85%	0,083345957	0 dBm	
65,49045732	66,17022	1,04%	0,082337109	0 dBm	
75,42545989	77,37068	2,58%	0,20787422	0 dBm	
85,37564055	86,96466	1,86%	0,202210903	0 dBm	
95,33624704	96,95826	1,70%	0,130815934	0 dBm	
105,3043209	105,4173636	0,11%	0,188188349	0 dBm	11 measurement points only

Table 12: Mean estimated distances, relative error and standard deviation for static measurements with obstacles in setup 2

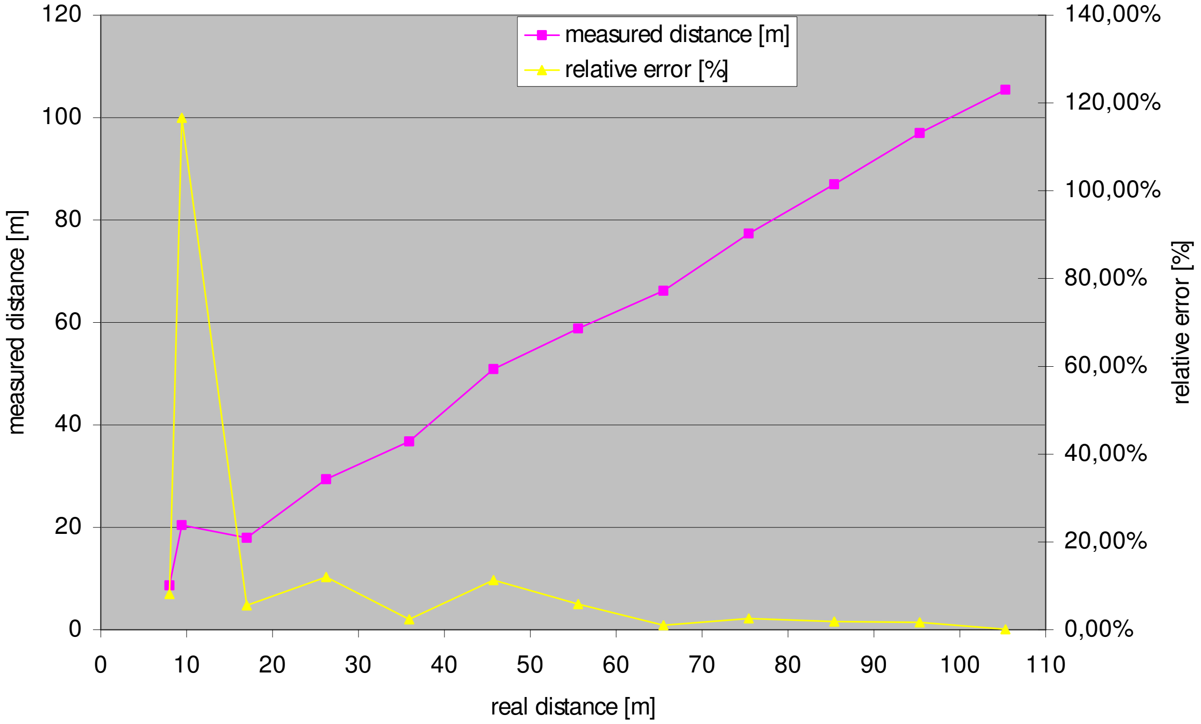

Fig. 25: Mean estimated distances and relative error for static measurements with obstacles in setup 2

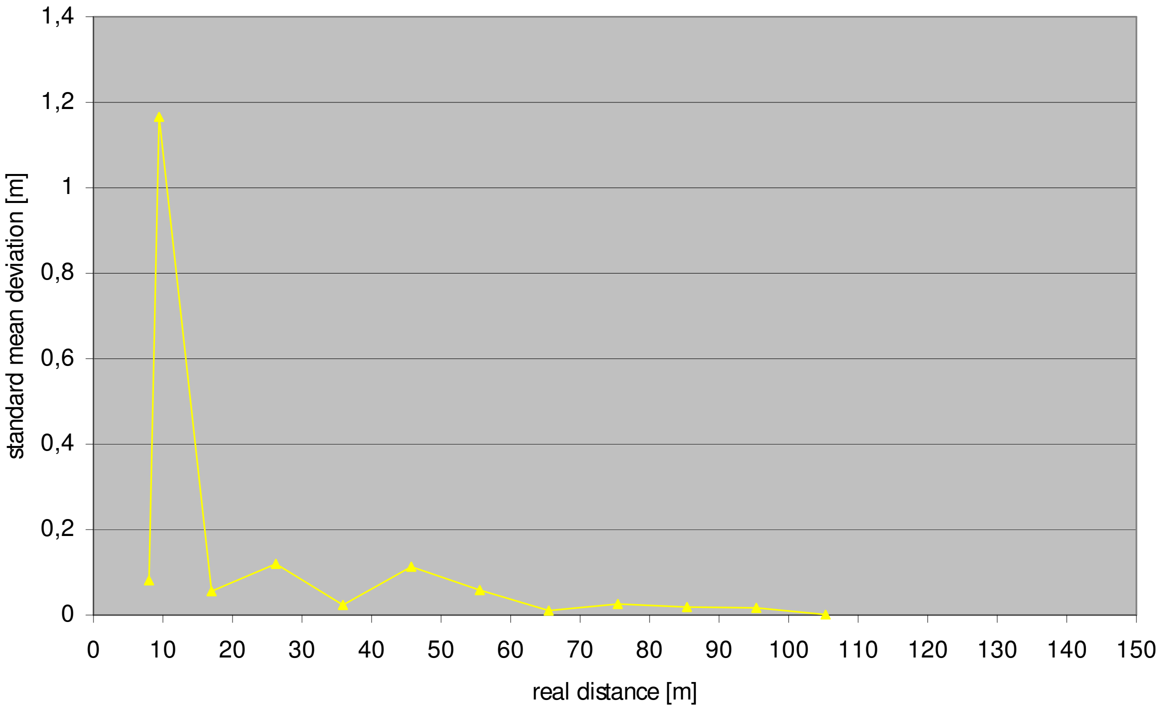

Fig. 26: Standard mean deviation for static measurements with obstacles in setup 2

Dynamic Measurements

Obstacle free measurements

Although taking dynamic measurements in this scenario was a little bit difficult due to missing space of acceleration, some measurements were performed.
The estimated distance are shown in Fig. 27 and basically show a good linearity. Due to the missing real values, no precision can be described.
The calculated speed is shown in Fig. 28. The dotted pink line show the estimations for each neighbored values

$$v(t_1)=\frac{s(t_1)-s(t_0)}{t_1-t_0}$$	Eq. 33

The solid blue line is the moving average, calculated as follows

$$\overline{v(t_1)}=0{,}9\cdot\overline{v(t_0)}+0{,}1\cdot v(t_1)$$	Eq. 34

The target speed of the vehicle after the acceleration phase (read from speedo) is 30 km / h.
It should be mentioned that the measurement works well for distances up to 70 … 80 m. For larger distances, the connection breaks down. However, the maximum achieved distance is 240 m.

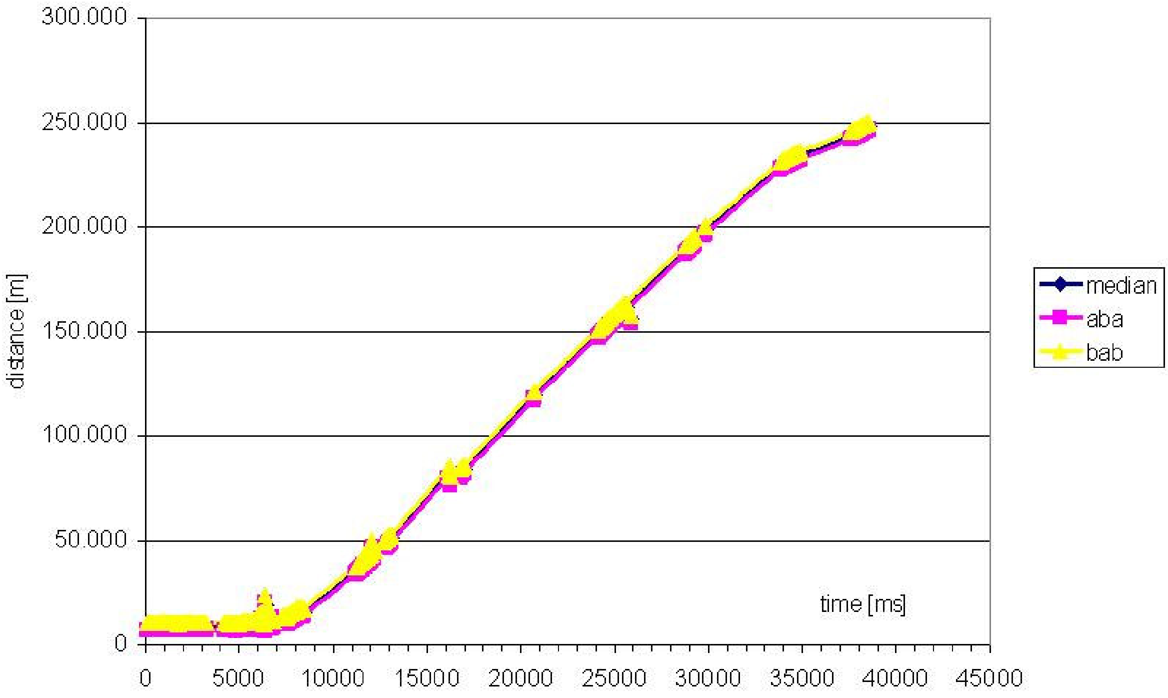

Fig. 27: Estimated distances for dynamic measurements without obstacles in setup 2

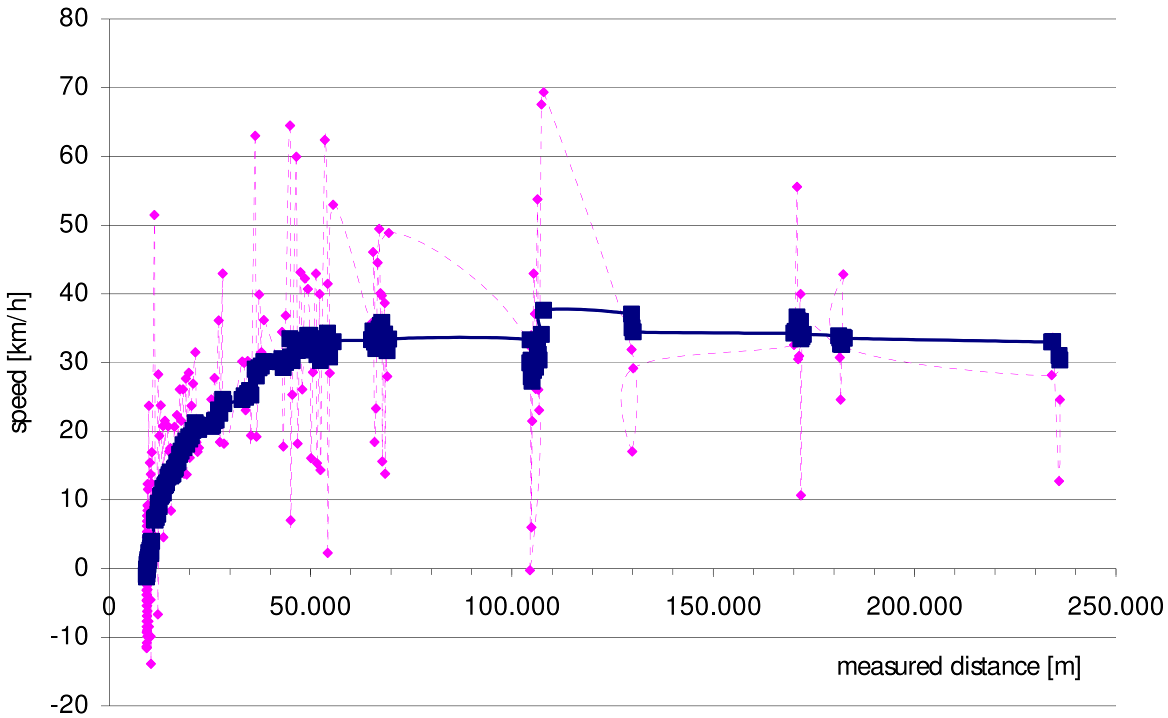

Fig. 28: Estimated speed for dynamic measurements without obstacles in setup 2; The dotted pink line is calculated along Eq. 33, the solid blue line along Eq. 34

7. Measurement results from setup 2 (Residential area) with ASIC

Overview

The measurements with the ASIC were taken in January 2007. Due to cold and adverse weather conditions, major problems were encountered with the Notebook equipment. Hence only a limited number of measurements could be performed during that day in Berlin. Those measurements examined the static use-cases without obstacles with a distance between 10 and 60 m. Longer ranges could not be achieved due to Notebook problems.

Static Measurements

Fig. 29 and 30 show the values directly measured from the transceiver for the two edge values 10 m and 60 m. The maximum absolute error of the median value in the case of 10 m is around 0.8 m, which corresponds to around 8%, in the case of 60 m around 0.42 m, corresponding to around 0.7 %.

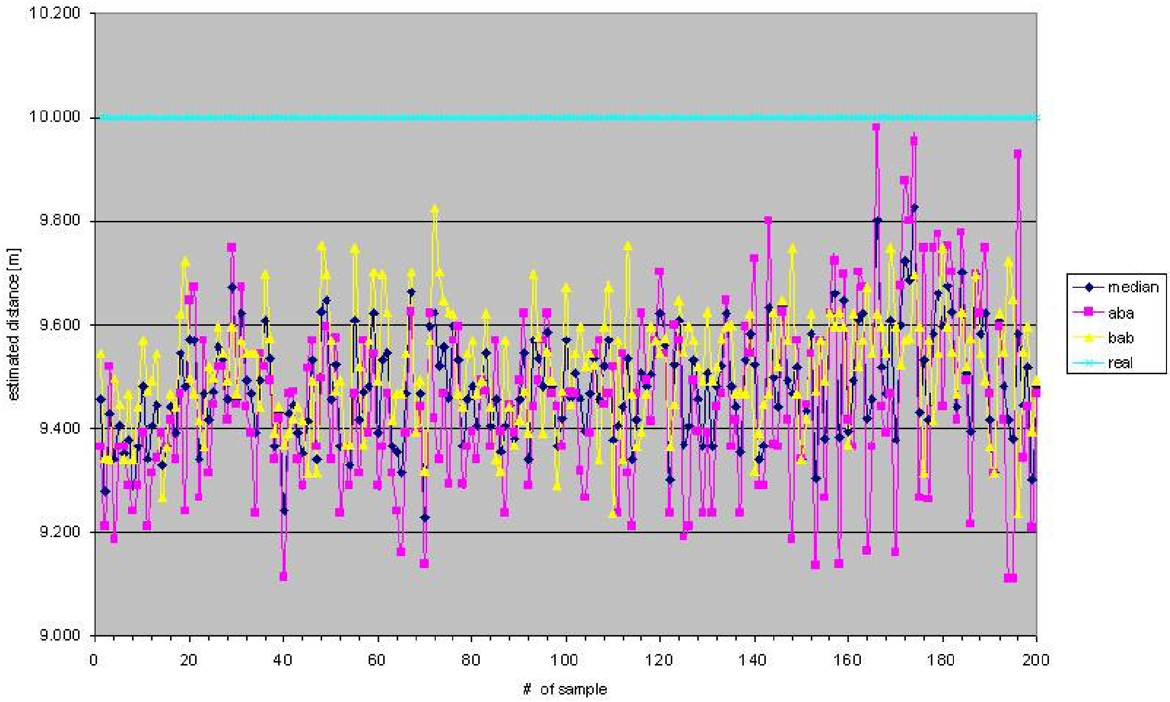

Fig. 29: Estimated distances for 200 samples using the nanoLOC ASIC; real distance is 10 m

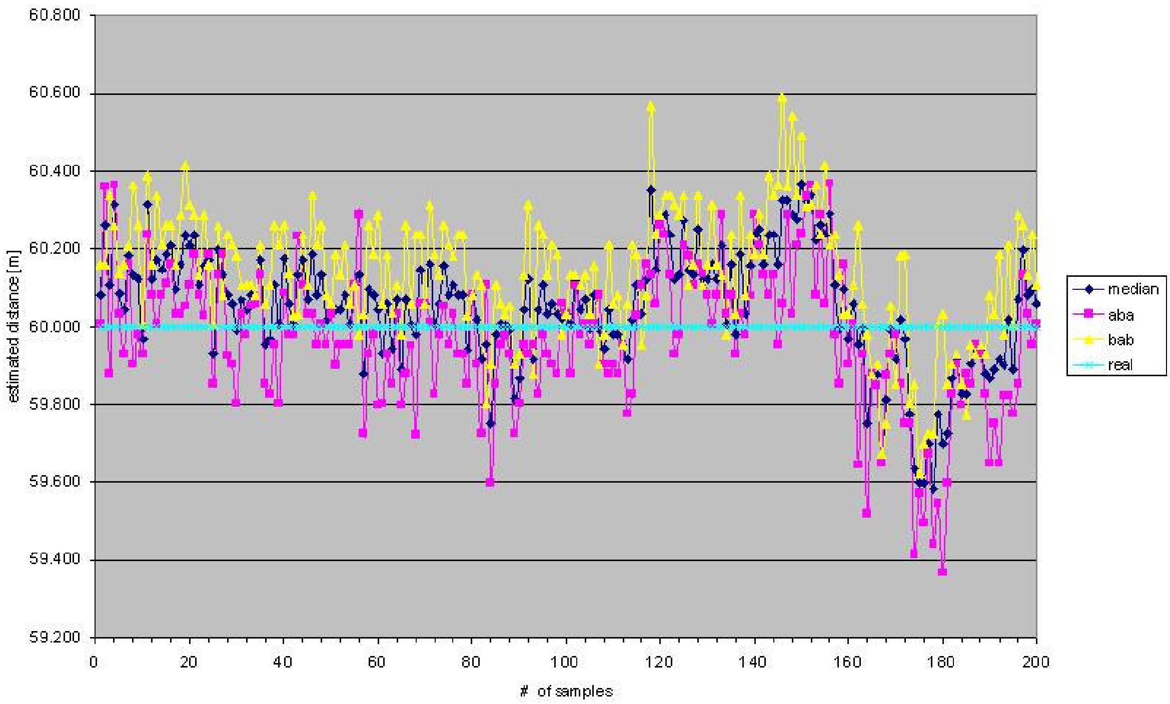

Fig. 30: Estimated distances for 200 samples using the nanoLOC ASIC; real distance is 60 m

Table 13 shows the statistical data to these measurements, which are depicted in Fig. 31 and 32.

real distance [m]	measured distance [m]	mean relative error [%]	max relative error [%]	standard mean deviation [m]
10	9,48	-5,20%	-7,72%	0,10727
20	19,856	-0,72%	-1,76%	0,08267
30	29,682	-1,06%	-2,14%	0,09903
40	40,579	1,45%	-2,18%	0,1266
50	50,635	1,27%	1,85%	0,10728
60	60,054	0,09%	-0,70%	0,15008

Table 13: Mean estimated distances, mean and maximum relative error and standard deviation for static measurements without obstacles in setup 2 using the nanoLOC ASIC

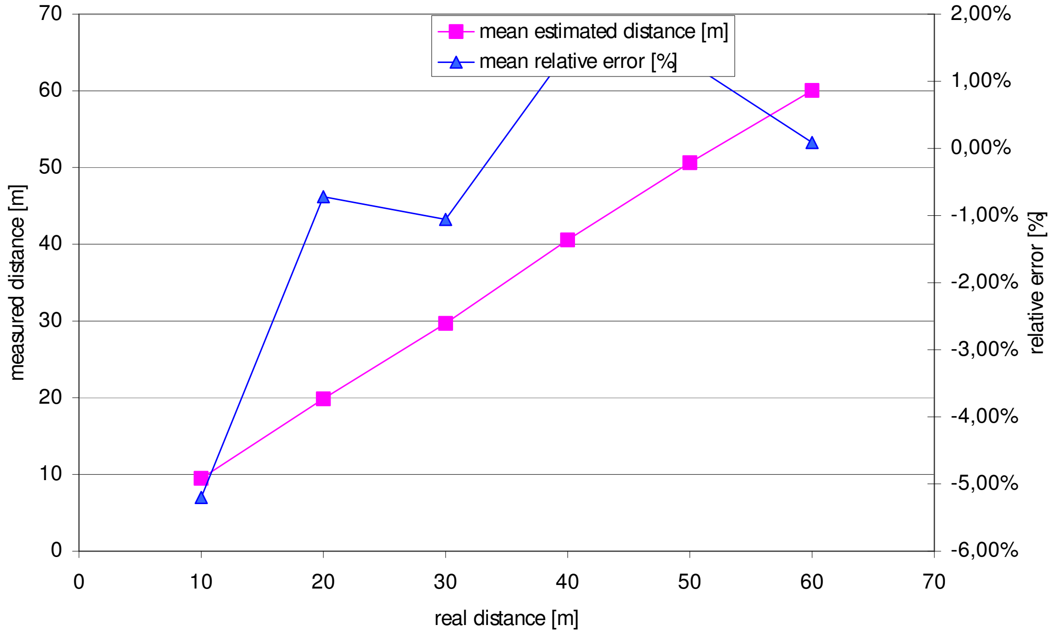

Fig. 31: Mean estimated distances and relative error for static measurements without obstacles in setup 2 using the nanoLOC ASIC

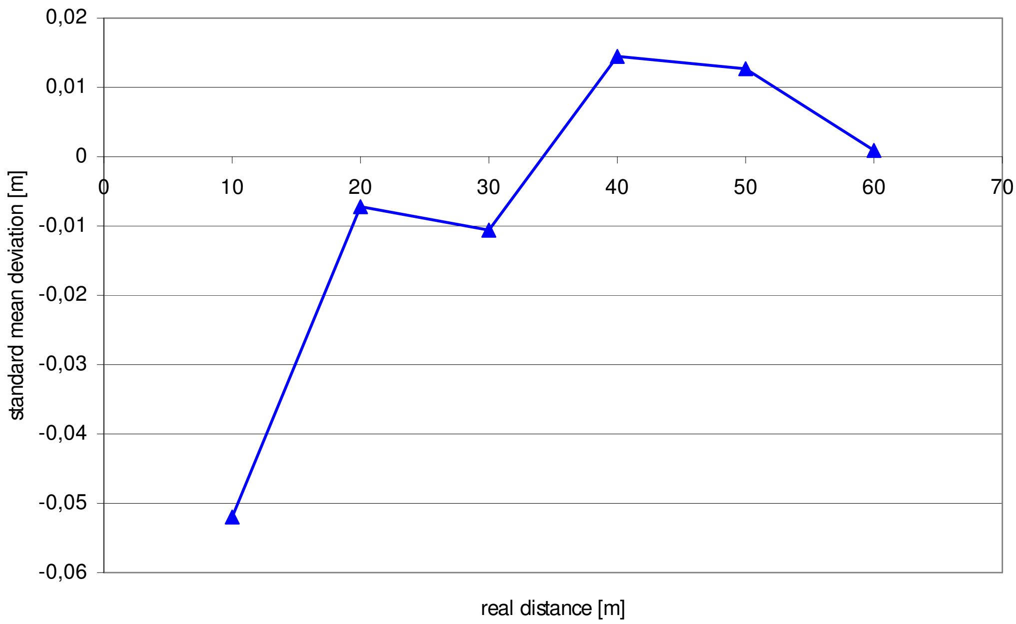

Fig. 32: Standard mean deviation for static measurements without obstacles in setup 2 using the nanoLOC ASIC

8. Further activities

The following activities should be performed:

- Further test setup, as described in ch. 0.
- More powerful post-processing, i.e. Kalman-filtering
- Synchronized dynamic measurements with real position data

9. References

[1] R. Roberts, "Ranging Subcommittee Final Report", IEEE P802.15.04-0581r0, 18.10.2004, available at (21.7.2006): http://grouper.ieee.org/groups/802/15/pub/04/15-04-0581-00-004a-ranging-subcommittee-final-report.doc

[2] R. Hach, "Symmetric Double Sided – Two Way Ranging", IEEE-15-05-0334-00-004a, available at (21.7.2006): http://www.ieee802.org/15/pub/2005/15-05-0334-00-004a-symetric-double-sided-two-way-ranging.ppt.